Summer 2024

Ontogenetically Driven Changes in the Endocranial Anatomy of Maiasaura Peeblesorum and its Implications for Sensory Functions

Emma Puetz
Missouri University of Science and Technology

Department:

Recommended Citation

ONTOGENETICALLY DRIVEN CHANGES IN THE ENDOCRANIAL ANATOMY

OF *MAIASAURA PEEBLESORUM* AND ITS IMPLICATIONS FOR SENSORY

FUNCTIONS

by

EMMA ROSE PUETZ

A THESIS

Presented to the Graduate Faculty of the

MISSOURI UNIVERSITY OF SCIENCE AND TECHNOLOGY

In Partial Fulfillment of the Requirements for the Degree

MASTER OF SCIENCE IN GEOLOGY & GEOPHYSICS

2024

Approved by:

Francisca Oboh-Ikuenobe, Advisor
James Logan King
John Patrick Hogan

ABSTRACT

Hadrosaurids exhibited extreme morphological diversity and behavioral characteristics that can be compared with other, closely related members of Dinosauria – particularly through the study of neuroanatomy. X-ray CT generated endocrania of the Late Cretaceous saurolophine hadrosaur *Maiasaura peeblesorum*, known as the "good mother" dinosaur, offers a unique opportunity to compare complex ecological behaviors between non-avian dinosaurs and their modern archosaur relatives. The 3D reconstruction software ORS Dragonfly provided linear and volumetric measurements taken from the digital cranial endocast and endosseous labyrinths of three ontogenetically varied *M. peeblesorum* specimens from the Two Medicine Formation in Montana that were used to calculate the olfactory acuity, total and cerebral encephalization quotients, and hearing frequencies. Endocranial anatomical data of *M. peeblesorum* specimen OTM F138 suggests that adults had a cerebral relative volume (CRV) of 49.5%, a high reptile encephalization quotient of 2.2-2.3, an average to high olfactory acuity of 1.76, and a hearing frequency range of 57-3380 Hz. Late juvenile and subadult ontogenetic specimens (TMDC F139 and TMDC F140) had a CRV of 39.4-42.6%. These cerebral volumes are ~6% higher than the CRV value calculated for other related hadrosaurs and are among the highest values across Dinosauria, suggesting that complex behaviors were expected. The data is consistent with the advanced social and nesting behavior observed in the fossilized record of this exemplar taxon that preserves numerous growth stages. These preliminary neuroanatomical descriptions and sensory calculations for *M. peeblesorum* are critical in understanding how sensory acuity and behavior could have changed ontogenetically and interspecifically.

ACKNOWLEDGMENTS

TABLE OF CONTENTS

LIST OF ILLUSTRATIONS

LIST OF TABLES

NOMENCLATURE

Symbol   Description

YPM-PU   Yale Peabody Museum at Yale University, New Haven, Connecticut, USA

MOR   Museum of the Rockies, Bozeman, Montana, USA

OTM   Old Trail Museum, Choteau, Montana, USA

TMDC   The Montana Dinosaur Center, Bynum, Montana, USA

PU   Princeton University, Princeton, New Jersey, USA

TCMI   The Children's Museum of Indianapolis, Indianapolis, Indiana, USA

BFR   Best Frequency Range of Hearing

MBH   Mean Best Hearing

BF   Best Frequency of Hearing

MF   Maximum Frequency of Hearing

REQ   Reptile Encephalization Quotient

MPZ   Museo de Ciencias Naturales de la Universidad de Zaragoza, Zaragoza,
Spain

AMNH   American Museum of Natural History, New York City, New York, USA

FPDM   Fukui Prefectural Dinosaur Museum, Fukui, Japan

UALVP   University of Alberta Laboratory for Vertebrate Paleontology, Edmonton,
Alberta, Canada

NCSM   North Carolina Museum of Natural Sciences, Raleigh, North Carolina,
USA

RAM   Raymond M. Alf Museum of Paleontology, Claremont, California, USA

BSPG   Bayerische Statssammlung für Palaontologie un Geologie, Munich,

Germany

MB.R   Museum für Naturkunde, Berlin, Germany

AEHM   Amur Natural History Museum of the Far Eastern Institute of Mineral

Resources, Russia

RBINS   Royal Belgian Institute of Natural Sciences, Brussels, Belgium

MNHN   Muséum national d'Histoire naturelle, Paris, France

MAP   Museo Aragonés de Paleontologia, Teruel Spain

IGM   Mongolian Institute of Geology, Ulaan Bataar, Mongolia

ZPAL   Institute of Palaeobiology of the Polish Academy of Sciences, Poland

1. INTRODUCTION

1.1. PALEONEUROLOGY

Paleoneurology is a branch of paleontology that qualitatively and quantitatively describes the endocranial anatomy in extinct organisms to understand the most vital organ in the central nervous system: the brain (Buchholtz and Seyfarth, 1999, 2001; Lautenschlager and Hübner, 2013). However, the brain is rarely preserved as an actual fossil, since taphonomic processes typically destroy the soft, organic tissues of the body such as neuroanatomy (Brasier et al., 2017). The most common evidence of neuroanatomy in the fossil record is recovered from the osteological remnants that surrounded the brain and the 3D form the space that the brain occupied within the braincase. The term 'cranial endocast' refers to the internal spaces of the braincase that housed the brain and its associated surrounding soft tissues in life (Dufeau et. al, 2012; Lautenschlager & Hübner, 2013, Balanoff and Bever, 2017; Hu et. al 2020). The morphology and anatomy of the endocrania enable paleontologists to make inferences about the brain, behaviors of extinct animals, and overarching macroevolutionary trends in neuroanatomy across phylogenies.

1.2. NON-AVIAN DINOSAUR PALEONEUROLOGY

A popular misconception in the past stereotyped non-avian dinosaurs as having small brains and limited cognitive abilities (Jerison, 1969). With time, this belief has been challenged and disproven through the study of dinosaurian paleoneurology: the subfield of paleoneurology applied to ornithischian and saurischian taxa. The overall goal of this subfield is to grasp a deeper understanding of the neuroanatomical features of the non-

avian dinosaurs and investigate how the nervous and sensory systems changed throughout their evolution during the Mesozoic. Over the last two centuries, paleoneurologists have been qualitatively and quantitatively describing the cranial endocasts of numerous dinosaurian taxa to understand the anatomical, morphological, and evolutionary trends of the non-avian dinosaur nervous system (Marsh, 1884a, 1884b; Edinger, 1929; 1942; Jerison, 1955; 1969; 1973; Jerison and Barlow, 1985; Giffin, 1989; Rogers, 1998; Buchholtz and Seyfarth, 2001; Evans, 2005; Franzosa and Rowe, 2005; Gleich et al., 2005; Witmer and Ridgely, 2008; Evans et al., 2009; Walsh et al., 2009; Witmer and Ridgely, 2009; Zelenitsky et al., 2009, 2011; Lauters et al., 2013; Lautenschlager and Hübner, 2013; King et al., 2020; Sakagami and Kawabe, 2020; Button and Zanno, 2023; Lauters et al., 2023).

Since the youngest specimens of the non-avian dinosaurs are 66 million years old, the likelihood that soft anatomy of the brain being preserved in the braincase is incredibly low. The first ever reported evidence and study of fossilized dinosaurian endocranial tissue was conducted by Brasier et. al (2017) who noted that the rare taphonomic process replaced blood vessels, capillaries, meningeal, and potentially superficial cortical tissues with collophane and microcrystalline siderite in a phosphatic layer. This was revealed by scanning electron microscopy from the natural endocast of an Early Cretaceous Iguanodontid - a dinosaur distantly related to the "duck-billed" hadrosaurs (Brasier et al., 2017). For this preservation to occur, it was hypothesized that the dinosaur died adjacent to or within a eutrophic anoxic freshwater body, since precise anoxic environmental conditions are necessary for phosphate to preserve soft tissue (Briggs et al., 1993). The assumption is that the head of the dinosaur became rapidly partially buried under the

sediment where preservation and taphonomic processes could begin (Brasier et al., 2017). This study was crucial and revolutionary for better understanding the fine anatomical features of the soft tissues within the non-avian dinosaur's braincase. In most cases, the cranial endocast is sufficient for allowing paleoneurologists to describe and quantifiably utilize the inner morphological features of the osteological braincase. Through these paleoneurological studies, new insight into the endocranial body of non-avian dinosaurs have provided answers to macroevolutionary questions regarding the brain and sensory systems and better understanding of these still unknown extinct organisms and modern archosaurian taxa.

1.3. SIGNIFICANCE AND OBJECTIVE OF STUDY

Parental care is a behavioral, social, and intellectual trait commonly exhibited by mammals, avians, and some reptiles (Balshine, 2012). Before 1978, this characteristic was not associated with dinosaurs, as they were commonly believed to be similar to modern reptiles with a cold, neglecting type of parental behaviors, and therefore incapable of maternal care. The discovery of a nest-like structure with fifteen nestling dinosaurs, namely *Maiasaura peeblesorum*, changed this belief and some of our ideas about the social structure and complexity of dinosaurian behaviors. (Horner and Makela, 1979).

Maiasaurua peeblesorum is a saurolophine hadrosaur whose fossil record is well represented in the Upper Cretaceous Campanian Two Medicine Formation of Montana. The dinosaur species has preserved all ontogenetic growth stages from eggs to mature adults throughout the formation. Deemed the "good-mother lizard" due to the discovery of the first nestling-aged dinosaurs and nesting sites, *M. peeblesorum* quickly gained fame

and sparked the interest of paleontologists due to the abundance of ontogenetically diverse fossils found within the unique preservational conditions of the Two Medicine Formation (Figure 2.1). The ontogenetic series of *M. peeblesorum* have been studied extensively due to the mass number and preservation of specimens (Horner and Makela, 1979; Horner, 1983; Horner et al., 2000; Woodward et al., 2015; Prieto-Marquez et al., 2018; McFeeters et al., 2021) but a reconstruction of the cranial endocast remained to be made. The preservation of fossilized evidence interpreted to reflect complex behaviors in *M. peeblesorum* (e.g. nesting behavior, gregariousness) provides a unique opportunity to observe how the brain of a behaviorally complex non-mammalian organism differs from and/or relates to other related taxa that are not known for the same behaviors. Similarly, insights into the taxon's sensory systems, such as olfaction and hearing frequencies, and volumetric analyses can provide information as to how these functional traits are consistent with the ability of an organism to exhibit these complex behaviors.

Understanding variations in the cranial endocast and sensory systems is vital in inferring how they affect the evolutionary success of extinct and extant organisms. Furthermore, quantitative and qualitative analysis of the morphological and anatomical changes in the cranial endocast through an ontogenetic series allows for an unprecedented insight into the development of the cranial endocast and sensory systems. More importantly, the applications of these first inferences of the cranial endocast of *M. peeblesorum* can provide insight into macroevolutionary trends within neuroanatomy and behavior throughout ornithopods and across Archosauria. Late Cretaceous hadrosaurs were extremely diverse and evolutionary highly specialized, allowing for extensive knowledge to be gained from the study of their characteristics. Understanding if the cranial endocast,

and by inference the brain, of *M. peeblesorum* was a monospecific specialization unseen in the endocrania of related taxa is crucial to further examine the relationship between the brain's morphology, likelihood of displaying of complex behaviors, and macroevolutionary trends in the neuroanatomy evolution.

The objective of the present study is to develop and better understand the relationship between complex behaviors and morphology of the endocranial anatomy in non-avian dinosaurs. Three braincases of *M. peeblesorum* were CT-scanned, respective endocasts were reconstructed, and then qualitatively and quantitatively analyzed for paleoneurological implications. Thus, the ontogenetic development of the endocrania and sensory systems will be inferred.

2. THE TWO MEDICINE FORMATION

The Two Medicine Formation of North America is situated along the eastern slopes of the Rocky Mountains and is approximately 600 meters thick, thinning to the east (Rogers, 1990). The formation was deposited in a fluvial-deltaic environment that occurred during the both the Telegraph Creek-Eagle regressive - Claggett transgressive and Claggett regressive – Bearpaw transgressive phases of the Western Interior Seaway beginning approximately 80 mya, during the Campanian stage of the Upper Cretaceous (Varricchio and Horner, 1993; Rogers, 1998; Stidham and Hutchinson, 2001). The deposition during this regressive phase led to the formation being comprised of nonmarine lithologies of fine to medium sandstones, variegated mudstones, and siltstones sourced from the Cordilleran highlands (Rogers et al., 1993, Falcon-Lang, 2003; Foreman et al., 2007). Volcaniclastic materials, including bentonite clay, also appears in the formation and were derived from the Elkhorn Mountain Volcanics that were primarily active during the Campanian stage of the Late Cretaceous (Viele and Harris, 1965; Chadwick, 1981; Rogers et al., 1993; King, 1997). $^{40}Ar/^{39}Ar$ dating of biotite and plagioclase from four of the bentonite clays spread through the formation to provide approximate age of 82.6-74.0 Ma (Rogers et al., 1993).

The Two Medicine Formation is underlaid and overlaid by the shallow marine Virgelle Sandstone Formation and Bearpaw Formation, respectively (Varricchio and Horner, 1993; Rogers 1998), and was contemporaneously deposited with the Judith River Formation of eastern Montana (Rogers et al., 1993) and Judith River Group of Alberta and Saskatchewan (Eberth and Hamblin, 1993). For simplicity, the Two Medicine Formation is subdivided into five lithofacies (Horner et al., 2001). Lithofacies 1, the lowermost unit
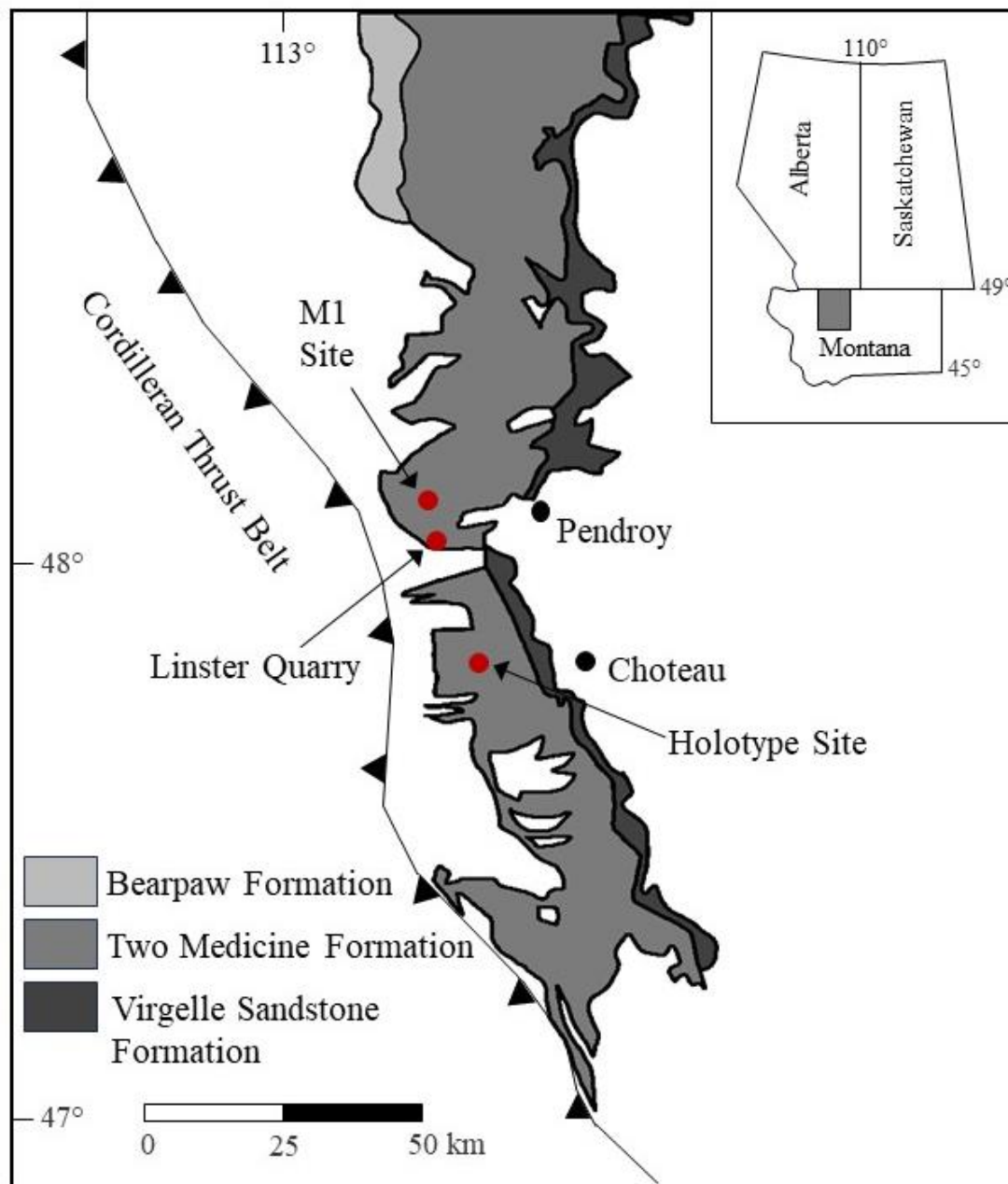
Figure 2.1 Geologic map of the Two Medicine Formation, adjacent formations, and *M. peeblesorum* bonebed localities (red circles). Edited from Falcon-Lang (2003).

immediately above the Virgelle Sandstone, is sandstone-dominated and representative of a

proximal shoreline paleoenvironment. Lithofacies 2 is dominated by mudstone that is

correlative to the "Chaggett shaley interval" (Lorenz, 1981; Lorenz and Gavin, 1984) in

eastern Montana. Lithofacies 3 comprises interbedded fluvial sandstones and mudstones attributed to the regression of the Claggett Sea and referred to as a Judithian sequence. Lithofacies 4 is a thin lacustrine section representing the debut of the transgressive event of the Bearpaw resulting from increased basin subsidence rates (Rogers, 1998). This is the only lithofacies where *M. peeblesorum* species has been found (Horner et al., 2001), however other fossilized material of various dinosaurian, crocodilian, fish, reptilian, avian, and plant taxa have been observed throughout the formation (Horner et al., 2001). Finally, lithofacies 5 is dominated by fluvial facies, such as sandstones, that were deposited during the continued transgression of the Bearpaw Sea. There was a shift to a marginal marine transitional bed (Bearpaw Shale and Horsethief Sandstone) above this unit.

Paleoecological studies of the Two Medicine Formation reveal that there are numerous dinosaurian species that have only been found in this formation, including the aforementioned chronologically related Judith River Formation and Judith River Group to the east and north, respectively. Specimens recovered from the formation were first formally discovered and documented in 1911 by Eugene Stebinger, who found the first recorded vertebrate fossils while working in the area as a geological surveyor (Gilmore, 1917). Over the past few decades, continuous excavations and research throughout the formation have documented numerous species of saurolophine and lambeosaurine ornithopods *Maiasaura peeblesorum* (Horner and Makela, 1979), *Gyposaurus latidens* (Horner, 1992), *Hypacrosaurus stebingeri* (Horner and Currie, 1994) and *Prosaurolophus blackfeetensis* (Horner, 1992), ceratopsians *Einiosaurus procurvicornis* and *Achelousaurus horneri* (Sampson, 1995), theropods *Daspletosaurus* sp. (Carr et al., 2017), *Bambiraptor feinbergi* (Burnham et al., 2000), and thyreophorans *Euoplocephalus* sp. and

Edmontia sp. (Horner et al., 2001). These taxa comprise just a portion of the fossilized Animalia taxa found in the Two Medicine Formation.

The discovery of dinosaurian eggs and the first-ever dinosaur nestlings found in a nest structure in the Willow Creek anticline west of Chouteau, Montana in 1978 (Gavin, 1986) was the event that sparked global interest in the Two Medicine Formation. To date, dinosaur eggs have been found on every continent (Grellet-Tinner et al., 2006) and 37 oospecies comprising 13 oogenera and eight oofamilies of dinosaur eggs have been documented (Liang et al., 2009). After the initial discovery of hadrosaur eggs in the Two Medicine Formation, other dinosaurian eggs ichnotaxa were uncovered in the formation, including theropod (*Troodon*), hypsilophodonitid (*Orodromeus makelai*), and a small, possibly avian egg (Hirsch and Quinn, 1990; Jackson et al., 2015). While the abundance of eggs found in the formation was imperative to understanding the taphonomic and preservation of eggshell material, the perinatal nestling dinosaurian bones found alongside a nest structure and adult specimen was revolutionary (Horner and Makela, 1979). This discovery was crucial to the development of the first interpretations about the ecological behavior and relationship of dinosaurs – specifically parental behavior (Horner and Makela, 1979) allowing for the unique debut of *Maiasaura peeblesorum*.

3. LITERATURE REVIEW

The historical overview of dinosaurian paleoneurology (Appendix 1), current research trends, and descriptions of past and present methods of reconstructing the endocranial body provide the context for the rest of this thesis. A review of the general form and function of dinosaur neuroanatomy can be found in Appendix 2. Dinosaurian paleoneurology will hereafter be referred to as "paleoneurology" in this section.

3.1. MODERN RESEARCH TRENDS

Over the past century, paleoneurological research has significantly expanded to utilize emerging technologies and explore previously unavailable observations. Due to the vast number of dinosaurian taxa discovered since the development of paleoneurology as a subfield of paleontology, qualitative analyses of the gross anatomy of braincases from newly described taxa are still important to the overarching goal of the field as they provide data for broader studies. Many cranial endocasts descriptions for ornithischian (Evans, 2005; Evans et al., 2009; Lauters et al., 2012; Saveliev et al., 2012; Lautenschlager and Hübner, 2013; Paulina-Carabajal et al., 2016; Brasier et al., 2017; Sakagami and Kawabe, 2020; Button and Zanno, 2023) and saurischian taxa (Rogers, 1998, 1999; Franzosa and Rowe, 2005; Sanders et al., 2005; Witmer and Ridgely, 2009; Lautenschlager et al., 2012; Carabajal, 2012; Hurlbert et al., 2013; Bronzati et al., 2019; Cerroni and Carabajal, 2019; King et al., 2020; Müller, 2022;) have been utilized to better understand the morphology of their endocranial cavities. The wide range of dinosaurian taxa being used to model and describe their neuroanatomy enables further insight into how the dinosaurian endocast has

changed through time and the impacts the changing morphological features had on the neurosensory abilities within a clade or species.

Since the first quantitative study of paleoneurological analysis occurred in the late 1960's (Jerison, 1969), new mathematical methods are enabling paleonneurological researchers to develop a better understanding of the neurosensory system of non-avian dinosaurs. The focus of many paleoneuroanatomical studies has been centered around the olfactory abilities of both carnivorous and herbivorous taxa since the need to sense predator-prey relationship or the inter- and intraspecific communications that were crucial to their survival. The evolution of olfaction acuity in numerous theropod dinosaurs (Witmer and Ridgely, 2009; Zelenisky et al., 2009; Zelenitsky et al., 2011), such as *Tyrannosaurus rex* (Zelenitsky et al., 2009), and ornithischians (Zelenitsky et al., 2009; Sakagami and Kawabe, 2020; Button and Zanno, 2023) has been measured using a ratio of the greatest linear measurement of the olfactory bulbs to the greatest linear measurement of the cerebral hemispheres (Zelenitsky et al., 2011). This analysis has been used to infer the olfaction acuity of dinosaurian taxa, resulting in a greater understanding of behavioral traits and the changes of olfactory acuity through Dinosauria (Zelenitsky et. al., 2009).

Calculations of hearing acuity among non-avian dinosaurs have also been frequently studied in recent years (Gleich et al., 2005; Witmer and Ridgely, 2009; Evans et al., 2009; Lautenschalger et al, 2012; King et al., 2020; Sakagami and Kawabe, 2020; Button and Zanno, 2023). Gleich et al. (2005) were the first to conceptualize the ability to calculate the hearing frequencies ranges of dinosaurs from their study correlating the length of the basilar papilla to attainable hearing frequencies in modern birds. Their observations recorded that if the basilar papilla had a smaller length, the birds would hear higher

frequencies, and vice versa for birds with basilar papillae of longer lengths. Since the cochlear duct can be digitally segmented in well-preserved dinosaurian braincase, the basilar papilla length can be approximated as two-thirds the length of the cochlear duct and used to calculate the hearing frequencies (Gleich et al., 2005; Evans et al., 2009). However, it is worth noting that extrapolating these methods from modern birds with small masses to extinct dinosaurs with very large masses, could limit the results and affect the accuracy due to unknown factors such as the space filled by soft anatomy and differences in body temperature regulation (Gleich et al., 2005). Walsh et al. (2009) derived a method to calculate the hearing frequencies for dinosaurs taking into account the body mass difference between taxa; this was done by logarithmically scaling the reconstructed cochlear duct length to the basisphenoid complex of the osteological braincase. Evans et al. (2009) combined the ideas of these two methods to calculate the hearing frequencies of lambeosaurines hadrosaurs and utilized the cochlear duct length in the equations of Gleich et al. (2005). Choosing to use the cochlear duct length rather than the basilar papilla length stems from the inability to know how much volume the basilar papilla composed within the cochlear duct bony structure within extinct dinosaurs (Gleich et al., 2005; Walsh et al., 2009; Evans et al., 2009). Nonetheless, all three of these methods allowed for new comparisons and predictions to be made about the attainable hearing frequencies, vocalization complexity, and potential for sociality based on the hearing ranges and behaviors of extinct dinosaurs.

3.2. DEVELOPMENT OF ENDOCAST RECONSTRUCTION METHODS

In order to study paleoneurological trends in extinct organisms, the cranial endocast must be reconstructed and described. The cranial endocast is reconstructed from the endocranial cavity that would have housed all the soft anatomy of the brain and neurological system within the braincase. Therefore, the cranial endocast does not reveal the exact volume, anatomy, and shape of just the brain, but rather it preserves the total volume and external shape and anatomy of the inner braincase. The methodologies utilized to expose or reconstruct this inner anatomical feature have dramatically evolved in many ways over the last century. Originally centered entirely on chance discoveries in the field and destructive methods, advances in technology have immensely increased the complexity of descriptions and interpretations that are made from the cranial endocast. However, these modern analytical techniques would not have been developed without the creation and improvements of their earlier techniques.

3.2.1. Steinkerns. Steinkern, stone "stein" and grain or kernel "kern" in German, is a type of fossil that preserves the empty spaces of a fossil (Hopson, 1979). This is naturally achieved by an infilling and lithification of detrital material in a hollow cavity that had once been filled by soft anatomy. Once lithified, the mold preserves the inner anatomical endocast of the original fossil, and can be studied if the osteological fossil decomposes as the lithified material is often more resistant to weathering (Brasier et al., 2017). Qualitative and quantitative details can be described and calculated, respectively, about the cranial anatomy from the steinkern of a cranial endocast if sufficient anatomical detail has been preserved. Steinkerns were popularly utilized in older paleoneurological research (Werneberg et al., 2021) due to the lack of modern reconstruction techniques

however, these types of fossils still have utility in current research (e.g. Brasier et al., 2017; Werneberg et al. 2022). While studying a natural endocast can be a nondestructive analytical technique, the drawback of the method is that the steinkern cannot be assigned to a particular genus or species without the preservation of a specimen alongside the cast. In the fortunate cases when a steinkern preserved inside the osteological braincase, destructive methods are to be used to remove the fossil from the inside of the braincase (Newton, 1888).

3.2.2. Sectioning. The process of serial sectioning was introduced by Sollas (1904) as a method to remove small incremental layers of a fossil to expose internal structures. Sollas developed and perfected this method over a wide variety of studies on taxa of graptolites (Sollas, 1904), an ophiurid (Sollas, 1904), numerous fish (Sollas, 1904; Sollas and Sollas, 1904), *Dicynodon* (Sollas and Sollas, 1913), *Ichthyosaurus* (Sollas, 1917), *Lysorophys* (Sollas, 1920), foraminifera (Sollas, 1921), homininaes (Sollas, 1926), and other fossil groups (Sollas, 1915). The purpose of sectioning comes from the fact that the internal structure of the braincase cannot be seen from the external view, and therefore destructive sectioning of the braincase was the only method to view the internal structure. This process entails grinding away layers in <100 µm intervals and then sketching, photographing, or, in more recent times, photographically scanning the fossil. Serial segments could then be reconstructed with pliable material, such as wax or clay, to make a 3D image of the internal structure of the braincase. In his description of the technique, Sollas referreds to the process as "a means for obtaining a deeper insight into the objects of his study lies ready to hand" (Sollas, 1904). In this statement, one can interpret Sollas as proposing the methods of sectioning as a way to readily reconstruct the cranial endocast

of extinct organisms, rather than wait for the preservation of natural steinkerns. However, significant drawbacks to this method are the extreme time consumption and the complete destruction of the specimen used in the study. For example, for the skeletal anatomy of Devonian fish described by Jarvik (1954), he spent more than 25 years to grind and reconstruct over 500 slices with wax. Moreover, due to the uneven natural and wide array of bones in the osteological braincase, manual sectioning can pose problems, such as inconsistency in the thickness ground away, incorrect identification of bones, or bias between paleontologists, that will result in the inaccurate reconstruction of the cranial endocast (Sandy, 1989).

  3.2.3. Latex Casting. For the purpose of non-destructive analysis of an endocast, the reconstruction method of latex casting was popularized and standardized in the early 1900's (Holloway, 2018). Latex casting creates an internal mold of endocranial region of the osteological braincase with soft, pliable material, such as silicone, latex, or rubber (Edinger, 1948). This is done by injecting, pouring, and filling in the empty neural spaces with latex or a similar material which allows paleoneurologist to examine the internal and undersurface structures, such as vascularization or dural tissues, of the braincase in greater detail. Unfortunately, this method requires the braincase to be meticulously cleaned, sectioned, and prepared so that no internal matrix obstructs the view of those anatomical features (Jerison, 1973).

  The process of making the cast is relatively simple, especially compared to that of sectioning, measuring, and drawing the braincase microns at a time. The viscous silicone, latex, or rubber material is slowly poured into the foramen magnum, as the braincase is rotated around to cover the inner surface and fill in the empty foramina and canals. Fine

powder (e.g. talcum powder) can be used on the bone surface before this first pour to ensure the latex does not stick to the bone (Holloway, 2018). The initial layer of latex is allowed to solidify before pouring of the latex to fill the rest of the cavity begins. Once the cavity is filled and solidified to form a soft, pliable endocast, it can be pulled out of the osteological braincase via the foramen magnum (Edinger, 1968). However, there is the possibility of damaging the bones of the posterior and ventral region of the skull, and subsequently the endocranial cavity, during this removal process, the probability of which is higher with more modern and less fossilized specimens.

Limited latex casting has been performed on extinct specimens (including diniosaurs) due to the frequency in which braincases are infilled with sediment. In order to get an accurate representation of the anatomical features of the endocast with latex casting, all sediment must be removed from the inner surfaces of the osteological braincase. This task proves to be almost impossible in well-preserved specimens, as paleontologists will not be able to work around all the bones to ensure complete removal of material. This is especially true when specimens are not three-dimensionally preserved. The skull would more than likely need to be bisected to be prepped, and then reconstructed, which could then cause errors in the casting process and further future interpretations. Not to mention that this irreparably damages specimens, thus making this method dangerous or unusable on holotype specimens. With this being said, this method has successively been used before on dinosaurs. Evans (2005) provided evidence for vascular valleculae (i.e., impressions of blood vessels incised into the braincase) on the underside of the frontals in hadrosaur specimens with latex casting. Prior to the advent of modern digital reconstructive methods, latex casting was used more in modern specimens, such as horses (Edinger, 1948) and

primates (Radinsky, 1968), due to minimal infilling and taphonomic distortion of geologically young vertebrate specimens.

Latex casting has both advantages and drawbacks. Latex is easy to use, readily available and affordable, and has a low risk of chemically damaging the fossil, when used properly. Problems arise after the endocast has been created; due to the pliable structure of the material needed for extraction from the braincase, the reconstructed endocast is prone to losing shape or deforming after a period of time if not supported by another structured material (Edinger, 1948; Radinsky, 1968). Additionally, latex casts also can shrink or expand over time due to the curing process still occurring once outside the osteological braincase (Edinger, 1948). All of these create major problems for researchers, as the latex cast could no longer be used for any morphometric, volumetric, or surficial material research.

3.2.4. Computed Tomography and 3D Reconstruction. Due to the difficulties and destructive testing that are associated with older reconstruction methods of endocranial models, detailed documentation of paleoneurological studies were severely limited. With the technological advancement and the development of computed tomographic (CT) scanning, there was a rejuvenation and revolution of paleoneurology (Witmer et al., 2008; Witmer and Ridgely, 2009) By utilizing CT scanners alongside 3D reconstruction software, accurate and precise visualizations of internal structures can be documented, described, and measured without the need for invasive preparation of a fossil specimen. Therefore, destructive methods, such as the removal of all rock matrix, individually grinding away layers, and the long0term storage or viability issues of latex modelling, are eliminated in this reconstruction method. Applying CT scanning and 3D reconstruction to

paleoneurology has led to an abundance of endocranial models, endosseous labyrinths, and vascularization being investigated in a wide range of dinosaurs (Rogers 1998, 1999; Evans, 2005; Evans et al., 2009; Lauters et al., 2012, 2013, 2022; Balanoff et al., 2013; Button and Zanno, 2023) The first application of CT scanning in dinosaurian paleoneurology was undertaken by Rogers (1999) whereby an endocast of *Allosaurus fragilis* was compared to the endocast of crocodiles and birds. Since this method has only been implemented in the last three decades at the time of writing, it is constantly being used for different types of studies to understand the entire breadth of its potential.

The process of CT scanning is relatively simple: a fossil is placed into a CT scanner and scanned through the process of X-ray beams penetrating and rotating around the same to create 2D images at given intervals of measurement. These 2D images, called slices, are then layered on top of one another in a computer program to form a digital 3D image. This is a digitalized and much more accurate, far less damaging version of the "sectioning" methods done in the past. The X-rays of the scanner are absorbed differently based on the difference in the density of the fossil compared to the rock around it. In the 3D software, the density differences are used to perform the segmentation of specific regions of interest. The resolution of the slices is dependent on the intensity of the X-ray beam, the frequency of images taken, and the size and location of the focal point. Surprisingly, medical-grade scanners used by hospitals and research-grade scanners, such as high-resolution or μCT systems, vary significantly in beam energy intensity and focal point ranges. Medical-grade scanners have intensity ranges of 5-120 kilo-electronvolts (keV) and a focal point between 0.3-1.2 mm, while research-grade scanners can have intensity ranges of 10-450 keV and a focal point 0.5-220 μm. These translates to slice resolutions of ~1-2 mm vs 2-5 μm,

respectively, allowing the latter to provide for a much more detailed and higher resolution scan in more varied densities of rock types (Racicot, 2016). Research grade scanners can only be used on non-biological, or dead, items due to the high dosage of radiation in the scan; a medical scanner will produce ~0-20 mSv of low linear energy transfer radiation during routine examines, while microCT research scanners can produce radiation doses reaching up to 90000 mSv (Meganck and Liu, 2017). Exposure to this magnitude of radiation doses can cause severe histopathological damage to the tissues, lungs, bones, etc. (Meganck and Liu, 2017) within living specimens.

Drawbacks to CT scanners are relatively few when compared to older techniques; however, they do exist. The most common problem encountered is high attenuation – the blocking or distorting of X-ray beams that result in partial or complete blurring, whitening, and/or obstruction of the fossilized material leading to uninterpretable images. This occurs when the fossil has been permineralized with metallic or otherwise dense minerals during taphonomy, which affect the X-ray beams. However, this problem does not only occur in older fossilized specimens though since modern specimens that contain metallic materials (e.g. lead in bullets and shotgun pellets) will alter the X-ray penetration and scatter a bright white pattern across the scans. Attenuation can be measured using a signal-to-noise ratio (SNR) where signals are the X-ray photons and noise is pixel deviation from normal. Higher SNR values will mean a lower attenuation, and therefore the image is clearer and has less obstructions (Racicot, 2016). Conversely, a lower SNR value will mean a higher attenuation, therefore the image will have more blurring and distortion in the images and model, if one can be made.

The ease and functionality of CT scanning has made a wide range of impacts in the field of paleontology, not just paleoneurology. Popular applications include other internal anatomical modeling, finite element analysis, and computational fluid dynamics (Racicot, 2016). Finite element analysis can be used for functional morphological studies. Such studies analyze at the stresses, strains, and deformation on the osteological bodies of extinct organisms for feeding and locomotion (Cunningham et al., 2014) or even computationally modelling biomechanical processes, like calculating the bite force of *Tyrannosaurus rex* (Osborn, 1905). Computational fluid dynamics allows for the calculation and visualization of fluid and air flow through and around solid objects/volumes. Bourke et al. (2014) used this method to investigate the air flow within the nasal cavity of pachycephalosaurids and their relatives. Another major impact CT scanning has made to paleontology is the accessibility and ease of sharing information across platforms. In this digital age, we no longer need to carefully wrap and ship delicate fossils around the world for researchers to study. Instead, the fossil can be scanned, and that data can be sent anywhere for reconstruction and/or analysis. While availability and cost of using CT scanners was prohibitive in the past, both are becoming more readily accessible for research purposes and for more frequent usage for reconstructing of visual models.

4. *MAIASAURA PEEBLESORUM*

The hadrosaurid *Maiasaura peeblesorum* is an exemplar taxon among the non-avian dinosaur fauna of the Two Medicine Formation which provides an unprecedented glimpse into growth and behavioral patterns for Late Cretaceous hadrosaurids. In broader terms, *M. peeblesorum* was the first taxon to be found with numerous ontogenetic stages ranging from eggs to fully grown adults, which allowed for macroevolutionary ontogenetic trends to be thought of across all of Dinosauria (Horner and Makela, 1979). The species is well known for the discovery of perinatal material, the first documented hadrosaurid nest, and discovery of parental care amongst non-avian dinosaurs. Extensive field research in the Two Medicine Formation also led to the discovery of mass bone bed deposits containing numerous growth stages of the taxon (Varricchio and Horner, 1993) and the well-known "Egg Mountain" locality that preserves hundreds of eggs attributable to *M. peeblesorum*, alongside other dinosaurian and non-dinosaurian taxa (Hirsch and Quinn, 1990). These discoveries have enabled *M. peeblesorum* to become the "poster child" for the growth and ontogenetic development of the hadrosaurid clade. Contrary to the extensive number of fossilized materials found of the taxon, *M. peeblesorum* was only first discovered less than five decades ago (Horner and Makela, 1979).

4.1. DISCOVERY

The holotype material of *Maiasaura peeblesorum* was discovered in 1978 by Laurie Trexler near Choteau, Montana and is now housed in the Yale Peabody Museum at Yale University (YPM-PU 22405). This specimen is represented by a skull that is missing

portions of the right dentary and predentary (Horner and Makela, 1979). Its finding was, however, overshadowed by Marion Brandvold's 1979 discovery of eleven juvenile dinosaurs, jumbled together in a basin shaped depression resembling a nest (Horner and Makela, 1979). This was the first ever perinatal non-avian dinosaurian material to be described. Before this time, scientists were unsure if the soft, un-ossified and undeveloped bones of juvenile material would withstand harsh fossilization and taphonomic processes due to lack of evidence. The discovery of these *Maiasaura peeblesorum* hatchlings in a nest-like structure several hundred meters from another site containing nestlings (twice the size of the hatchlings) and adult material (all were later determined to be from the same species) sparked immediate interest in the taxon and area. Horner and Makela (1979) and Horner (1983) named and described the taxonomic classification of the holotype adult skull and juvenile bones of the new hadrosaurid dinosaur as *Maiasaura peeblesorum*. "*Maiasaura*" combines the Latin prefix "maia," meaning "good mother," and the Latin female conjugation of the suffix "saurus" to give the generic name of the taxon. The sex of the adult holotype has not been identified, but since the fossil evoked stereotypical ideas about a mother's natural instinct of taking care of infants, the dinosaur's name was created to highlight this discovery. The species name "*peeblesorum*" is in gratitude to the landowners of the fossil locality, the Peebles.

4.2. SYSTEMATIC PALEONTOLOGY

The saurischians and ornithischians are the two distinct and natural groups of Dinosauria in which all species are classified into. This classification scheme was created to group the dinosaurs on the basis their pelvis orientation; saurischians are the "lizard-

hipped" group and ornithischians are the "bird-hipped" group (Owen, 1842; Huene, 1914). Anatomically, the pelvic region of all vertebrates is composed of three bones – the pubis, ischium, and ilium – although the orientation is different for various groups. In saurischians, the pubis points ventrally and the ischium points caudally from the ilium. In ornithischians, the public points rostrally and the ischium points ventrocaudally from the ilium. These are the hip structures observed in modern reptiles and modern birds, respectively, therefore explaining the derivation of the names of the two groups. However, contrary to their pelvic arrangements, modern birds are known to have evolved from the saurischian group of dinosaurs (Ostrom, 1976).

The two main clades represented within Saurischia are the Theropoda, the typically (though not always) carnivorous bipedal dinosaurs featuring the famous dinosaurs *Tyrannosaurus rex* and *Velociraptor*, and the Sauropoda, the long-necked dinosaurs featuring the well-known *Brachiosaurus*. On the other side of the phylogenetic tree, the three main subgroups represented within Ornithischia are the Thyreophora, Marginocephalia, and Ornithopoda. These three ornithischian subgroups are subdivided further for greater specificity. Thyreophora contains the clades Stegosauria, the dinosaurs with a row of dorsal plates on their backs such as *Stegosaurus*, and Ankylosauria, the armored-plated dinosaurs featuring *Ankylosaurus*. Marginocephalia contains the two clades of dinosaurs represented by horns, frills, and domed heads, the Ceratopsians and Pachycephalosaurians, represented by the well-known *Triceratops* and *Pachycephalosaurus*, respectively. Ornithopoda is represented by the crested and non-crested duck-billed dinosaurs featuring *Parasaurolophus* and *Edmontosaurus*. The focus

of the present research is within the group Ornithischia, the clade Ornithopoda, and the family Hadrosauridae.

The ornithopods were a group of herbivorous dinosaurs that lived from the Jurassic to the end Cretaceous extinction across every present-day continent (Brett-Surman, 1997). The name of the clade was created by Othniel Marsh in 1881 and was derived from Latin, meaning "bird-feet," due to their three-toed foot shape resembling that of a bird and a walking style on their toes (Brett-Surman, 1997). The ornithopods are not directly related to present-day birds, because their pre-pubic bone hip structure projecting forward and away from the midline of the body, in contrast to the fused and midline oriented pubic bone of theropod dinosaurs and birds. The ornithopods varied in size and stance, ranging from small (less than 1 meter tall, and 2 meters long) to large (7 meters tall, and 20 meters long) and bipedal to quadrupedal. The clade was highly specialized for herbivory in the form of their teeth structure and feeding style; they had multiple highly specialized tooth rows, called a dental battery, that would shed and replace teeth when needed, cheek pouches, and the first mastication (chewing) seen in dinosaurs (Brett-Surman, 1997). The ornithopods are subdivided into numerous families that began appearing throughout the middle and late Mesozoic. Listed in order of appearance in the fossil record, these families are the heterodontosaurids, hypsilophodontids, dryosaurids, camptosaurids, tenontosaurids, iguanodontids, and hadrosaurids. The history of ornithopods and paleontological research is rich; *Iguanodon* was the second dinosaur ever to be discovered and described (Mantell, 1825) and numerous taxa have since been documented.

The hadrosaurid ornithopods were one of the most diverse and abundant dinosaurian clades of the Late Cretaceous in Eurasia, North and South America, and

Antarctica (Horner et al., 2004; Prieto-Marquez, 2010a: Prieto-Marquez, 2010b). They are referred to as the "duck-billed" dinosaurs because the maxilla and dentary bones of the mouth form a wide, flat structure that resembles a duck's bill in some species. The exact shape, size, and morphology of the bill changes immensely between taxa. The hadrosaurids are further divided into two subfamilies: the hollow-crested Lambeosaurinaes and the non-crested and solid crested Saurolophinae (Prieto-Marque, 2010a, 2010b). The Brachylophosaurini tribe (Gates et al. 2011), originally Maiasaurinae (Horner, 1992), falls into the latter of these two subgroups. Brachylophosaurinis are prominently found in Montana and are currently represented in four accepted unique and stratigraphically different taxa (McFeeters et al., 2021):

1. *Probrachylophosaurus bergei*: lower Judith River Formation (Freedman Fowler and Horner, 2015)

2. *Brachylophosaurus canadensis*: upper Judith River Formation (Sternberg, 1953; Prieto-Marquez, 2005, 2007; Murphy et al., 2007)

3. *Ornatops incantatus*: Judith River Formation of Montana and Menefee Formation of New Mexico (McDonald et al., 2021)

4. *Acristavus gagslarsonoi*: lower Two Medicine Formation (Gates et al., 2011)

5. *Maiasaura peeblesorum*: upper Two Medicine Formation (Horner and Makela, 1979; Horner et al., 2001; McFeeters et al., 2021)

The taxon *Brachylophosaurus goodwini* (Horner, 1988) from the Judith River Formation has been considered a junior synonym of *Brachylophosaurus canadensis* (Prieto-Marquez, 2005) but further study is being reviewed for the validity of relationship to this clade (Freedman-Fowler and Horner, 2015). The newly found taxon of

Brachlophosaurini, *Ornatops incantatus*, is being reviewed as fitting in a trichotomy with *Probrachylophosaurus* and *Brachylophosaurus*, with *Maiasaura* and *Acristavus* as successive forms (McDonald et al., 2021). The phylogenetic position of *M. peeblesorum* can be seen in Figure 4.1.
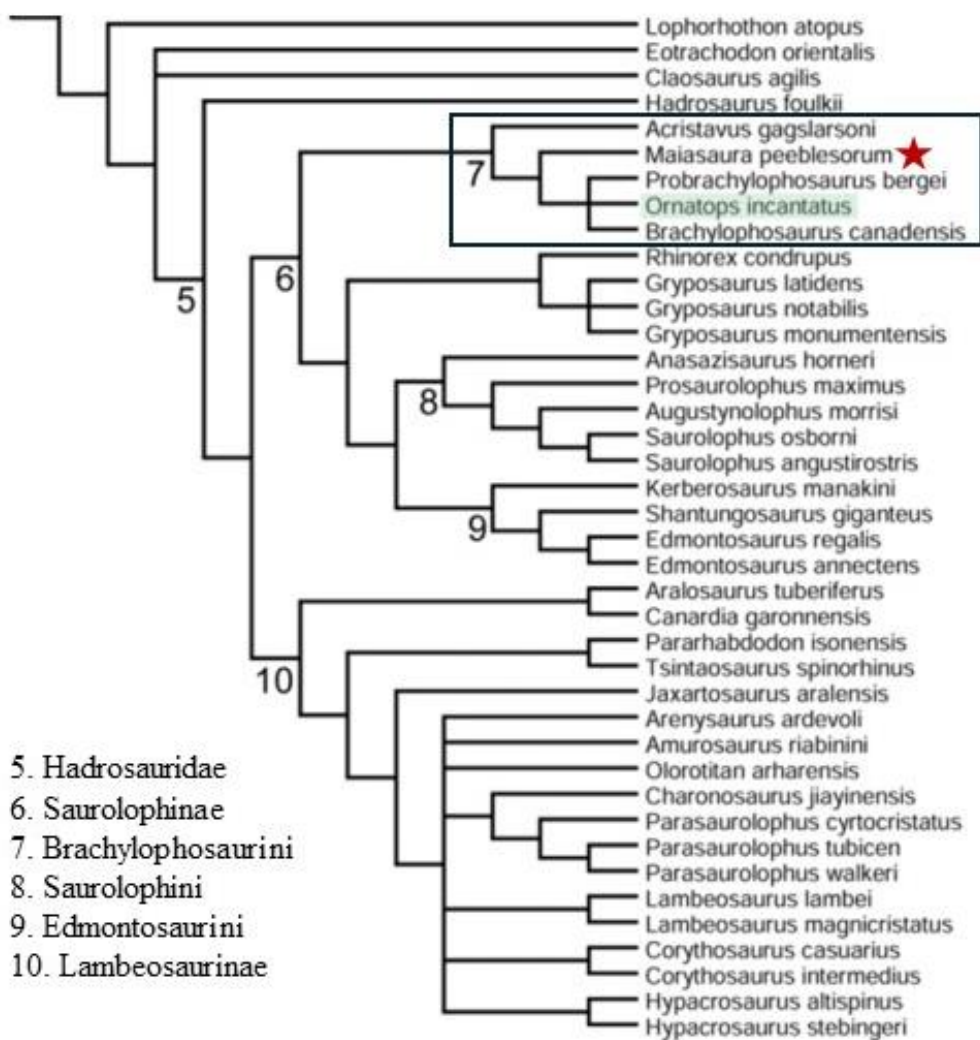
Figure 4.1 Phylogenetic tree of Hadrosauridae taxa created by McDonald et al. (2021) showing the position of the newly described *O. incantatus*. The relationship between *M. peeblesorum* (indicated by the star) and other members of Hadrosauridae can be seen. Edited from McDonald et al. (2021).

4.3. DESCRIPTION

The following sections give a brief description of the osteological characteristics of the cranium and ecological behaviors of *M. peeblesorum*.

4.3.1. Skull. The classification of genera of hadrosaurs is very specific because they were highly diverse. Throughout the Late Cretaceous hadrosaurs were abundant and estimated to comprise up to 75% of fossilized assemblages (Brett-Surman, 1979). The distinction between taxa stems almost entirely from cranial elements (Prieto-Marquez, 2007), since most hadrosaurs have very similar post-crania bodies plans (Brett-Surman, 1979) and the absence of morphological studies focusing on the post-crania anatomy (Prieto-Marquez, 2007). Horner and Makela (1979) set the crucial precedence for the differences of *Maiasaura peeblesorum* from other related hadrosaurids. The most distinguishing feature of *M. peeblesorum* is the short, solid, transversely oriented, and dorsally concave crest-like structure formed at the contact of the nasals, frontals, and prefrontals situated slightly posteriorly between the orbits (Horner and Makela, 1979 Horner 1983; Prieto-Marquez and Guenther, 2018; McFeeters et al. 2021). Surprisingly, the sister-taxa of *M. peeblesorum* do not record a further gradual developed *Maiasaura*-like crest, one of similar morphology, or a crest at all. The skull of *Acristavus gagslarsoni* records no cranial crest (Gates et al., 2011) and the skull of *Brachylophosaurus canadensis* has a solid, flat paddle shaped nasal crest that projects posteriorly across the dorsal skull roof (Freedman Fowler and Horner, 2015). *Probrachylophosaurus* bergi represents an intermediate and transitional stage of nasal morphology between *A. gagslarsoni* and *B. canadensis* that is represented by a small, triangular and posteriorly oriented nasal crest that slightly overhangs the supratemporal fenestrae. This crest is similar to the morphology

seen in that of younger ontogenetic stages of *B. canadensis* (Freedman Fowler and Horner, 2015). Furthermore, *Ornatops incantatus* is believed to be an intermediate stage between *P. bergi* and *B. canadensis*, since it has a posteriorly expanded nasofrontal suture that is indicative of a transversely elongated nasal crest that posteriorly overhangs the dorsal surface of the skull. However, the full extent of this crest is not preserved (McDonald et al., 2021).
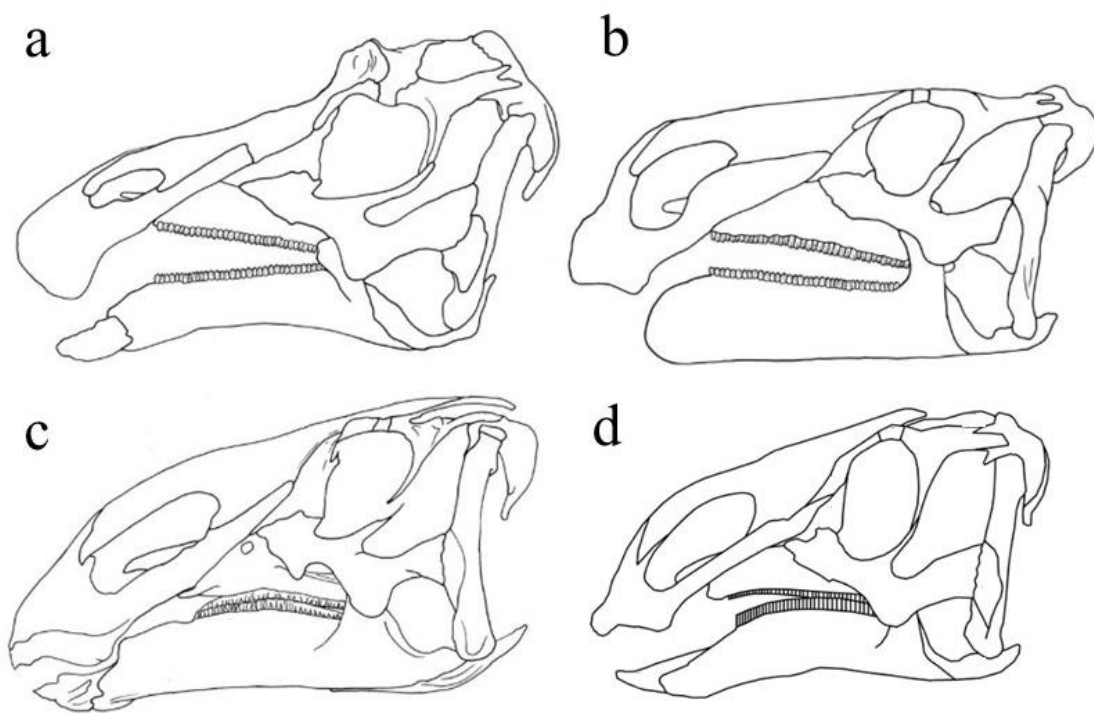
Figure 4.2 Line drawings of select Brachylophosaurini taxa including (a) *Maiasaura peeblesorum* TCMI 2001.89.2, (b) *Acristavus gagslarsoni* MOR 1155, (c) *Brachylophosaurus canadensis* (MOR 794), and (d) *Probrachylophosaurus bergei* (MOR 2919). Note the transverse-oriented ridge-like nasal crest in *M. peeblesorum* compared to the longitudinal, plate-like crest seen in *B. canadensis* and *P. bergei* and the non-crested skull of *A. gagslarsoni*. Figure edited from Gates et al. (2011) and Freedman Fowler and Horner (2015).

Additionally, the skull of *M. peeblesorum* has characters that further distinguish it from other Brachylophosaurini taxa (Figure 4.3). The anteriormost extent of the premaxilla is defined by an edentulous bill that has a lateroventrally deflected border, which is a common trait observed in lambeosaurines (Horner and Makela, 1979). Short narial openings are located on the snout anteriorolaterally to the elongated nasal bones that provide the extensively elongated facial region anterior to the orbits and transverse crest. This region dorsally overlies a long, shallow maxilla and elongated, thick dentary bones comprising the mouth region. An anterior maxillary process and notch is present in *M. peeblesorum*, as is present in all saurolophines. The predentary is wide and shallow with evenly spaced and round denticulate processes around the anterior edges. Between the maxilla and dentary, lies the highly specialized dental battery identified in ornithopods (Brett-Surman, 1997). Posterior to the nasal is the aforementioned distinctive crest formed at the concave boundary between the nasal and frontal bones. The frontal bones widen proportionately and thicken, relative to their length, throughout ontogeny (McFeeters et al., 2021). The orbits are dorsoventrally elongated and wide orbits, as is typical for ornithopods. Posterior to the orbits a thin, long, steeply angled quadratojugal process of the jugal is characteristic of *M. peeblesorum* (Horner and Makela, 1979; Prieto-Marquez and Guenther, 2018; McFeeters et al., 2021).

4.3.2. Braincase. The braincase of *M. peeblesorum* morphologically resembles that of other hadrosaurs (Evans, 2005; Evans et al., 2009; Prieto-Marquez, 2010) and contains the same osteological framework seen across all of Dinosauria (Giffin, 1989; Rogers, 1998; Balanoff et al., 2009; Carabajal, 2012; Sobral et al., 2012; Cerroni and Carabajal, 2019; Sakagami and Kawabe, 2020; Ballell et al., 2021; Knoll et al., 2021; Button and Zanno,

2023). Functionally, the braincase is designed to protect and house the brain, while also allowing cranial nerves and various anatomy to traverse from the brain to their region of interest.

The floor of the braincase, referred to as the basicranium, is composed of the anteriormost parasphenoid-basisphenoid complex, and posteriormost basioccipital (Figure 4.4). As observed in numerous *M. peeblesorum* specimens of varying ontogenetic stages (McFeeters et al., 2021), the contact between the parasphenoid and basisphenoid is indistinguishable, as similarly visible in other hadrosaurs (Prieto-Marquez, 2010). Of the two osteological elements, the parasphenoid is the anteriormost and forms a rostrally protruding subrectangular to pointed cultriform process, in lateral view, that lies anteroventrally to the olfactory apparatus (Figure 4.4a-b). The basisphenoid is the posteriormost element of the fused complex and laterally contacts with the laterosphenoid and prootic bones and dorsally with the basipterygoid process. In ventral view, the basisphenoid has an hourglass shaped, while in lateral view it appears as a thick wedge-shaped structure, anteriorly thinning slightly until the protrusion of the parasphenoid (Figure 4.4f, a-b, respectively). The basipteygoid processes are two subrectangular extensions, in lateral view, that are medially bilaterally symmetrical protruding ventrolaterally from the basicranial region of the braincase. The degree of ventrolateral projection is slightly varied between ontogenetic stages (McFeeters et al., 2021). A smaller, similarly shaped, flattened, posteroventral protrusion, called the interbasiptergyoid process, is located slightly posterior to the two basipterygoid processes on the midline that separates the processes. The paired alar processes are flat, large portions of the basisphenoid that project posterioventrally. Foramina for the ventralmost extent of the
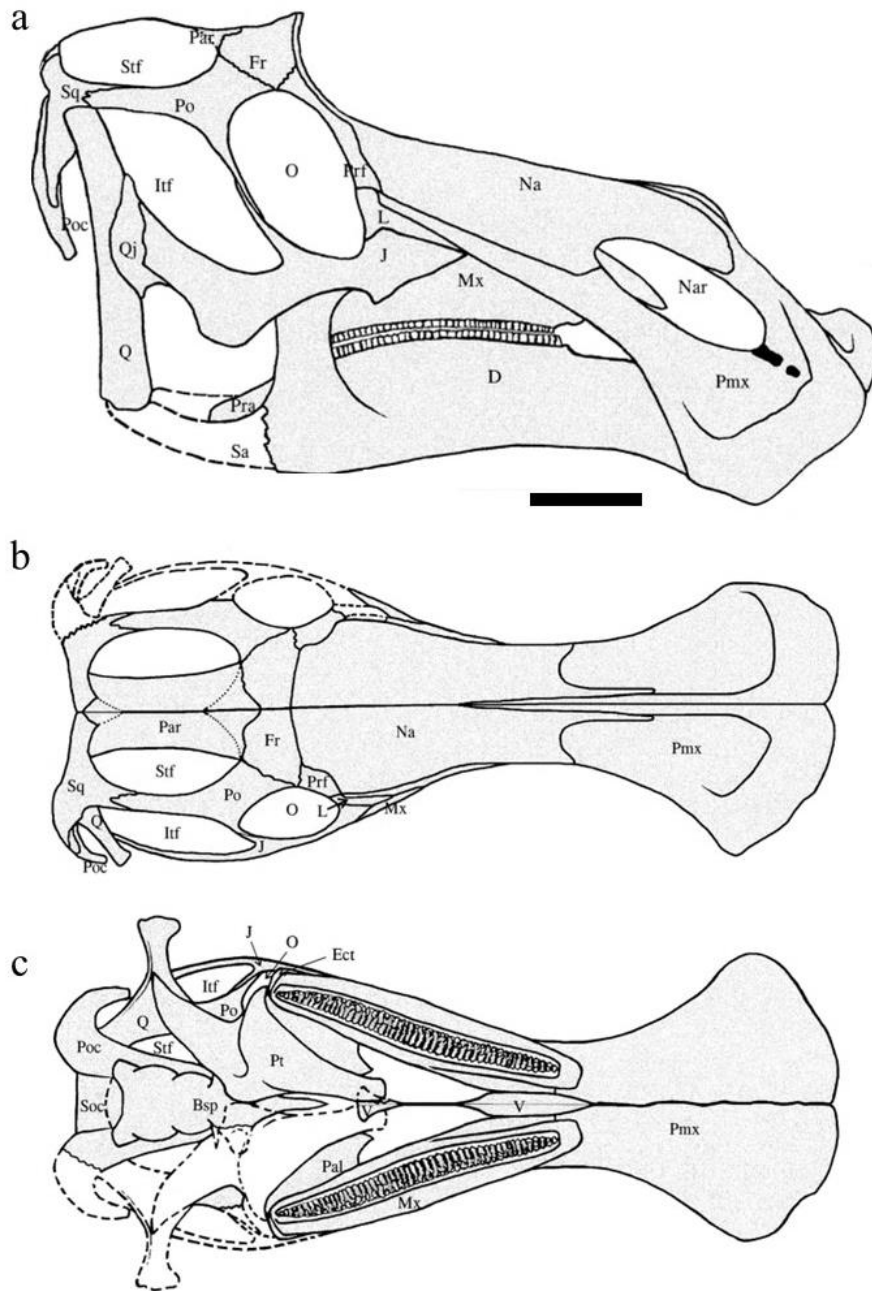
Figure 4.3 Labelled skull of *M. peeblesorum* specimen OTM F138 in (a) lateral, (b) dorsal, and (c) ventral views. Figures edited from an unpublished thesis by David Trexler (1995). Dashed lines indicate missing bones from the specimen. Scale bar = 100 mm. Figure 4.3 cont. Abbreviations: Bsp = basisphenoid; D = dentary; Ect = ectopterygoid; Fr = frontal; Itf = infratemporal fenestra,; J = jugal; L = lacrimal; Mx = maxilla; Na = nasal; Nar = narial opening; O = orbit; Par = parietal; Pal = palatine; Pmx = premaxilla; Po = postorbital; Poe = paroccipital process; Pra = prearticular; Prf = prefrontal; Q = quadrate; Pt = pterygoid; Q = quadrate; Qj = quadratojugal; Sa = surangular; Soc = supraoccipital; Sq = squamosal; Stf = supratemporal fenestra; V = vomer.

internal carotid arteries can be seen on the ventral surface of the basisphenoid, directly posteriodorsal to the basipteygoid process and situated lateroventral to the alar process so that alar process hides the foramen in lateral view. The posteromost region of the basicranium, and ventralmost region of the braincase, is the basioccipital. A distinct fused line between the posterior basisphenoid and anterior basioccipital can be seen on the ventral surface of most specimens as a V-shaped contact (Figure 4.4f; McFeeters et al., 2021) forming the anterior and posterior halves of the basal tubera. The basioccipital has a rounded square shape and is situated in contact with the basisphenoid anteriorly and the exoccipitals dorsally. The posterior region of this feature, in addition to the exoccipital-opisthotic bone complex and ventral margin of the foramen magnum, forms a portion of the lobe-shaped occipital condyle.

Anteriorly to posteriorly, the presphenoid, orbitosphenoid, laterosphenoid, prootic, exoccipital-opisthotic complex, and supraoccipital make up the transversely median region of the braincase including portions of the anterior, lateral, dorsal, and posterior regions (Figure 4.4; Horner, 1983; McFeeters et al., 2021). Foramen for CN II-V and VII-XII laterally exit the braincase through these bones or along the contact between these bones and the portion of the basicranial in that respective region. The presphenoid occurs is a thin, plate-like bone situated ventral to the frontals and anteriodorsal to the orbitosphenoid. Functionally, the presphenoid helps protect the olfactory apparatus, as it composes the lateral and ventral walls of the region, in combination with the dorsal nasal and frontal bones. Posterior to the presphenoid, ventral to the frontals, anterior to the laterosphenoid, and dorsal to the parabasisphenoid structure, the orbitosphenoids are paired bones that come in contact with each other posterior to the olfactory apparatus. In progressive
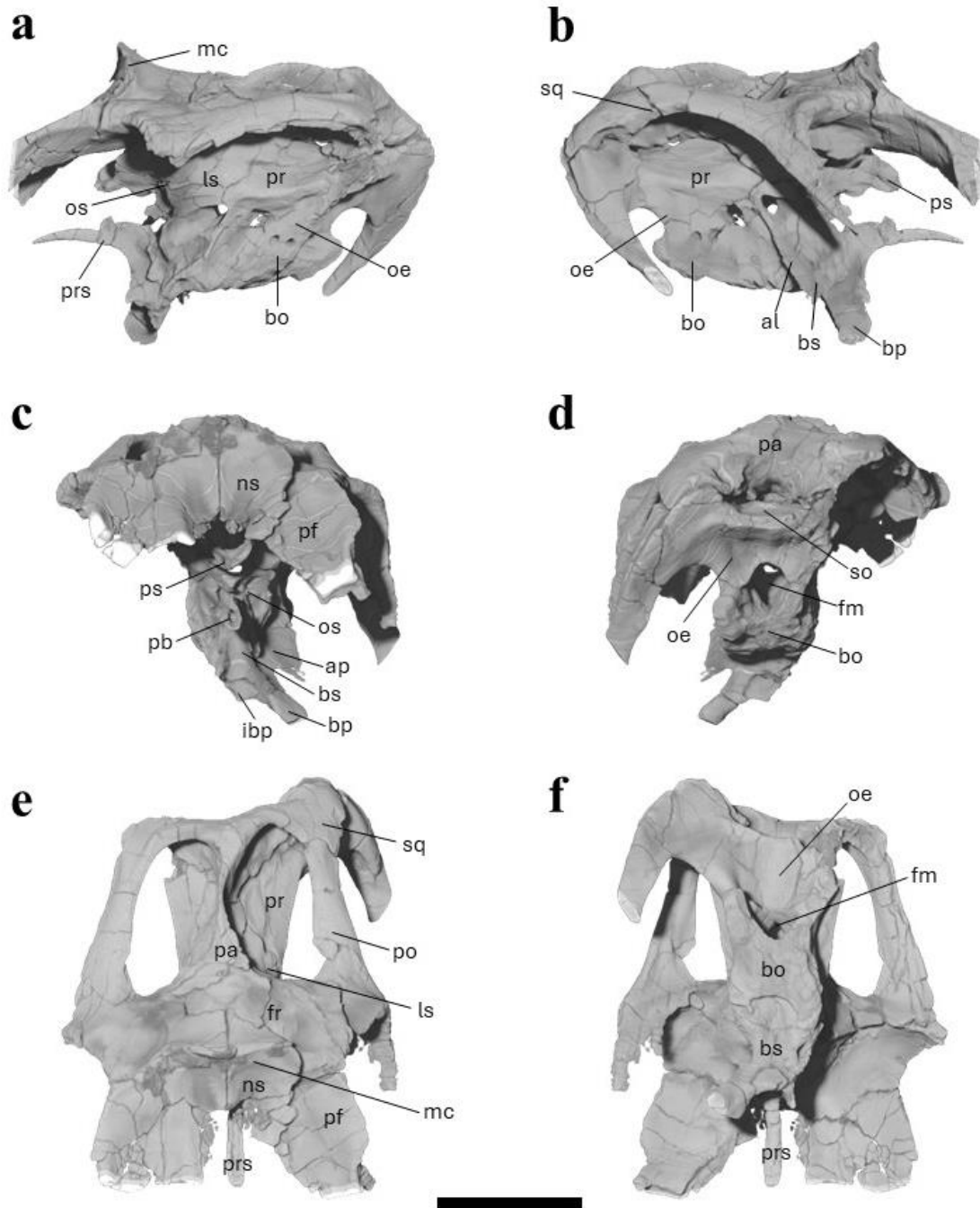
Figure 4.4 Labelled bones of the braincase on *M. peeblesorum* OTM F138. Scale bar = 100 mm. Abbreviations: ap = alar process; bo = basioccipital; bp = basipterygoid process; bs = basisphenoid; eo = exoccipital-opisthotic; fm = foramen magnum; fr = frontal; ibp = interbasipterygoid process; ls = laterosphenoid; mc = *Maiasaura* crest; ns = nasal;; os = orbitosphenoid; pa = parietal; pf = prefrontal; po = postorbital; pr = prootic; prs = parasphenoid; ps: presphenoid; so = supraoccipital; sq = squamosal.

ontogenetic stages, the orbitosphenoid can occur with increasing degrees of fusion to the frontals and laterosphenoids (McFeeters et al., 2021), but morphologically appears as thin and square-to-rectangular shaped, in lateral view, in all growth ages. McFeeters et al. (2021) noted that there was not a distinct and separate foramen for CN IV in the *M. peeblesorum* specimen preserved in this region (ROM 60261) that is seen in other hadrosaurs, but rather a small, horizontal groove that is ventrally truncated by the foramen for CN II. They attribute this to possible taphonomic and preservational conditions because there is a crack running through the region. This same cracking is the likely cause of this missing anatomy since the braincase of OTM F138 does have a separate foramen for CN IV. The paired laterosphenoid bones are situated posterior to the orbitosphenoid, dorsal to the basisphenoid, anterior to the prootic, and ventrolaterally to the parietals (Figure 4.4a-b). It is roughly triangular in shape, with the broad portion seen dorsally and tapered end ventrally, with a process overhanging the basisphenoid, and is bordering the foramina for CN III (anteriodorsally), CN V (anteriorly), and CN VI (anteriodorsally). An anteriorly traversing horizontal groove from the foramen for CN V, specifically for the ophthalmic branch (CN V_1), has been noted on the lateral face of the laterosphenoid (McFeeters et al., 2021). Posterior to the laterosphenoid, are the paired prootic bones which comprise the middle portion of the lateral wall of the braincase (Figure 4.4a-b). The dorsoventrally oriented approximately triangled shaped structure is also in contact with the parietal dorsally, exoccipital-opisthotic complex posteriorly, and the basisphenoid ventrally. Ventral to the prootic and posterior to the contact with the exoccipital-opisthotic complex, a pocket shaped structure is seen in all examined braincases of *M. peeblesorum* and *Brachylophosaurus* (McFeeters et al., 2021). Also present in the prootic region are CN VII

and the vestibular fenestra for the endosseous labyrinth complex. The exoccipital-opisthotic complex is fused in all described braincases of *M. peeblesorum*, and therefore referred to as one bone structure, conventionally the exoccipitals (Evans, 2009). The parietal, squamosal, and supraoccipital are situated posterodorsally along the braincase and the basioccipital is oriented ventral to the exoccipital-opisthotic complex (Figure 4.4). The metotic foramen and CN XII are located on the lateral walls of exoccipital on each side of the foramen magnum. The foramen magnum occurs as a large, oval shaped opening on the posteriormost surface of the braincase and is formed by the basioccipital and exoccipital which makes up the ventral and dorsolateral margins, respectively, of the foramen (Figure 4.4d). The supraoccipital, a differentially thick plate-like bone, forms the dorsal margin of the foramen magnum. A ridge that overhangs the foramen magnum is formed by the contact between the supraoccipital and exoccipital, but the exact definition of the ridge is variable between specimens, likely due to a combination of ontogeny and taphonomic processes (Figure 4.4d; McFeeters et al., 2021).

For *M. peeblesorum*, the dorsal roof of the braincase, anterior to posterior, is comprised of the frontals, parietals, and supraoccipital (Figure 4.4e). The frontals are situated directly dorsal to the cerebrum region of the endocrania cavity, as the ventral surface of the bones is where vascularization for various ornithopod taxa has been noted previously (Evans, 2005; Evans et al., 2009). Anterior to these paired and connected bones, a broad and continuous contact with the nasal and prefrontals to form the *Maiasaura*-crest is seen in dorsal and lateral view (Figure 4.4e, a-b, respectively). Posteriorly, the frontals contact with both the postorbitals and parietals however, the postorbitals are situated posterolateral to the frontals and anterior to the squamosals (Figure 4.4e). Forming the

posteriormost region of the dorsal roof of the neurocranium cavity is the parietals; the paired bones connect medially to form a triangular shaped platform, and individually appear as a plate-like element with laterally expanded anterior and posterior ends. At its anterior end, it is in contact with the frontal and postorbital bones, while at its posterior end, the bone thins and is wedged between the squamosals. The paired squamosal bones form the posterior margins and posterolateral corners of the dorsal braincase and skull roof (McFeeters et al., 2021). Anterior to the squamosals are the supraoccipitals, which form the dorsal, lateroposterior, and posterior encasing of the endocrania cavity.

        4.3.3. Ecological Characteristics. *Maiasaura peeblesorum* were large in size, growing up to 7 meters long (Horner et al., 2000) and having a body mass of up to 4 metric tons (Wosik et al., 2019). They were also herbivores, with studies on coprolite samples showing they ate angiosperms, grasses, and recurringly, possibly seasonally, rotting conifer wood (Chin, 2007). *M. peeblesorum* can be interpreted as scale-covered organisms, like their hadrosaur relatives, unlike some small theropods. Skin impressions of hadrosaurs, including *Corythosaurus* (Brown, 1916), *Edmontosaurus* (Manning et al., 2009), and *Brachylophosaurus* (Murphy et al., 2007), have been recorded in the fossil record (Bell, 2014). However, skin impressions have never been documented for hatchling or nestling hadrosaurs (Bell, 2014). *M. peeblesorum* would have walked bipedally during youth but shifted to quadrapedalism during adulthood. A study conducted by Cubo et al. (2015) on the biomechanics of exostoses pathologies on numerous tibiae of *M. peeblesorum* was conducted to understand the biomechanics of the organism. Their findings showed that the pathologies resulted from overexertion rather than from predator evasion, suggesting that

M. peeblesorum underwent a shift in their posture through ontogeny from perinatal bipedalism to adult quadrupedalism (Dilkes, 2001; Cubo et al., 2015).

Assemblages of *M. peeblesorum* dominate Lithofacies 4 of the Two Medicine Formation (Horner et al., 2001) with the approximate geologic age of 75.4 Ma (Rogers and Swisher, 1996; Roger, 1998). Two specific sites in this lithofacies, the Willow Creek Anticline (also known as Egg Mountain) and the Badger Creek locality, record extensive bonebeds filled with the remains of each ontogenetic stage of life of *M. peeblesorum* from eggs to somatically mature adults (Horner and Makela, 1979; Horner and Weishampel, 1988; Horner, 1982; Varricchio et al., 1997, 1999; Horner et al., 2000, 2001). The discovery of well represented ontogenetic stages has allowed for numerous and comprehensive studies on the ontogenetic series of *M. peeblesorum* to be conducted to better understand the growth rates, paleoecology, survival rates, and biomechanics of the organism.

4.4. ONTOGENETIC SIGNFICANCE

Ontogenetic growth stages for *Maiasaura peeblesorum* were defined by Horner et al. (2000) on the basis of body size, osteohistological data gathered from femora, and the association of each specimen to other eggs, nests, and/or adults. These stages are small nestling, large nestling, small juvenile, large juvenile, subadult, and adult, and their approximate sizes are represented in Figure 4.3.

Femur lengths of small nestlings show they were approximately 45 cm in length and grew to be approximately 7 meters in length in adulthood (Horner et al., 2000). Microanalysis on the tibiae of *M. peeblesorum* showed the taxa reached a 95% asymptotic
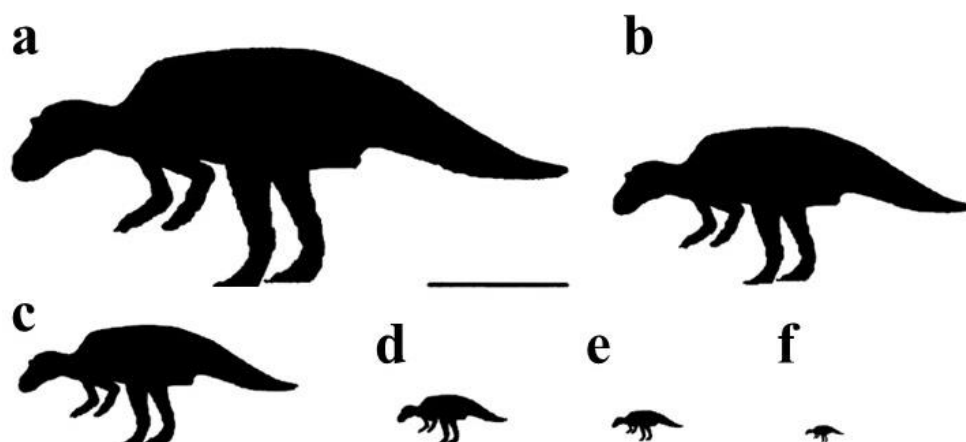
Figure 4.5 Comparison of approximate body sizes of the six growth stages of *M. peeblesorum* observed by Horner et al. (2000) through osteohistologic features: (a) adult (~7 meters), (b) subadult, (c) large juvenile, (d) small juvenile, (e) large nestling, (f) small nestling (~45 centimeters). Scale bar = 2 meters. Edited from Horner et al., 2000.

body mass around the age of 9 years old (Woodward et al., 2015) based on the fossils from a mass bone bed in the Willow Creek Anticline, described by Varricchio and Horner (1993). An underrepresentation in tibia specimens from *M. peeblesorum* yearlings (deemed as tibia lengths less than 30 cm) was observed, suggesting that the young had very low mortality rates and abnormally high survival rates (Woodward et al., 2015; Wosik et al., 2020). These rates likely led to a higher presence of youth and is attributed to the species exhibiting social behaviors and residing in protective herds, as seen from the mass bone beds (Varrichio and Horner, 1993). Furthermore, myologoical studies of the presence of muscles scarring in nestling *M. peeblesorum* provided an unprecedented, although limited, view into ontogenetic developmental changes of muscles in hadrosaurs (Dilkes, 2000). Dilkes (2000) found a surprisingly large number of muscle scar remnants throughout the nestlings' bones despite the incomplete ossification of the bones. Muscle scars on the

nestling correlate with the prominent scar location on adult specimens; however, taphonomic processes probably limited ontogenetic patterns in myology (Dilkes, 2000). These studies were influential in describing the developmental and morphological changes observed in *M. peeblesorum* and could be applied to greater understanding of ontogenetic growth in Late Cretaceous hadrosaurs and other taxa in Dinosauria.

5. MATERIALS AND METHODS

5.1. BRAINCASES

The three *Maiasaura peeblesorum* braincases (OTM F138, TMDC F139, and TMDC F140) used for this study come from the Upper Cretaceous Two Medicine Formation in Teton County, Montana. They were all recovered geographically close to the locality where the holotype specimen (PU 22405) was discovered. All three braincases used in this study are housed at The Montana Dinosaur Center in Bynum, Montana.

The largest braincase, OTM F138, is a nearly complete and well-preserved braincase that has only undergone minor taphonomic deformation and fracturing. Furthermore, all the bones of the braincase (see Section 4.3.2 for list and description of bones), are present and well defined (Figure 4.4), allowing for easy segmentation of the endocranial cavity. The skull of the specimen is missing the left surangular, a portion of the left pterygoid, the left paroccipital process, the left jugal the encloses the ventral portion of the orbit, right jugal, right lacrimal, and right quadrate. The OTM F138 specimen was discovered and collected by John Brandvold Jr. in 1990 from the M1 site, which is located approximately 20 kilometers west of Pendroy, Montana. This site is also 31 km northwest of where the holotype of *Maiasaura peeblesorum* (PU 22405) was discovered by Laurie Trexler in 1978. The M1 site contained only the *M. peeblesorum* OTM F138 specimen, which included numerous disarticulated bones and bone fragments that were reconstructed to form the majority of an adult *M. peeblesorum*. The full composite skeleton (Figure 5.1) was described in detail by Dave Trexler in an unpublished thesis (1995). OTM F138 was discovered in a sandstone lens that laterally tapered into a siltstone/mudstone layer. Argon-

argon dating of the stratigraphic units above and below the collection site was conducted by Rogers et al. (1993) and provided the geologic age between 79.2 and 74 mya for the OTM F138 specimen.
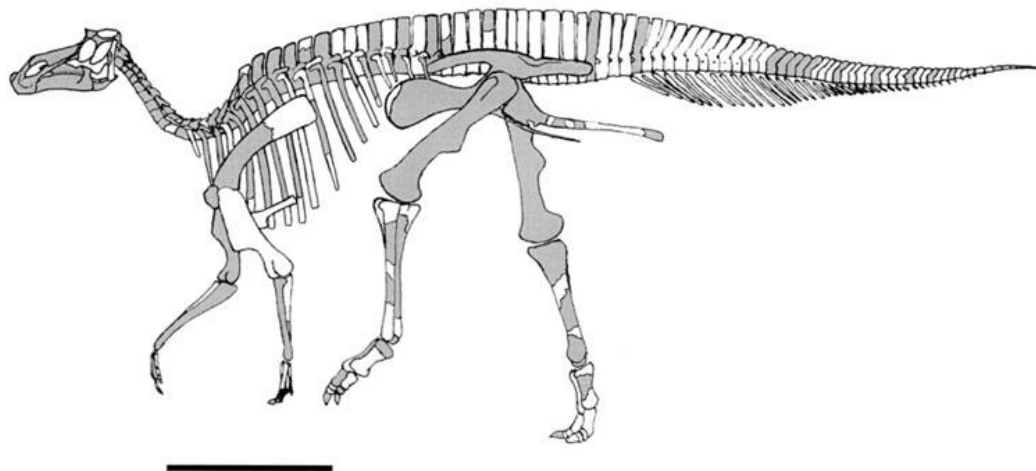
Figure 5.1 Composite skeleton in left lateral view of *Maiasaura peeblesorum* OTM F138 recovered from the M1 site outside of Pendroy, Montana. Missing portions are shown without shading in white. Scale bar = 1 meter. Edited from Trexler (1995).

The two smaller braincases, TMDC F139 (Figure 5.3) and TMDC F140 (Figure 5.4) were recovered in the Linster Quarry in the Upper Campanian strata of the Two Medicine Formation in Teton County, Montana. The Linster Quarry mass bone bed included numerous hadrosaurid materials that were all identified as *Maiasaura peeblesorum*, including five other braincases (see McFeeters et al., 2021) and TCMI 2001.89.2 (see Gates et al., 2011, Figure 2B), undescribed tyrannosaurid material, and the holotype of dromaeosaurid *Bambiraptor feinbergi* (Burnham et al., 1997, 2000; McFeeters et al., 2021). The two braincases were identified as *Maiasaura peeblesorum* based on a
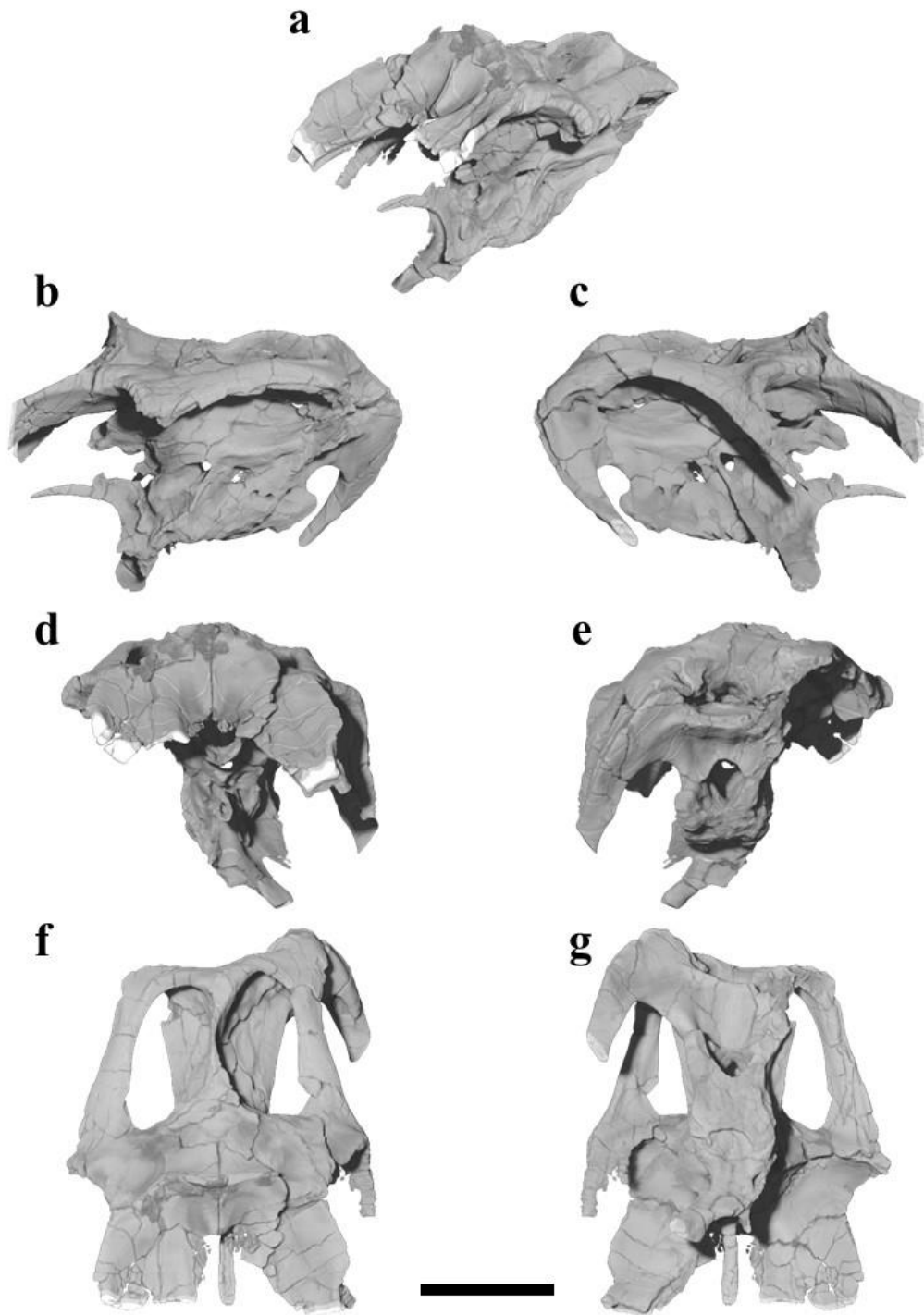
Figure 5.2 Digital models of the braincase and partial skull of OTM F138 in (a) left lateral oblique, (b) left lateral, (c) right lateral, (d) anterior, (e) posterior, (f) dorsal, and (g) ventral views. Scale bar = 100 mm.
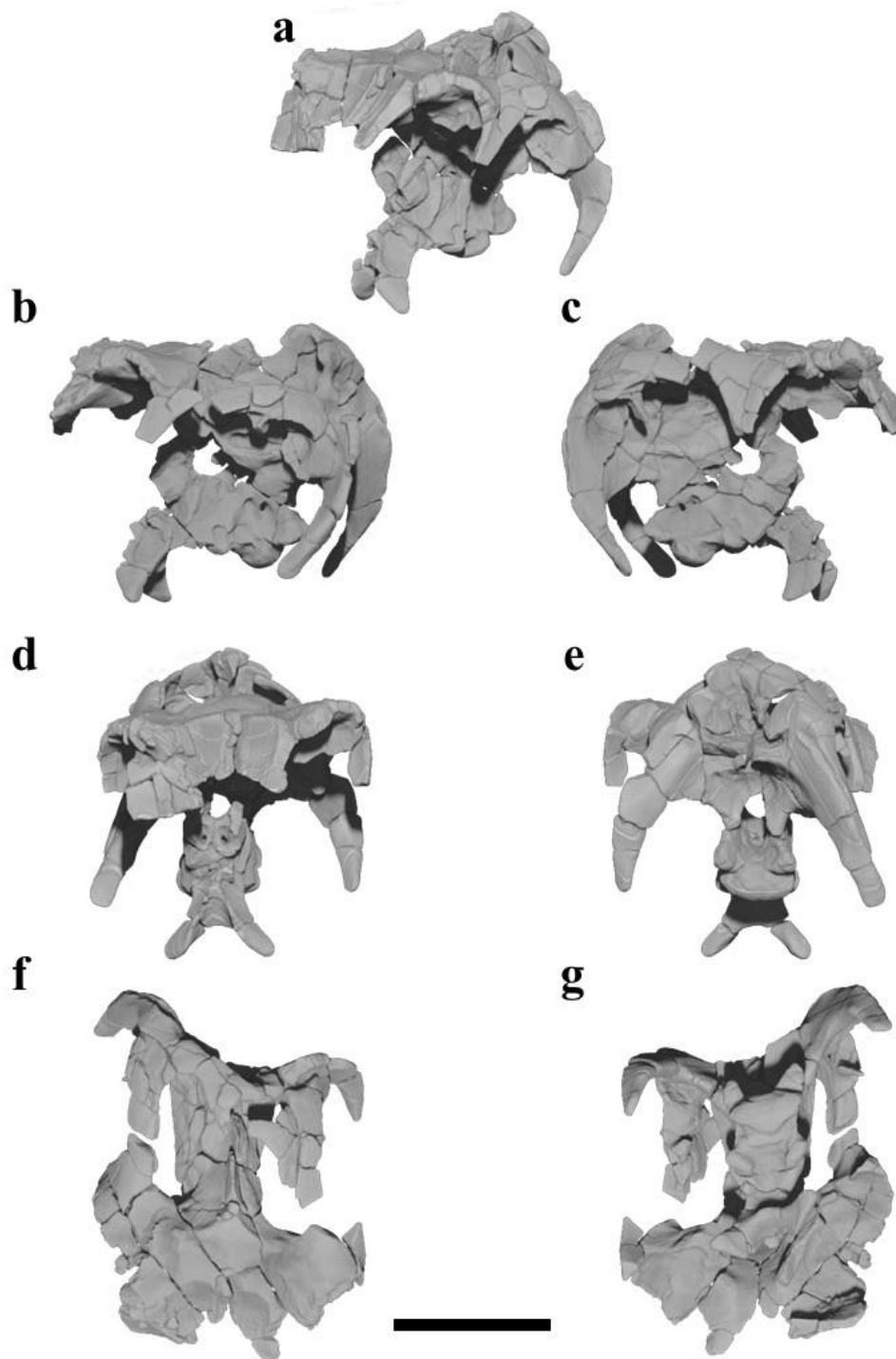
Figure 5.3 Digital model of the braincase and partial skull of TMDC F139 in (a) left lateral oblique, (b) left lateral, (c) right lateral, (d) anterior, (e) posterior, (f) dorsal, and (g) ventral views. Scale bar = 100 mm.

44
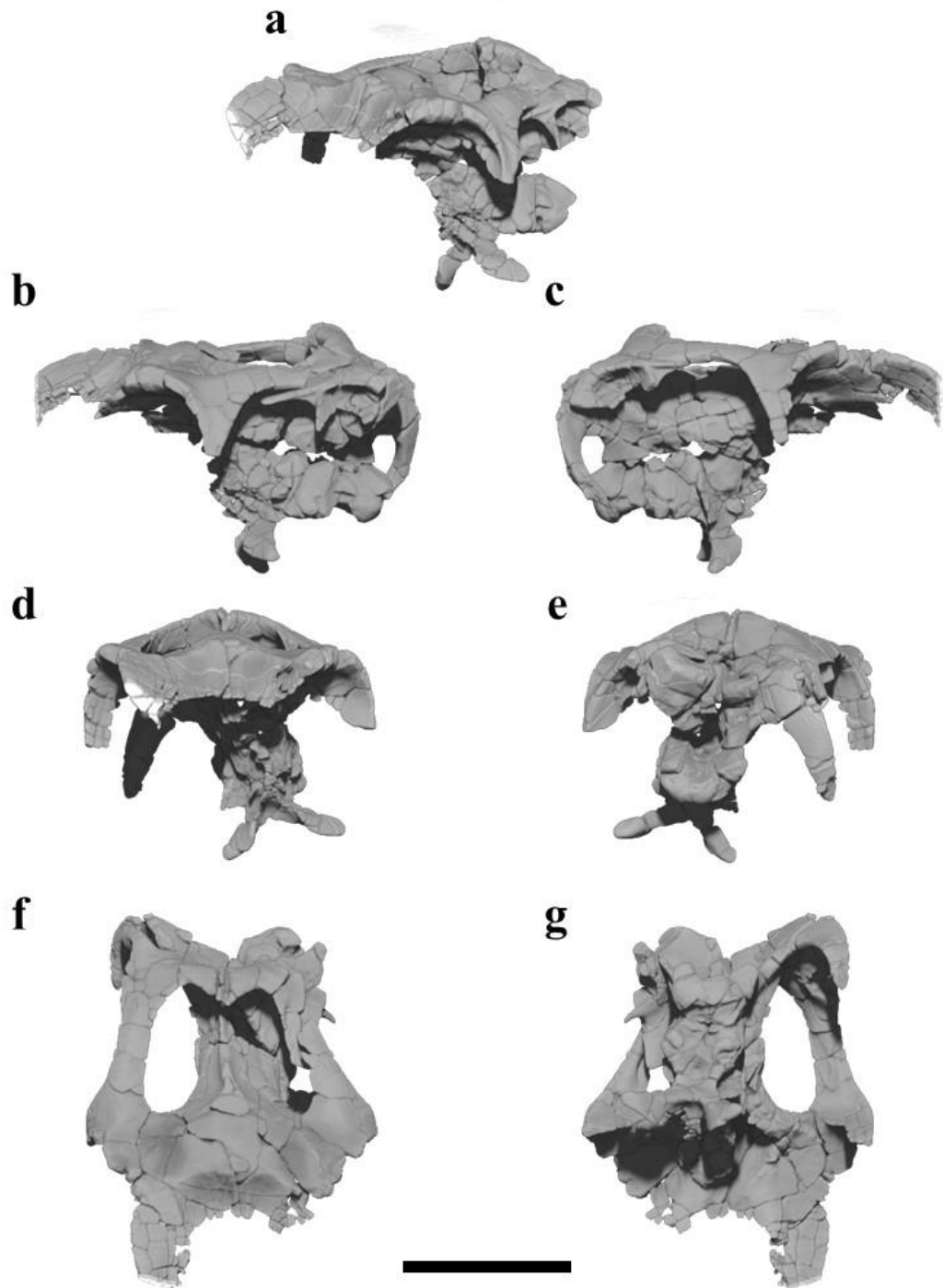
Figure 5.4 Digital model of the braincase and partial skull of TMDC F140 in (a) left lateral oblique, (b) left lateral, (c) right lateral, (d) anterior, (e) posterior, (f) dorsal, and (g) ventral views. Scale bar = 100 mm.
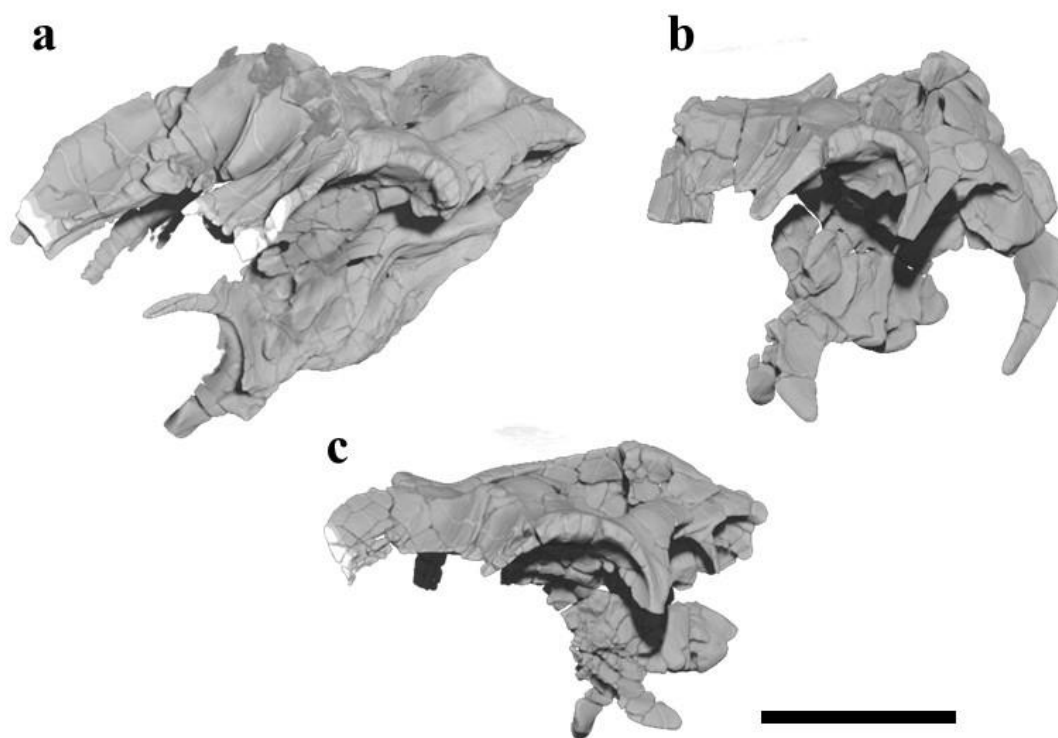
Figure 5.5 Comparison of braincase and partial skulls of (a) OTM F138, (b) TMDC F139, and (c) TMDC F140 in left lateral oblique view. Note the mature development and morphology of the *Maiasaura*-like crest in OTM F138 compared to the underdeveloped crest in TMDC F139 and TMDC F140. Scale bar = 100 mm.

transversely oriented crest that is present at the nasofrontal sutural contact for both specimens. However, the crest appears more prominent in TMDC F139 than in TMDC F140. Furthermore, evidence of secondary hadrosaurid taxa has yet to be found in the Linster Quarry mass bone bed (McFeeters et al., 2021). The two braincases themselves are poorly preserved with numerous bones missing and cracks traversing through the lateral walls of the braincase. TMDC F139 specifically appears to have undergone sever taphonomic deformation due to an apparent anteroposterior shortening of the braincase, and furthermore skull.

5.2. ENDOCRANIAL RECONSTRUCTION

The three skulls were CT-scanned using a GE Lightspeed VCT whole body CT scanner at the Benefis Teton Medical Center in Chouteau, Montana at a slice resolution of 5 mm. The scan data were then imported in ORS Dragonfly Version 2022.2 Build 1409 for segmentation and analysis of the endocranial body at Missouri University of Science and Technology. The endocranial body, each pair of cranial nerves, and the endosseous labyrinths were individually segmented as regions of interest (ROI) in Dragonfly. The different anatomical features were constructed as separate ROIs for simplicity of calculating volumes of the features after segmentation was completed. The process of segmentation included scrolling through the 2D CT scan slices and manually tracing the borders of the negative space that would have house the anatomical features. This was done slice by slice for the dorsal-ventral, anterior-posterior, and lateral window views of the CT scans to ensure proper segmentation of the features and correct identification of taphonomic features (i.e., from cracks or deformation), as ROIs. While time consuming, manual segmentation was preferred over 3D augmentations or training artificial intelligence to ensure accuracy. Once segmentation was completed, the ROIs were quantitatively measured on the 2D window views. All linear measurements of the cranial endocast (e.g., heights, widths, lengths, etc.) were made using the straight ruler tool, and all non-linear measurements (e.g., semicircular canals) were made using the curved ruler tool. All volumes (e.g., total endocrania, cerebral hemispheres, etc.) were calculated using the Multi-ROI Object Analysis tool.
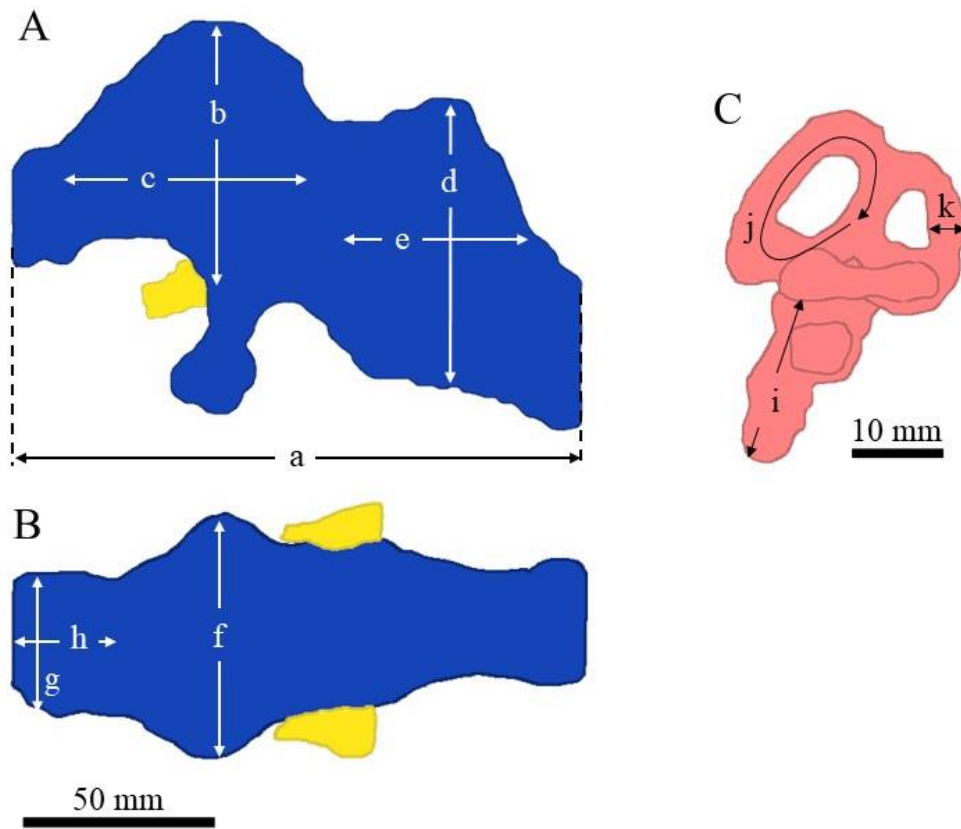
Figure 5.6 Depiction of the linear measurements taken from the reconstructed endocasts of *M. peeblesorum* in (A) lateral and (B) dorsal view of the endocranial cavity, and (C) lateral view of the endosseous labyrinth. Measurements taken are as follows: (a) total cranial endocast length; (b) cerebral hemisphere height; (c) cerebral hemisphere length; (d) cerebellum height; (e) cerebellum length; (f) cerebral hemisphere width; (g) olfactory bulb width; (h) olfactory tract length; (i) cochlear duct length; (j) semicircular canal length; (k) semicircular canal thickness.

5.3. FLEXURE

The cephalic and pontine flexures were measured based off a similar approach utilized by Hopson (1979) and Lautenschalger and Hübner (2013). The angles for both flexures were measured on the central-most CT slice of the endocranial cavity in 2D lateral view on Dragonfly. The cephalic flexure was measured as the angle between the

rostrocaudal axis of the forebrain and the oblique axis of the midbrain. The rostrocaudal axis of the forebrain traverses from the rostralmost to caudalmost extent of the cerebral hemispheres, and the oblique axis of the midbrain traverses from the caudalmost extent of the cerebral hemispheres and terminates at the rostralmost extent of the cerebellum. The pontine flexure was measured as the angle between the oblique axis of the midbrain and the rostrocaudal axis that traverses from the rostralmost extent of the cerebellum to the foramen magnum.
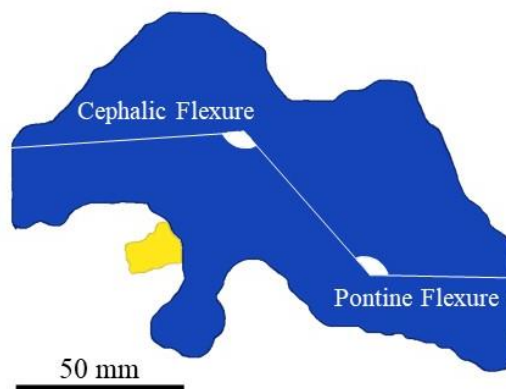
Figure 5.7 Depiction of the cephalic and pontine flexure measurements taken from cranial endocast of *M. peeblesorum.*

5.4. OLFACTION RATIO

The olfaction ratio was calculated as the ratio of the maximal width of the olfactory bulb to the maximal width of the cerebral hemispheres, using the methods established by Zelenitsky et al. (2009). The two sections were measured in dorsal view of the endocast on Dragonfly. This ratio was then logarithmically scaled for comparison to other ornithischian and saurischian dinosaurs, with a specific focus on saurolophines and lambeosaurines.

5.5. ENDOSSEOUS LABYRINTH AND HEARING FREQUENCIES

The calculation of the hearing frequencies of *Maiasaura peeblesorum* was conducted with the methods of Gleich et al. (2005), Walsh et al. (2009), and Evans et al. (2009) to allow for the broadest comparison across Ornithopoda. Each method utilizes different measurements to achieve the hypothesized attainable hearing frequency for the extinct taxa. For the method of Walsh et al. (2009), the length of the endosseous cochlear duct was measured (in mm) on both the left and right inner ears in lateral view on Dragonfly. These values were then scaled against the length of the basicranial, which was measured as the length of the basisphenoid and basioccipital, but not including the parasphenoid process, in ventral view on Dragonfly. This scaled cochlear duct value (SCD: Equation 1) were logarithmically scaled and used to calculate the best frequency range (BFR: Equation 2) and mean best hearing range (MBH: Equation 3) of *M. peeblesorum* using the equations of Walsh et al. (2009):

$$SCD = Log_{10}(\frac{endosseous\ cochlear\ duct\ length}{basicranial\ length}) \qquad (1)$$

$$BFR = (6104.3 * ECD) + 6975.2 \qquad (2)$$

$$MBH = (3311.3 * ECD) + 4000.8 \qquad (3)$$

For comparison, the values for the best frequency of hearing (BF: Equation 6) and maximum frequency of hearing (MF: Equation 7) were also calculated for each labyrinth using the equations of Gleich et al., (2005). Noteworthy is that this method was devised from the study of modern bird audiograms, therefore extrapolation errors have been noted by Gleich et al. (2005) to possibly occur when applying this method to extinct, large archosaurs. Recent dinosaurian endocranial studies have employed this calculation for testing the attainable hearing, therefore it was calculated in this study for the widest range

of auditory comparisons. In the Gleich et al. (2005) method, the basilar papilla length (L: Equation 5) is approximated since this is the anatomy responsible for the acquisition of the auditory sense and the structure is destroyed during taphonomic processes and is therefore not measurable in extinct taxa. The cochlear duct bony structure is the anatomy that would have housed the basilar papilla in life, therefore the basilar papilla is approximated to be two-thirds the length of the cochlear duct (Gleich et al., 2005):

$$L = \frac{2}{3}(endosseous\ cochlear\ duct\ length) \tag{5}$$

A two-thirds volumetric filling of the basilar papilla is approximated rather than a complete filling because the cochlear duct housed other soft-tissue structures alongside the basilar papilla, such as the lagenar macula and perilymphatic space (Wever, 1978; Gleich et al., 2005). From the approximated basilar papilla length (L), the best frequency of hearing (BF) and maximum frequency of hearing (MF) can be calculated using the equations derived by Gleich et al. (2005):

$$BF = 5.7705e^{(-0.25*L)} \tag{6}$$

$$MF = (1.8436 * BF) + 1.026 \tag{7}$$

Another method employed by Evans et al. (2009) took the methods derived by Gleich et al. (2005) and without scaling the cochlear duct length to find an approximate length of the basilar papilla. Therefore, the altered equations utilized were:

$$BF = 5.7705e^{(-0.25*CD)} \tag{8}$$

$$MF = (1.8436 * BF) + 1.026 \tag{9}$$

where CD is equal to the measured length of the cochlear duct. This alternative to Gleich et al. (2005) assumes the basilar papilla is related to the length of the cochlear duct in reptiles (Baird, 1970; Wever, 1978; Manley, 1990; Gleich and Manley, 2000; Gleich et al.,

2005) however, the exact length correlation between the two is unknown. As these calculation methodologies were employed by a study focusing on ornithopod sensorineural calculations, this calculation will also be performed on the *Maiasaura peeblesorum* specimen of this study as well for comparison.

The total length, maximum vertical diameter (height), horizontal diameter (width), and cross-sectional thickness measurements of the three semicircular canals were measured using the respective tool. Thickness measurements were taken in both the lateral and rostrocaudal, or dorsoventral for the lateral canal, and then averaged to find the most accurate diameter measurement of each canal. Due to the orthogonal orientation of the anatomy, the view perspective had to be oriented differently for each canal so linear measurements could be taken within a parallel slice of the endocast. These measurements were gathered from both the left and right endosseous labyrinths.

5.6. REPTILE ENCEPHALIZATION QUOTIENT (REQ)

The comparison of the volume of the brain to the body mass of an organism to infer behavioral and cognitive traits of an organism – termed an encephalization quotient - was devised by Jerison (1969, 1973, 1979). The reptile encephalization quotient (REQ) was then created by Hurlburt (1996) to apply Jerison's observations to reptiles, birds (BEQ), and mammals (MEQ) to gain a greater comprehensive and distinct classification system for the groups.

The REQ was chosen to compare the brain to the body size of hadrosaurs, due to their closer relationship with reptiles than with birds or mammals. The REQ is calculated using the equation of Hurlburt (1996), as follows:

$$REQ = (M_{Br}) / (0.0155 * M_{bd}^{0.553}) \hspace{2cm} (10)$$

where M_{Br} is equal to the mass of the brain in grams, and M_{bd} is equal to the body mass in grams. The M_{Br} was calculated by taking the volume of the reconstructed endocast, which was measured in Dragonfly using the "Statistical Properties – Volume" tool and multiplying the value by 1.036 gcm^{-3} to account for brain tissues. The M_{bd} can be applied for either quadrupedal or bipedal dinosaurs estimated through the equations of Anderson et al. (1985):

$$Quadredpedal: W = 0.078(C_f + C_h)^{2.73} \hspace{2cm} (11)$$

$$Bipedal: W = 0.16(C_f^{2.73}) \hspace{2cm} (12)$$

where W is equal to the approximated weight of the dinosaur (in kilograms) and C_f and C_h are equal to the minimum circumferences of the femur and the humerus (measured in millimeters), respectively. Hadrosaurids, like all ornithopods, provide a unique case whereby they are generally thought to be facultatively bipedal, rather than truly bipedal during adulthood (Forster, 1997; Horner et al., 2004). Ontogenetic changes and retaining the ability for both biomechanical stances have been widely accepted as the reason for the differential walking methods observed in ornithopods (Norman, 1980; Forster, 1997; Dilkes, 2001; Horner et al., 2004; Maidment and Barrett, 2014; Barrett and Maidment, 2017). Therefore, both equations will be used, following a similar methodology by Evans et al. (2009) to represent both postures.

The brain of *Maiasaura peeblesorum* was estimated to fill 50% of the endocranial cavity, which is typical for non-avian dinosaurs, due to the lack of valleculae. However, preserved valleculae have been noted in several hadrosauridae and ornithopod specimens (Evans, 2005; Evans et al., 2009; Godefroit et al., 2012a; Lauters et al., 2013, Knoll et al.,

2021), leading to the interpretation that the brain filled a greater proportion of the endocranial cavity, such as 60% or 73%. Therefore, the REQ of *M. peeblesorum* was calculated for both 50% and 60% endocranial fill for comparison to other hadrosaurid and ornithopod specimens.

5.7. CEREBRUM RELATIVE VOLUME (CRV)

The cerebrum/endocranial volumetric measurement is the ratio between the volume of the cerebral hemispheres on the total volume of the brain (Larsson et al., 2000; Button and Zanno, 2023). The total volume of the brain utilized is the area located within the endocranial cavity and excludes the olfactory apparatus, infundibulum, pituitary, vascularization, and all the cranial nerves. This ratio was calculated to better interpret the importance of the development and size of the cerebral hemispheres relative to the other brain anatomy.

6. RESULTS

6.1. OTM F138 ENDOCAST

The cranial endocast of OTM F138 is the largest of the three *Maiasaura peeblesorum* endocrania reconstructed for this study, measuring 149.0 mm (Table 6.1) from the anteriormost extent of the olfactory bulbs to the foramen magnum and composing a volume of 253.3 cm^3 (Table 6.1). As typically seen in ornithopods (Lauters et al., 2012), the cephalic and poutine flexure were able to be measured. These two flexure angles measure 128.5 degrees and 132.7 degrees (Table 6.1), respectively. They indicate that the brain was likely growing at a slightly faster rate than the braincase, as a straighter flexure – that is closer to 180 degrees – would represent a braincase growing at a faster pace than the brain, while the inverse case accounts for a more defined flexure – that is closer to 90 degrees (Lautenschlager and Hübner, 2023). The endocast of OTM F138 is well-preserved and allows for detailed observations into the neuroanatomy that would have been housed in the braincase of *M. peeblesorum* during life.

    6.1.1. Forebrain. The olfactory apparatus is present at the anteriormost end of the cerebrum, with the widest preserved portion interpreted as being the olfactory bulbs and the segment of the olfactory tract between olfactory bulbs and cerebrum being able to be reconstructed. The maximum measurable length of the olfactory apparatus is 23.9 mm (Table 6.1). The olfactory bulbs are observable as a dorsoventral and lateral expansion of the anterior olfactory tract, acquiring a lobe-shaped appearance in lateral, dorsal, and ventral views, and slight upside-down triangular shape in anterior view. The rostralmost region of the olfactory bulbs are not preserved, which is attributed to poor preservation of
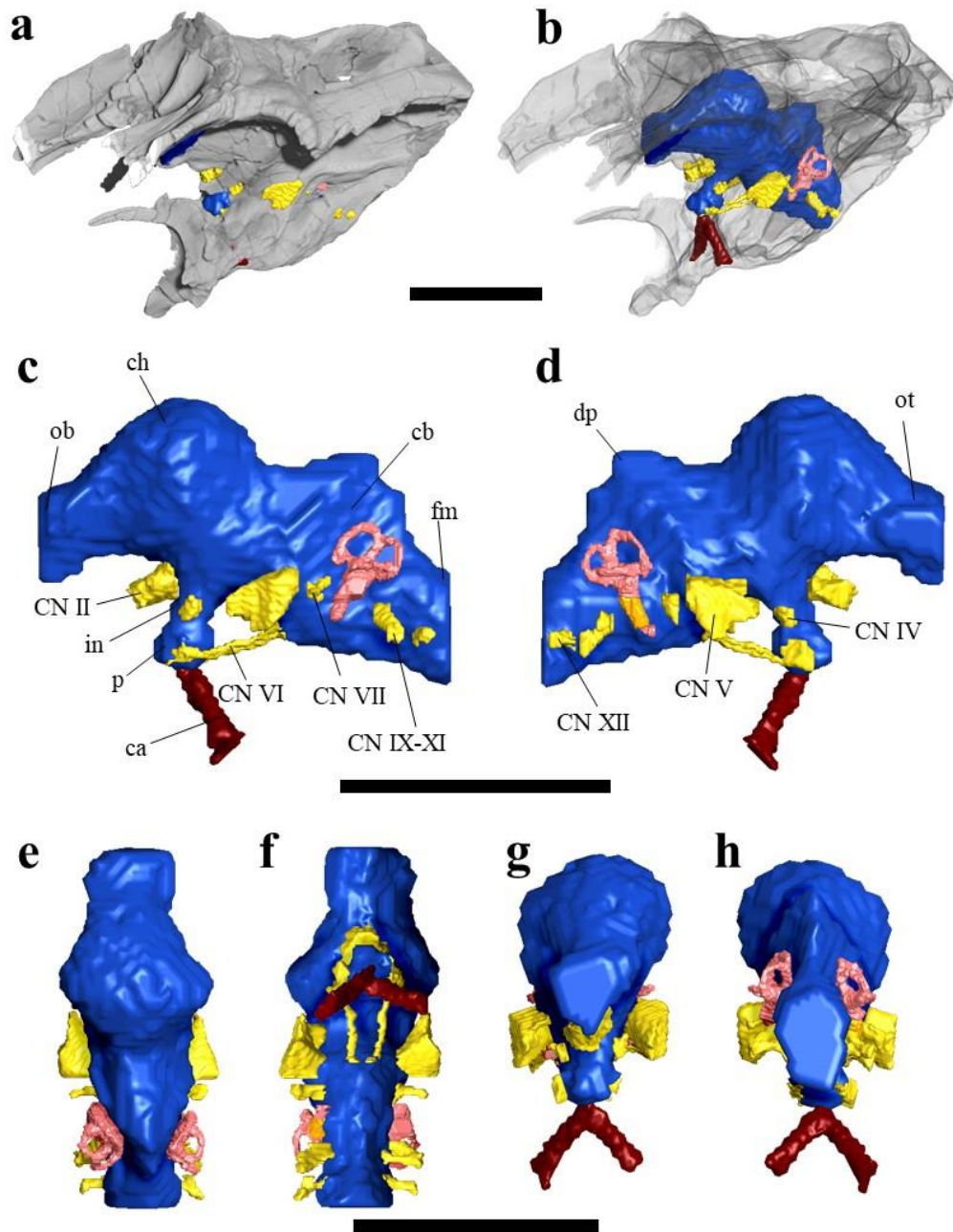
Figure 6.1. Reconstructed cranial endocast of OTM F138. (a) Opaque and (b) translucent skull with infilled endocranial cavity in oblique left lateral view. (c) Labelled left lateral view. (d) Right lateral view. (e) Dorsal view. (f) Ventral view. (g) Anterior view. (h) Posterior view. Colors as follows: blue = endocranial cavity, yellow = cranial nerves, pink = endosseous labyrinth, red = internal carotid arteries, orange = hypothesized endosseous labyrinth reconstruction. Scale bar = 100 mm. Abbreviations: ca = carotid artery; cb = cerebellum; ch = cerebral hemisphere; CN = cranial nerve/foramen for cranial nerve; dp = dural peak; fm = foramen magnum; in = infundibulum; ob = olfactory bulb; ot = olfactory tract; p = pituitary.

Table 6.1. Measurements of OTM F138 endocast.

Element Measured	Measurements
Total length	149.0 mm
Total volume	253.3 cm^3
Cephalic flexure	128.5º
Pontine flexure	132.7º
Olfactory apparatus length	23.9 mm
Olfactory bulb maximum height	32.0 mm
Olfactory bulb maximum width	33.7 mm
Olfactory tract length	16.2 mm
Olfactory tract maximum width	25.8 mm
Cerebral hemisphere width	59.3 mm
Cerebral hemisphere length	61.2 mm
Cerebral hemisphere height	74.0 mm
Infundibulum height	16.7 mm
Infundibulum maximum width	23.3 mm
Infundibulum minimum width	15.1 mm
Angle of infundibulum	86.9º
Pituitary width	21.6 mm
Pituitary length	22.0 mm
Cerebellum width	32.7 mm
Cerebellum height	70.2 mm
Cerebellum length	50.3 mm
Foramen magnum height	41.6 mm
Foramen magnum width	27.6 mm

the bones housing this region. Due to the large expansion observed from the olfactory tract

to the bulbs typical of ornithopods (Evans et al., 2009; Lautenschlager and Hübner, 2013),

the hypothesized widest portion of the bulbs is preserved in the OTM F138 endocast. At its widest and tallest points, the olfactory bulb measures 33.7 mm and 32.0 mm, respectively (Table 6.1). The olfactory tract is a mediolaterally wide, foreshortened passage that slightly narrows posteriorly from the olfactory bulbs towards the cerebral hemispheres and measures 16.2 mm in length and 25.8 mm at its widest point (Table 6.1). The opening for the tract is irregularly conically shaped and is made by the ventral side of the frontal and septate rostral flanges of the presphenoid. The olfactory tract caudally transitions and expands in the lateral, dorsal, and ventral direction to meet the cerebrum.

The cerebrum appears to be the most prominent anatomical feature of the OTM F138 cranial endocast as a large, round mass in the forebrain region. A longitudinal fissure separating the cerebral hemispheres from one another could not be distinguished in the reconstruction. This lack of fissure preservation is likely due to the presence of thick dural mater that covered this region of the brain in life. Moreover, no vascularization could be reconstructed in this cranial endocast, which is surprising given the large volumetric area of the forebrain region comprised of the cerebrum and the likelihood this area would have been pressed against the osteological framework of the braincase, as commonly observed ornithopods (Evans, 2005; Evans et al., 2009; Godefroit et al., 2012a; Lauters et al., 2013). This lack of characteristic trait is likely attributed to the lower quality of the CT scanner used in this study in comparison with other Ornithopoda endocranial work. At its tallest and widest points, the cerebrum measures 74.0 mm and 58.4 mm, respectively, and it has a volume of 118.5 cm^3 (Table 6.1). The cerebrum measures 61.2 cm in length (Table 6.1) and accounts for 41.1% of the total endocranial length.

The optic nerve (CN II) is located ventral to the olfactory apparatus and rostrally to the ventral surface of the cerebrum. In hadrosaurs, this nerve exits the braincase through the orbitosphoid bone, and extends to the orbits to control fine motor movements of the eyes via one large oval-shaped foramen located directly on the midline of the ventral braincase. From its point of nucleation on the endocast, CN II is angled rostroventrally at 41.1 degrees before the lack of fossilized material does not allow for further segmenting of the nerve. Due to the poor preservation and cracks propagating through the region, the oculomotor nerve (CN III) could not be reconstructed.

The infundibulum is located ventral to the cerebrum (Figure 6.1). It extends almost directly ventrally with a slight rostral angle of 86.9° and a height of 16.7 mm (Table 6.1). Since the infundibulum extends further ventrally, it tapers sharply, therefore the maximum width of the stalk is found nearest the endocranial body (23.3 mm; Table 6.1) and the minimum width is seen where the stalk reaches the pituitary body (15.1 mm; Table 6.1). Extending mediolaterally from both lateral walls of the infundibulum stalk are the trochlear nerves (CN IV) (Figure 6.1). The pituitary is located directly ventral to the infundibulum, oriented in an oblique, posteroventral direction, and seen with an oval bulb-shaped feature in lateral view, with an equatorial rounded appearance in posterior and anterior view (Figure 6.1). A maximum width of 21.6 mm and maximum length of 22.0 mm (Table 6.1) was measured on the reconstructed pituitary body. The branching internal carotid arteries extend ventrally from the pituitary and form a wish-bone shaped structure, viewable in anteroposterior view, that is angled posterolaterally (Figure 6.1). The left and right branches of the internal carotid arteries measure 35.6 mm and 37.8 mm in length (Table 6.1), respectively. The widths of the internal carotid arteries are consistent except for a

slightly wider, flattened oval end that is observed at the ventralmost extent of both arteries, which represents the area where the arteries exited the basisphenoid. Whether the widening of the arteries is natural or an artefact of taphonomic processes is indeterminable.

6.1.2. Midbrain. Broadly speaking, the midbrain region of the endocast is unremarkable and uninformative due to the lack of distinguishable anatomical material found along the midbrain's surface. The optic lobes cannot be observed in the reconstruction, likely due to the thick dural covering in this region of the brain during life. Similar to the cerebrum, vascularization is not visible along the midbrain, either.

6.1.3. Hindbrain. The cerebellum is the prominent laterally flattened oval feature of the hindbrain region with numerous anatomical features extending from it. The cerebellum itself is 70.2 mm at its maximum height and 32.7 mm at its maximum width (Table 6.1), giving the anatomy a height-to-width ratio of 2.1. A cartilaginous dural peak located on the dorsal cerebellar surface can be viewed in lateral view (Figure 6.1) and is a common trait seen in dinosaurian endocasts (Lautenschlager and Hübner, 2013; Button and Zanno, 2023). This peak signifies the presence of a longitudinal dural venous sinus that would have traversed from the foramen magnum across the dorsal surface of the endocast during life (Witmer et al., 2008; Evans et al., 2009). The cerebellum measures 50.3 mm in length (Table 6.1) and accounts for 33.8% of the total endocrania body length. Since the cerebellum is the informational processing center for movement and balance, the cranial nerves extending from this region are centered are the innervation of these functions.

The trigeminal nerve (CN V) would have been housed in the most distinguishable foramen on the cranial endocast. It is located in the hindbrain region, situated between - and at the same height as - CN II and the foramen for the vestibulocochlear nerve (CN

VIII). Circular to subtriangular in shape, the foramen border is formed by the basisphenoid ventrally, while the laterosphenoid encloses the dorsorostral third and the prootic encloses the dorsocaudal third – since the laterosphenoid and prootic suture is located directly dorsal to CN V. Upon segmentation of the nerve, three apices projecting rostrodorsally, rostroventrally, and caudoventrally could be observed. The rostrodorsal and rostroventral angles project further than the caudoventral, making them appear more pronounced, and the average measured distance from one of the apices to the termination to the endocranial body is 24.5 mm. These three apices are interpreted to be the three branches of CN V: the ophthalmic branch (CN V_1), the maxillary branch (CN V_2), and the mandibular branch (CN V_3). In other non-avian dinosaurs, CN V_1 would have exited the foramen via the rostrodorsal "point" and traversed rostrally to the face via a horizontal sulcus on the laterosphenoid, while CN V_{2-3} would have exited the foramen via the rostroventral "point" and traversed rostroventrally along the basisphenoid before branching off to their respective regions of interest on the mouth (Ostrom, 1961; Evans, 2009).

The paired right and left abducens nerves (CN VI) are located on the rostroventral surface of the cerebellum as two foramina bilaterally adjacent to the midline of the endocast directly caudal to the pituitary. The two tracts for CNVI extends rostrally, with a slight ventral trend, from these two foramina on the cerebellum and connects to two foramina on respective lateral walls of the pituitary. This gives CN VI a "bridge" like structure between the two localities in the reconstructed endocast in lateral view (Figure 6.1). In life, these two nerve tracts would have been completely encased in the basisphenoid, while the posterior foramen connecting the tract to the endocranial body would have been enclosed by the basisphenoid ventrally, laterosphenoid anteriodorsally, and prootic posterodorsally.

Both CN VI tracts have very similar morphologies and lengths, thus giving further evidence that the braincase has undergone little deformation or taphonomic destruction in this region (Figure 6.1); the right and left spanning tracts are thin and narrow, with a diameter of 3.1 mm and 2.9 mm and lengths of 34.3 mm and 35.3 mm, respectively (Table 6.1). The two foramina that house CN VI within the lateral walls along the pituitary are larger and wider than the tracts themselves, with dimensions of approximately 6.0 mm x 4.0 mm (Table 6.1); therefore, a large oval-shaped bulb at the rostralmost extent was reconstructed for the two CN VI tracts.

The facial nerve (CN VII) extends laterally from the cerebellar region of the cranial endocast via a small foramen located in the prootic and is the smallest foramen observable on the osteological braincase of F138 (Figure 6.1). CN VII is centrally located between CN V and the endosseous labyrinths on both sides of the braincase. Interestingly, after reconstruction, the left CN VII appears to curve upwards and extends dorsally, while the right CN VII has a slight downward curve and extends ventrally (Figure 6.1). Similar to CN V, CN VII has two branches, the hyomandibular branch and the palatine branch, thus these two different orientations are inferred as showing the separate directions the nerve branches would have traversed in life. Both branches have been observed in ornithopods, with the hyomandibular branch traversing dorsally and the palantine branch traversing ventrally (Evans et al., 2009; Sobral et al., 2012). Therefore, it is inferred that the hyomandibular branch was reconstructed on the left lateral wall, while the palatine branch was reconstructed on the right lateral wall of the endocast of OTM F138, resulting in the different trending directions. The inability to reconstruct both branches of CN VII on the

right and left walls of the braincase is due to taphonomic destruction and poor preservation in this region.

The shared foramen for the vagus (CN X) and accessory (CN XI), and possibly glossopharyngeal (CN IX), nerves is centrally located between the endosseous labyrinth and the posteriormost foramen on the lateral wall of the endocranial body, the hypoglossal (CN XII) nerve foramen (Figure 6.1). The reconstructed CN X/CN XI nerve tract on the left lateral wall extends directly laterally from the braincase, while the reconstructed nerve tract on the right lateral wall extends slightly ventrocaudally. This difference is attributed to taphonomic distortion. There is debate whether CN IX exited the braincase through this foramen or through a different foramen situated directly posteriorly adjacent to the vestibulocochlear foramen (CN VIII) of the endosseous labyrinth in hadrosaurs (Evan et al., 2009; Prieto-Marquez, 2010b). However, due to cracks on both sides of the osteological braincase, this area directly posterior to CN VIII could not be reconstructed.

The brainstem is the posteriormost region of the cranial endocast where it extends caudally from the cerebellum and sharply narrows posterior to the dural peak. The brainstem terminates at the foramen magnum, with the caudalmost extent of the brainstem and opening for the foramen magnum measuring 41.6 mm in height and 27.6 mm in width (Table 6.1). One cranial nerve, the hypoglossal nerve (CN XII), extends laterally from the brainstem region of the endocast (Figure 6.1). This nerve is reconstructed on both walls, although there is a slight caudal projection to the nerve. This projection is more prominent on the right lateral wall than the left wall.

6.1.4. Endosseous Labyrinth. The endosseous labyrinth is nearly complete on both sides of the endocast, although the midsection of the right cochlear duct, ventral to

the vestibule, could not be reconstructed due to taphonomic damage (Figure 6.1 and 6.2). In lateral view, both labyrinths have a posteriorly angled tilt to the overall structure (Figure 6.1 and 6.2). The morphology of the endosseous labyrinths have a distinct resemblance to that of other hadrosaurs (Evans et al., 2009), with the three semicircular canals each oriented in their own plane and orthogonal to each other, as observed in all tetrapods (Figure 6.2) (Walsh et al., 2009). Similarly, all three canals have a rounded circular appearance in lateral view, as seen in the rounded-sub triangular shaped morphology reconstructed in most non-avian dinosaurian taxa (Figure 6.2) (Lautenschlager et al.; 2012; King et al., 2020; Sakagami and Kawabe, 2020; Button and Zanno; 2023). The anterior semicircular canal stands taller than the posterior semicircular canal, with left measured heights of 18.5 mm and 17.8 mm and right measured heights of 17.0 and 14.6 mm, respectively (Table 6.2). Anatomically, this height difference between the anterior and posterior canal trend occurs across all tetrapods in varying degrees and morphologies (Walsh et al., 2009). The left lateral semicircular canal has a height of 16.3 mm, while the right has a height of 12.5 mm (Table 6.2); this large difference is notably due to the right lateral wall of the endocast being slightly deformed and fragmented, causing the right lateral canal to be more ovoidal in shape rather than the morphologically typical circular shape. Horizontal diameter widths of the left anterior, lateral, and posterior canals measure 16.5 mm, 16.1 mm, 16.7 mm, while the right measure 16.1 mm, 16.2 mm, and 14.4 mm, respectively (Table 6.2). Length measurements were also taken of the three of the left and right inner ears, showing that the anterior semicircular canal was the longest (44.2 mm and 41.4 mm), the lateral semicircular canal was the shortest (36.2 mm and 35.9 mm), and the posterior semicircular canal length was in between the two (41.2 mm and 38.0 mm) (Table

6.2). This follows the trend seen in most derived ornithopods where the anterior canal is the longest semicircular canal (Evans et al., 2009). The thickness of each canal stays roughly constant throughout, except for where the ampulla of the anterior and posterior semicircular canals is located.

Thickness measurements were taken in the middle region of each canal in both the rostrocaudal, and dorsoventral for the lateral semicircular canal, and lateral directions and then averaged to avoid influence of the ampulla or reconstruction errors: the anterior, lateral, and posterior diameters for the left endosseous labyrinth are 3.4 mm, 3.2 mm, and 2.9 mm, while the right are similarly 3.0 mm, 2.9 mm, and 3.1 mm (Table 6.2). Overall thickness varies taxonomically, although it is commonly observed in tetrapods that the thicknesses of the canals are relatively similar with each other (Walsh et al., 2009). The ampullae of the respective canal are located along the ventral extent and appear as thickened areas connected to the vestibule regions (Figure 6.2). The thickness of the left and right crus communis are 4.2 mm and 4.4 mm (Table 6.2), forming a slightly thicker region than the individual canals.

The cochlear duct, which would have housed the basilar papilla in life, extends ventrally from the vestibule region with the same posterior tilt relative to the endocast as the rest of the endosseous labyrinth (Figure 6.2). As aforementioned, a significant portion of the right cochlear duct is missing due to taphonomic damage to the braincase. Fortunately, the ventralmost extent of the right cochlear duct could be segmented, thus allowing for a measurement of the cochlear duct length to be approximated. As the dorsalmost and ventralmost regions of the cochlear duct are present, a hypothesized cochlear duct was reconstructed to connect the two regions (shown in orange in Figure 6.2
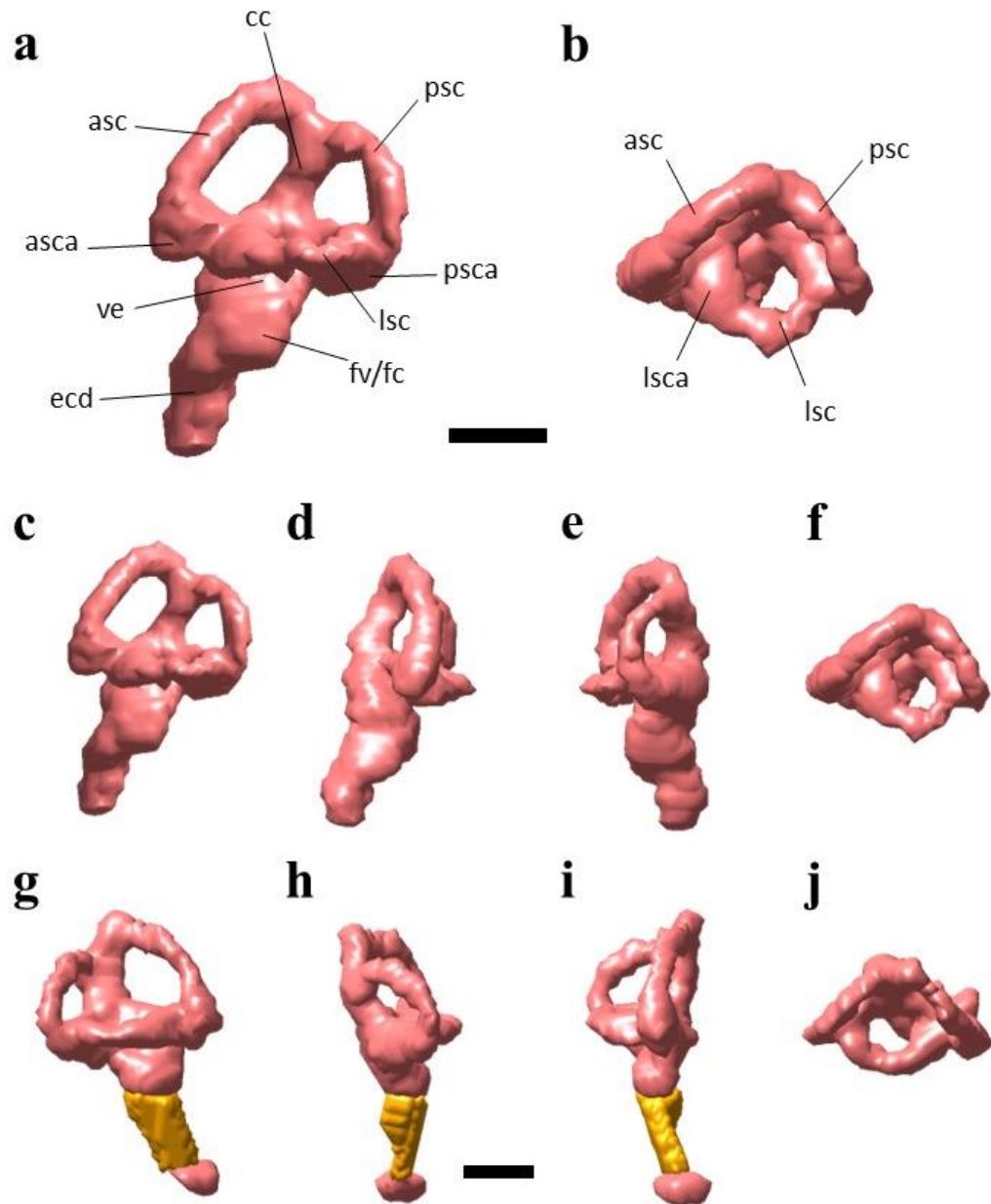
Figure 6.2 Reconstructed endosseous labyrinth of *M. peeblesorum* OTM F138. Labelled left endosseous labyrinth in lateral (a) and dorsal (b) view. The left (c-f) and right (g-j) inner ears are shown in lateral (c,g), anterior (d,h), posterior (e,i) and dorsal (f,j) views. Scale bar = 10 mm. Abbreviations: asc = anterior semicircular canal; asca = ampulla of the anterior semicircular canal; cc = crus communis; ecd = endosseous cochlear duct; fv/fc = fenestra vestibuli and fenestra cochleae; lsc = lateral semicircular canal; lsca = ampulla of the lateral semicircular canal; psc = posterior semicircular canal; psca = ampulla of the posterior semicircular canal; ve = vestibule.

Table 6.2. Measurements of Endosseous Labyrinth of OTM F138 Endocast.

Elements Measured	Measurement	
	Left	Right
Total height	41.2 mm	43.3 mm
Anterior semicircular canal length	44.2 mm	41.4 mm
Lateral semicircular canal length	36.2 mm	35.9 mm
Posterior semicircular canal length	41.2 mm	38.0 mm
Anterior semicircular canal height	18.5 mm	17.8 mm
Lateral semicircular canal height	16.3 mm	12.5 mm*
Posterior semicircular canal height	17.0 mm	14.6 mm
Anterior semicircular canal width	16.5 mm	16.1 mm
Lateral semicircular canal width	16.1 mm	16.2 mm
Posterior semicircular canal width	16.7 mm	14.4 mm
Anterior semicircular canal thickness	3.4 mm	3.0 mm
Lateral semicircular canal thickness	3.2 mm	2.9 mm
Posterior semicircular canal thickness	2.9 mm	3.1 mm
Cochlear duct length	18.2 mm	18.8 mm
Cochlear duct maximum width	9.4 mm	7.5 mm
Cochlear duct minimum width	3.3 mm	4.8 mm
Crus communis thickness	3.8 mm	4.4 mm

* Measurements inferred to have been altered by taphonomic processes.

(g-i)), but the tilt or width could not be determined with accuracy. From the vestibule, the left and right cochlear ducts measure 18.2 mm and 18.8 mm, respectively, (Table 6.2), which is relatively long compared to other ornithopods (Evans et al., 2009; Button and Zanno, 2023). The separation between the fenestra vestibuli and the fenestra cochleae

could not be differentiated in the left endosseous labyrinth or observed in the right endosseous labyrinth. Both of these are attributed to taphonomic distortion.

6.2. TMDC F139 ENDOCAST

Maiasaura peeblesorum specimen TMDC F139 is the medium-sized braincase and volumetrically cranial endocast, but lengthwise the smallest cranial endocast, reconstructed for this study. The endocast measures 107.2 mm (Table 6.3) from the posteriormost section of the olfactory tract that is in contact with the cerebrum to the foramen magnum. The endocranial cavity has a volume of 134.4 cm^3 (Table 6.3). Intense deformation and fracturing of the braincase severely affected the reconstruction and quantitative analysis of the endocast. A combination of anterioposterior and dorsoventral compressional deformation is hypothesized to have occurred due to atypical cephalic and pontine flexure angles of close to 90 degrees measured for the medium-sized nature of the TMDC F139 specimen. The cephalic flexure measured 115.8 degrees and the pontine flexure measured 118.3 degrees (Table 6.3), which are 12.7 degrees and 14.4 degrees more acute, respectively, than the flexures measured on OTM F138. It is hypothesized that both directions of compression occurred because the endocast has undergone significant length and height shortening, therefore compounding the taphonomic processes to the two methods and further making comparisons between specimen and across ornithopods difficult. Portions of bones from the braincase are intersecting and protruding dorsally, laterally, and ventrally into the endocranial cavity as well, causing difficulty in segmentation and reconstruction of how the endocranial anatomy would have appeared in

Table 6.3. Measurements of TMDC F139 Endocast.

Element Measured	Measurements
Total length	129.7 mm
Total volume	134.4 cm^3*
Cephalic flexure	115.8°*
Pontine flexure	118.3°*
Olfactory tract length	6.3 mm
Olfactory tract maximum width	24.0 mm
Cerebral hemisphere width	48.5 mm*
Cerebral hemisphere length	52.6 mm
Cerebral hemisphere height	48.9 mm*
Infundibulum height	6.2 mm
Cerebellum width	20.8 mm
Cerebellum height	61.3 mm
Cerebellum length	36.6 mm
Foramen magnum height	33.6 mm
Foramen magnum width	23.0 mm

* Measurements inferred to have been altered by taphonomic processes.

vivo. This in turn led to volumetric calculation errors, which similarly makes comparing endocasts challenging. While both lateral walls of the braincase have severe breakage and fracturing, the completeness of the medial-caudalmost regions of the left wall and caudalmost region of the right wall allow for a few cranial nerves to be reconstructed.

6.2.1. Forebrain. The anteriormost region of TMDC F139 endocast consists of a small portion of the olfactory tract (Figure 6.3) that is viewable in all orientations. This anatomy is interpreted to be the olfactory tract, rather than just the anteriormost extent of the cerebral hemispheres due its contact and relative position with the nasal and prefrontal
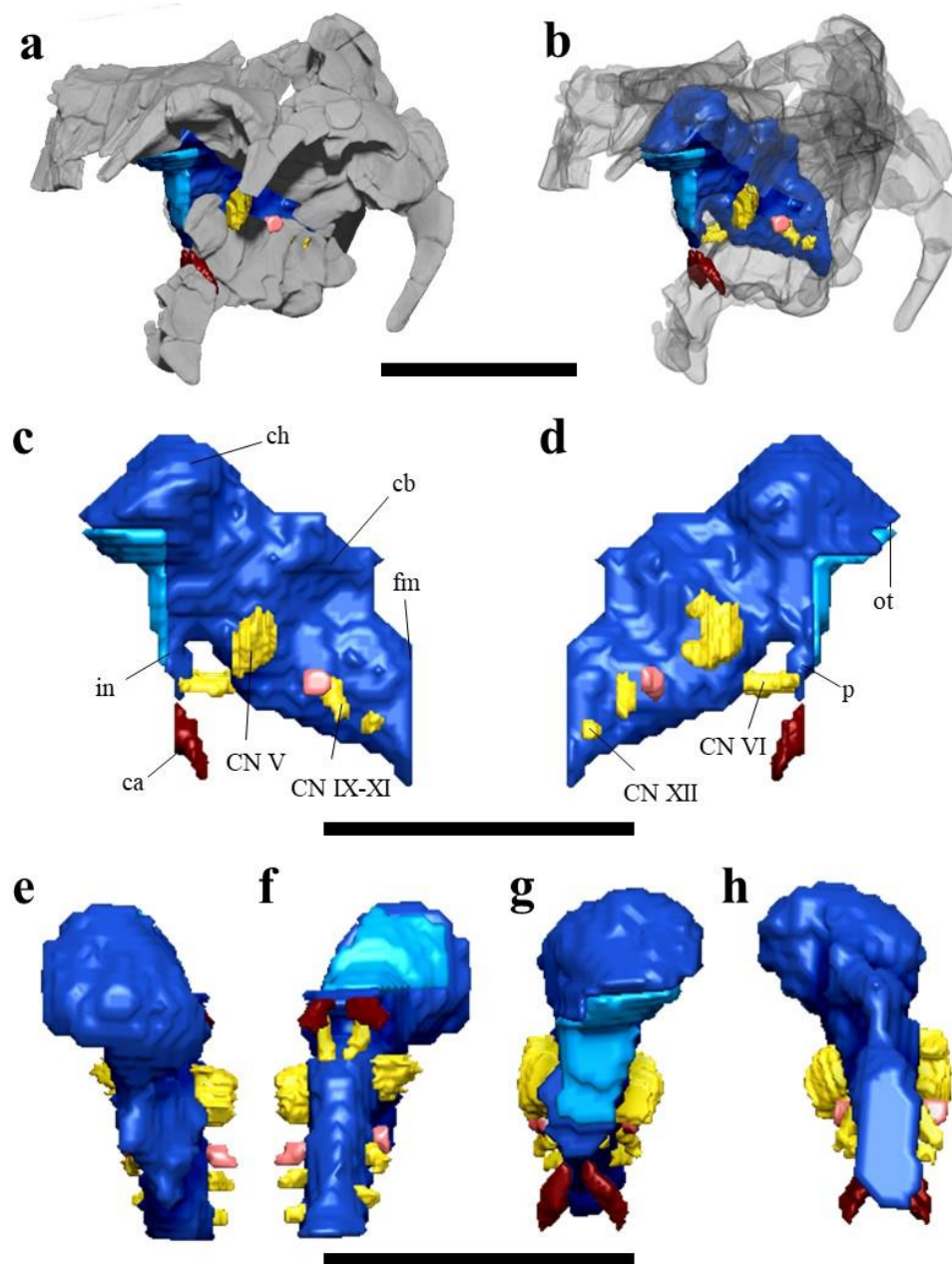
Figure 6.3 Reconstructed cranial endocast of TMDC F139. (a) Opaque and (b) translucent skull with infilled endocranial cavity in oblique left lateral view. (c) Labelled left lateral view. (d) Right lateral view. (e) Dorsal view. (f) Ventral view. (g) Anterior view. (h) Posterior view. Colors as follows: blue = endocranial cavity, light blue = hypothesized endocranial cavity reconstruction, yellow = cranial nerves, pink = endosseous labyrinth, red = internal carotid arteries. Scale bar = 100 mm. Abbreviations: ca = carotid artery; cb = cerebellum; ch = cerebral hemisphere; CN = cranial nerve/foramen for cranial nerve; dp = dural peak; fm = foramen magnum; in = infundibulum; ob = olfactory bulb; ot = olfactory tract; p = pituitary.

bones of the skull. Only the dorsal region of this hypothesized posteriormost olfactory tract could be reconstructed because of the incomplete preservation of the parabasisphenoid encasing the ventral region of the tract. The olfactory bulbs and anteriormost olfactory tract could not similarly be reconstructed due to the lack of preservation of the nasal, prefrontal, and parabasisphenoid bones. The preserved olfactory tract measures 6.3 mm in length and 24.0 mm in width (Table 6.3). The olfactory tract continually widens from its anteriormost extent to the cerebrum region, unlike the olfactory tracts observed in ornithopods where this is a constant equidimensional height and width tract seen until the significant expansion of the cerebrum (Evans, 2005; Evans et al., 2009; Lautenschlager et al, 2013). This is attributed to taphonomic distortion or errors during reconstruction preparation methods of the braincase.

The cerebrum region of TMDC F139 caused numerous difficulties during segmentation. In lateral view, the cerebrum is observed as a large, circular shaped region of the forebrain that appears to be nearly equidimensional (Fig 6.3). However, in the dorsoventral and anteroposterior view, the cerebrum is seen as an asymmetrical oval shaped mass that is obliquely oriented in relation to the rest of the endocranial body (Figure 6.3). Taphonomic deformation and poor preservation, alongside an assumed difficult reconstruction during mechanical preparation, of the braincase likely caused this unusual shape of the cerebral region. Measurements of the cerebral hemispheres were still taken, but the measurements and interpretations were noted to be skewed due to this significant alteration. At its tallest and widest point, the cerebrum of TMDC F139 measures 48.9 mm and 48.5 mm, respectively (Table 6.3). The measured length was 52.6 mm (Table 6.3), which accounts for 40.6% of the total endocranial cavity length. No longitudinal fissure

nor vascularization could be seen on the cranial endocast, which again likely owes to the dural covering of the brain. Even if observable with the dural covering, it is likely that the poor preservation of the specimen would still prevent an accurate description of these features.

Ventral to the cerebral hemispheres, portions of the posterior infundibulum, pituitary, and internal carotid arteries were reconstructed (Figure 6.3). However, similar to the rest of the braincase, this area is very fractured, resulting in sparse information to be confidently gained from the region. The incomplete infundibulum is very short (6.2 mm, Table 6.3) and only distinguishable by a slight narrowing directly ventral to the cerebrum before expanding laterally and ventrally into the pituitary (Figure 6.3). The dorsoposterior portion of the pituitary is preserved, but due to the limited amount of anatomy observed and osteological constraint on the area, measurements were not taken. The internal carotid arteries extend further ventroposteriorly with a wishbone shaped structure (Figure 6.3). Due to missing portions of basisphenoid and parasphenoid bones, the dorsalmost and ventralmost areas of the internal carotid arteries that serve as the connection between the two branches and the pituitary could not be reconstructed, as have been observed. Therefore, the arteries appear to be floating in the reconstructed view, although they should dorsally terminate at the pituitary. The length of the right and left internal carotid arteries reconstructed are 26.7 mm and 27.2 mm, respectively (Table 6.3).

6.2.2. Midbrain. Due to the anteroposterior compressed nature of the endocast, there is hardly a midbrain region of TMDC F139 that could be reconstructed. The cerebral hemispheres sharply taper both dorsoventrally and laterally to form a small saddle shaped depression on the dorsal and ventral face of the endocast (best viewable in lateral view)

before caudally expanding dorsoventrally and slightly laterally to form the cerebellum (Figure 6.3). There is a much larger dorsoventral than lateral expansion in the cerebellum, which is observable in both lateral, dorsal, and ventral views (Figure 6.3). Similar to OTM F138, this region of the brain is uninformative due to the lack of surface anatomy housed in this region.

6.2.3. Hindbrain. The cerebellum is the large, discoid shaped feature of the hindbrain region (Figure 6.3). Similar to the forebrain region, the cerebellum is deformed and not bilaterally symmetrical. Different dorsal, lateral, and ventral portions of the braincase housing this region are intact – meaning they were reconstructed to be intact by mechanical preparation methods – or missing, making segmenting only possible through interpolation between two points that preserved identifiable anatomy. The cerebellum measures 61.3 mm at its maximum height and 20.8 mm at its maximum width (Table 6.3), giving a height-to-width ratio of 2.9. Two peaks are present on the dorsal cerebellar surface in lateral view (Figure 6.3), but it is uncertain whether this is the preservation of the longitudinal dural venous sinus and dorsal peak or produced by preparation reconstruction errors. The cerebellum measures 36.6 mm in length (Table 6.3), accounting for 28.2% of the total endocranial length.

Due to the large, cross-sectionally round nature of the trigeminal nerve foramen, the approximate location for CN V could be deduced on both lateral walls of the endocast. The nerve is interpreted to be laterally branching from the rostral region of the cerebellum along the longitudinal midline of the endocranial body. Since the left lateral wall of the braincase is better preserved in the hindbrain, the location of CN V was first approximated on the left side of the endocast and then interpreted on the right lateral wall of the braincase.

The location of the nerve foramen on the left wall was relatively easy to distinguish. However, cracking on the contact of the laterosphenoid and prootic bone in the dorsal and rostrolateral regions of the foramen made it difficult to approximate the size of the anatomy. The right wall of the braincase is missing the fused contact line of the laterosphenoid, prootic, and basisphenoid bones, creating a large longitudinally oriented crack where the trigeminal (CN V), facial, and vestibulocochlear nerves would exit the braincase (Figure 6.3). Therefore, the lack of preservation of the rostral nor caudal lateral walls of the foramen prevented any size approximation. Only the slight curves on the dorsal and ventral sides of the longitudinal crack on the right wall allowed for an approximate location to be deduced on the right wall.

The paired "bridge-like" right and left abducens nerves extend rostrally from two bilaterally symmetrical foramina located on the rostroventral surface of the cerebellum, observable in reconstructed lateral view. The nerves are oriented directly rostral with no deviation from the midline of the endocast, through foramina tracts that traverse through the basisphenoid bone and terminate at the respective lateral walls of the posteriormost region pituitary. Contrary to those in OTM F138, the tracts are highly shortened and thickened with left and right passage lengths of 15.4 mm and 15.9 mm and diameters of 5.4 mm (Table 6.3). This is interpreted to be from anteroposterior deformation, and therefore possibly deforming the foramina tracts in response to the stress.

The facial nerve (CN VII) could not be reconstructed on either lateral wall of the braincase. Due to the known location of CN VII caudal to the trigeminal nerve (CN V) in ornithopods (Evans et al., 2009; Lautenschlager and Hübner, 2013), it is inferred that CN

VII could be located it one of the cracks propagating from the trigeminal nerve (CN V) on the left lateral wall of the braincase.

The location of the vestibulocochlear nerve (CN VIII) was approximated in the same way as the trigeminal nerve (CN V); the left lateral wall of the braincase preserves the foramen with cracks propagating dorsally from the opening, while the right lateral wall preserves a portion of the ventral "u"-shape border of the foramen. Therefore, this region on the right lateral wall of the braincase was interpreted to be CN VIII. The foramen for CN VIII is located caudally to CN V and exits the braincase in the median-to-caudal region of the cerebellum (Figure 6.3).

Similar to OTM F138, a single foramen is believed to have allowed the glossopharyngeal (CN IX), vagus (CN X), and accessory (CN XI) nerves to exit the braincase. This foramen is located centrally between the foramen for the vestibulocochlear (CN VIII) and hypoglossal (CN XII) nerve in the exoccipital bone and is visible on both walls of the braincase (Figure 6.3). The opening for CN IV-VI is in the rostralmost region of the cerebellum and is caudolaterally oriented, rather than directly laterally as seen with the other cranial nerves (Figure 6.3).

The brainstem region could be segmented with ease due to the posteriormost bones of the braincase being relatively well preserved, especially when compared to the anteriormost region of the braincase. The brainstem extends caudally from the cerebellum where a very sharp taper defines the end of the cerebellum, creating an observed 21.0 mm height difference between the two anatomical features and viewable in lateral view (Figure 6.3). This extreme dorsoventral tapering is most likely attributed to the anterioposterior deformation of the braincase and compression of the endocast. The caudalmost extent of

the brainstem and opening for the foramen magnum measures 33.6 mm in height and 23.0 mm in width (Table 6.3). The hypoglossal nerve (CN XII) extends from the lateroventral region of the brainstem and was reconstructed on both sides of the braincase (Figure 6.3).

      6.2.4. Endosseous Labyrinth. Neither the endosseous labyrinth is not preserved in TMDC F139 due to the extreme breakage and fracturing of the lateral walls of the braincase in this region. Therefore, no hearing frequencies could be calculated for this braincase.

6.3. TMDC F140 ENDOCAST

      The cranial endocast of TMDC F140 is the volumetrically smallest of the three *Maiasaura peeblesorum* cranial endocasts reconstructed for this study and comprises a volume of 123.8 cm^3 (Table 6.4). Noteworthy though is that this measurement excludes the olfactory apparatus volume, due to the lack of preservation of the anatomy. The endocast of TMDC F140 is longer than TMDC F139, as it measures 137.5 mm (Table 6.4) from the hypothesized middle portion of the olfactory tract to the foramen magnum. The cephalic flexure measured 148.8 degrees and the pontine flexure measured 156.9 degrees (Table 6.4), giving the endocranial body an elongated shape relative to OTM F138 and TMDC F139. This elongated endocrania shape is most typically seen in younger ontogenetic stages of ornithopod dinosaurs (Lautenschlager et al., 2013). The braincase is poorly preserved and was reconstructed from hundreds of small pieces, but it does not appear to have undergone severe deformation that altered the original shape of the cavity.
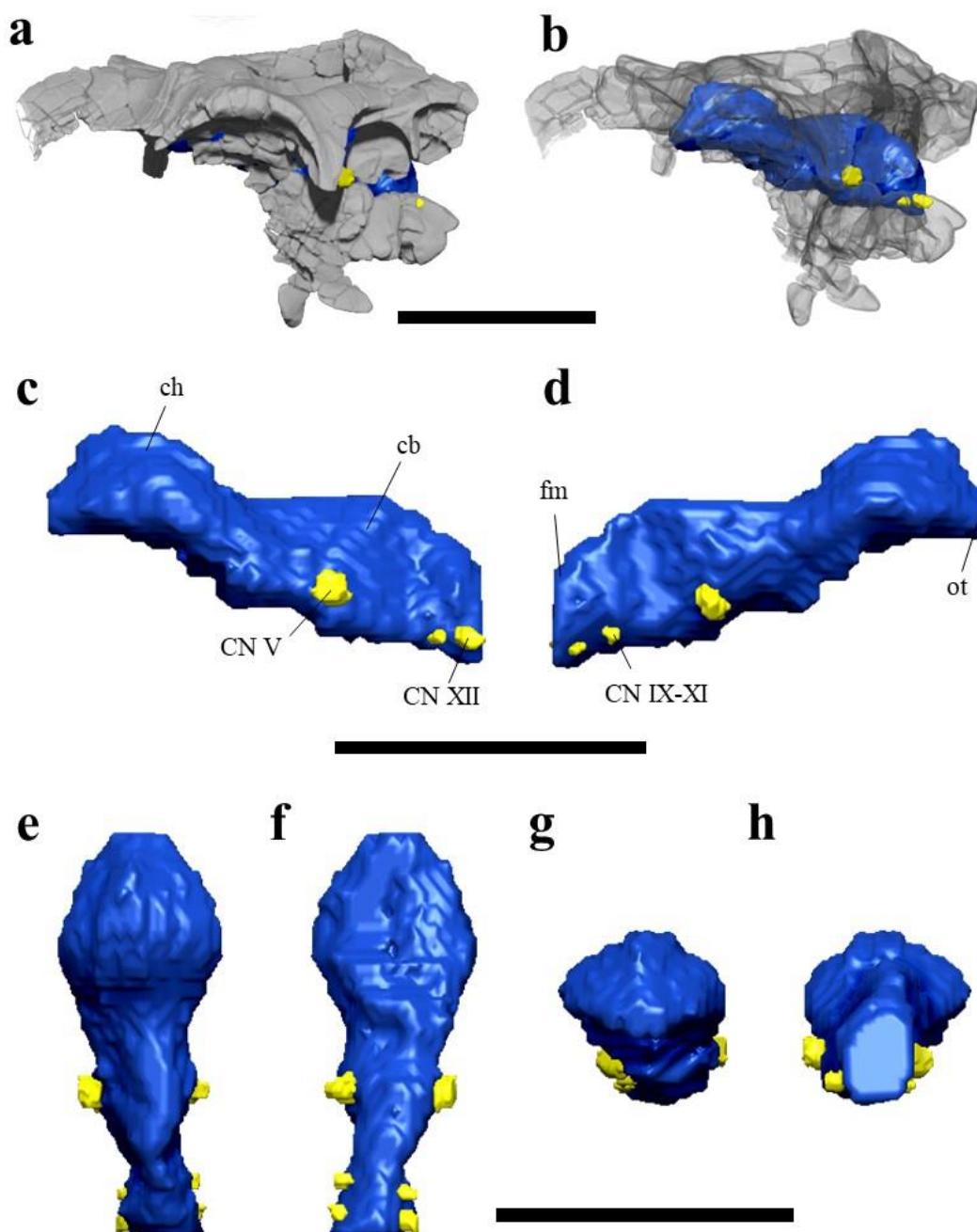
Figure 6.4 Reconstructed cranial endocast of TMDC F140. (a) Opaque and (b) translucent skull with infilled endocranial cavity in oblique left lateral view. (c) Labelled left lateral view. (d) Right lateral view. (e) Dorsal view. (f) Ventral view. (g) Anterior view. (h) Posterior view. Colors as follows: blue = endocranial cavity, yellow = cranial nerves. Scale bar = 100 mm. Abbreviations: ca = carotid artery; cb = cerebellum; ch = cerebral hemisphere; CN = cranial nerve/foramen for cranial nerve; dp = dural peak; fm = foramen magnum; in = infundibulum; ob = olfactory bulb; ot = olfactory tract; p = pituitary.

Thus, the main body of the endocranial cavity could be reconstructed with little difficulty. Since the caudoventral, lateral walls, and ventral bones of the braincase are very fragmented, numerous anatomical features of the forebrain (optic nerve, oculomotor nerve, trochlear nerve, infundibulum, pituitary, and internal carotid arteries) and hindbrain (abducens nerve, facial nerve, vestibulocochlear nerve, and endosseous labyrinth) could not be reconstructed (Figure 6.4). These intense fractures and cracks running through the braincase prevented the distinction between the suture lines of the bones comprising the braincase as well.

Table 6.4. Measurements of TMDC F140 Endocast.

Element Measured	Measurements
Total length	137.5 mm
Total volume	123.7 cm^3*
Cephalic flexure	148.8º
Pontine flexure	156.9º
Olfactory tract length	3.6 mm
Olfactory tract maximum width	21.5 mm
Cerebral hemisphere width	53.7 mm
Cerebral hemisphere length	49.9 mm
Cerebral hemisphere height	36.5 mm
Cerebellum width	21.0 mm
Cerebellum height	48.0 mm
Cerebellum length	37.3 mm
Foramen magnum height	32.0 mm
Foramen magnum width	22.8 mm

* Measurements inferred to have been altered by taphonomic processes.

6.3.1. Forebrain. The anteriormost anatomy visible on TMDC F140 is the portion of the olfactory tract directly anterior and in contact with the cerebral hemispheres. Neither the olfactory bulbs nor anterior region of the olfactory tract are preserved due to the lack of the prefrontal and nasal bones constraining this area. The olfactory tract that was reconstructed is 3.6 mm in length and 21.5 mm in width (Table 6.4). This short tract expands caudally to the cerebrum region.

The cerebrum appears as an elongated, oval shaped structure in lateral view and circular-bulb shaped structure in dorsoventral view in the forebrain region of the endocast (Figure 6.4). As in the other specimens, a longitudinal fissure that separates the cerebral hemispheres could not be distinguished in the reconstruction, which is likely due to the presence of thick dural mater in this region of the brain during life. A small bump on the anteriormost dorsal extent of the cerebrum where this longitudinal fissure would have traversed is present; however, this structure is likely an artefact of taphonomy or preparation rather than the preservation of an anatomical feature. This observation is based on the sharp, dorsally concave expansion of the olfactory tract to the cerebrum that is not typically present in ornithopod endocranial reconstructions (Figure 6.4) (Evans et al., 2009). No vascularization could be reconstructed in this cranial endocast, further supporting that this bump was likely due to postmortem processes rather than confined anatomy in this area. At its tallest and widest points, the cerebrum measures 36.5 mm and 53.7 mm, respectively (Table 6.4), and 49.9 mm (Table 6.4) in length, accounting for ~36.3% of the total endocranial length. The cerebrum tapers both dorsoventrally and laterally to form the midbrain region.

6.3.2. Midbrain. A wide saddle shape is seen on the dorsal and ventral surfaces of the endocast in lateral view (Figure 6.4), signifying the midbrain region between the cerebrum and cerebellum. Similar to the other two endocasts and other ornithopods, the midbrain of TMDC F140 is uninformative due to the absence of distinguishable anatomy visible in this region. Neither the optic lobes nor any vascularization could be seen. This is likely due to the thick dural covering that would have surrounded this region in life and because of the elongated shape of endocranial cavity. The stretched-out cavity shows that there was ample room for the brain anatomy, therefore furthering the likelihood no discernable or distinguished features will be seen. However, the mechanical reconstruction of the braincase from numerous bone pieces is further attributed to the absence of discernable in the endocast. At its caudalmost extent, the midbrain expands dorsoventrally and slightly laterally to form anteriormost extent of the cerebellum (Figure 6.4).

6.3.3. Hindbrain. The cerebellum is the elongated, laterally compressed oval-shaped feature of the hindbrain (Figure 6.4) with dimensions that are taller (48.0 mm) than wide (21.0 mm, Table 6.4). This gives a height to width ratio of 2.3, which is closer to the ratio calculated for OTM F138 (2.1) in comparison to 2.9 for TMDC F139, indicating that the cerebellum could increase more in width than height through ontogeny. The length of the cerebellum measures 37.3 mm (Table 6.4) and accounts for 27.1% of the total endocranial cavity length that was able to be reconstructed. A dural peak is not visible on the dorsal surface of the cerebellar surface, which is likely due to the elongation of the endocranial cavity during this ontogenetic stage.

Due to extreme fracturing in the braincase, only the trigeminal nerve (CN V) could be roughly reconstructed from the additional anatomical features that are known to extend

laterally from the cerebellum. Two longitudinally oriented cracks are present on both lateral walls of the braincase traversing directly through the median region where exact preservation of the nerves would be present (Figure 6.4). The estimated location of CN V was based on a second crack traversing dorsally perpendicular from the large longitudinally oriented crack on the left lateral wall of the braincase. At the truncation site of the dorsally oriented crack, a slight rounded region is observed at the ventral base of the opening. Knowing that a crack is more likely to develop from an already-existing opening in the braincase rather than a solid region and in compatibility with the rounded ventral base, CN V is inferred to have exited the braincase at this point. This is located in the rostral-to-median region of the cerebellum. The right lateral wall is in a worse preservational state than the left wall since the lateral wall dorsal to the longitudinal crack is overhanging the wall ventral to the crack.

The brainstem is the posteriormost region of the cranial endocast, extending caudally from the cerebellum. With this extension, the brainstem narrows, much more in height than in width, before slightly widening again to terminate at the foramen magnum. This caudalmost extent of the endocranial cavity and opening for the foramen magnum measures 32.0 mm in height and 22.8 mm in width (Table 6.4). Rostral to the foramen magnum, two foramina for cranial nerves were reconstructed. The shared foramen for the vagus (CN X) and accessory (CN XI), and possibly the glossopharyngeal (CN IX), nerves are seen extending laterally from the ventral region of the interpreted boundary of the cerebellum and brainstem. The hypoglossal nerve (CN XII) is observed caudal to the shared foramen and extends laterally from the lateroventral region of the brainstem. Similar to the methods used to approximate the aforementioned foramen locations, the foramen for
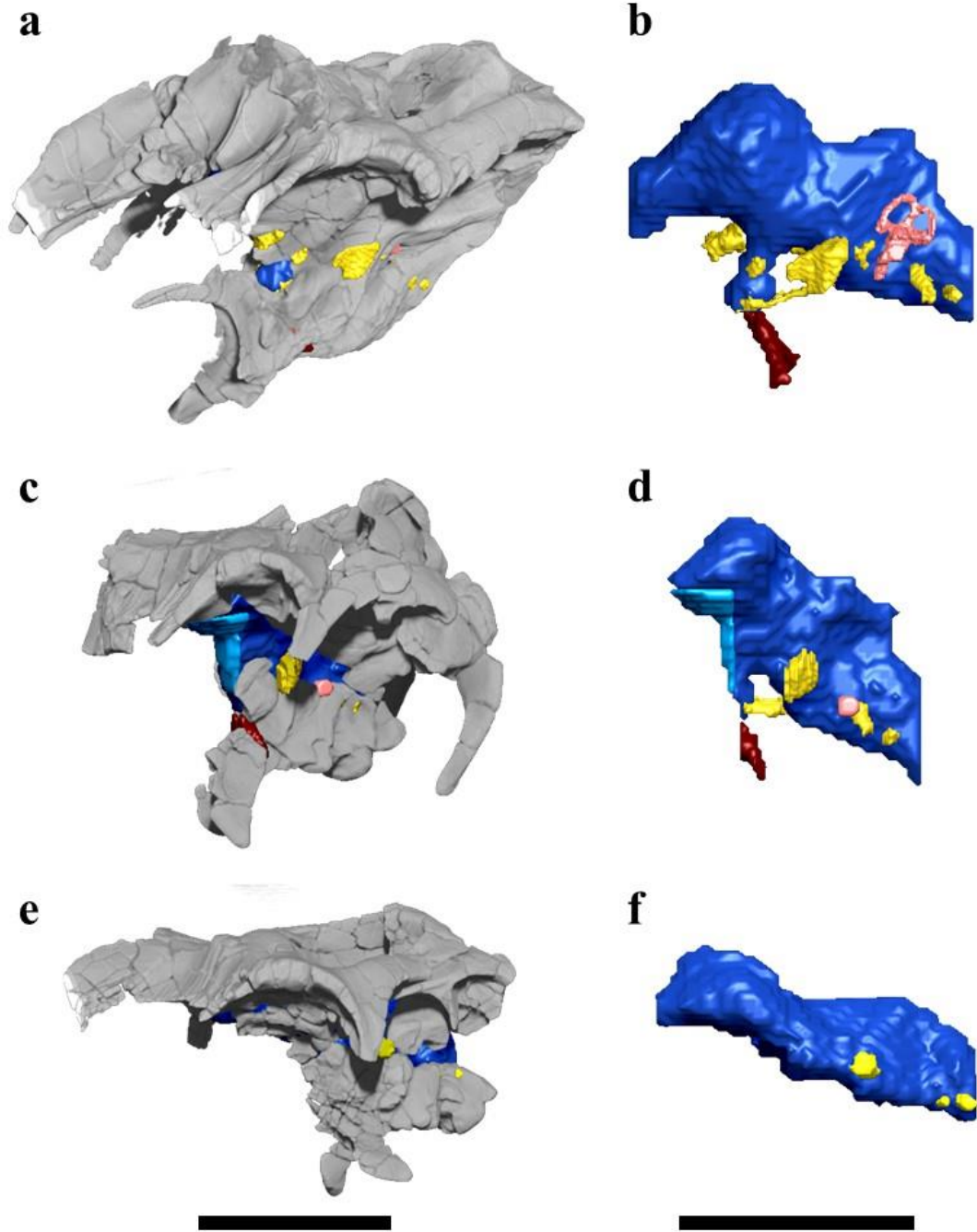
Figure 6.5 Comparison of braincases and reconstructed cranial endocasts of *M. peeblesorum* OTM F138 (a, b), TMDC F139 (c, d) and TMDC F140 (e, f).

both the shared CN IX-XI nerves and CN XII that could be observed on the left lateral wall of the braincase were bilaterally transformed and reconstructed on the right lateral wall.

6.3.4. Endosseous Labyrinth. The endosseous labyrinth is not preserved in TMDC F140 due to the extreme breakage and fracturing of the lateral walls of the braincase. Portions of the endosseous labyrinth, interpreted to be the semicircular canals were detected in a few segments on the left side of the braincase. These, however, could not be segmented as they did not connect or correlate with the overall structure that should be visible in the reptilian inner ear.

6.4. SENSORY AND ENCEPHALIZATION CALCULATIONS

The following sections describe the sensory and encephalization calculations employed on the *M. peeblesorum* endocasts.

6.4.1. Olfactory Ability. The olfactory ratio was calculated for OTM F138, but not for TMDC F139 and TMDC F140 due to the lack of preservation of the olfactory apparatus. The olfactory apparatus that was reconstructed accounts for 5.7% of the total endocranial volume in OTM F138, which is marginally greater than typical in adult saurolophine hadrosaurids (Evans et al., 2009). While the anteriormost portion of the olfactory bulb was not preserved for OTM F138, the interpreted widest portion of the olfactory bulb was able to be measured. The logarithmically scaled olfactory ratio that was calculated for OTM F138 was 1.76, which is slightly higher than the average value calculated for other ornithischians (Table 6.5).

Table 6.5. Olfactory ratio calculations of numerous dinosaurian taxa.

Family	Taxa	Specimen ID	Olfactory ratio	Source
Hadrosauridae	*Maiasaura peeblesorum*	OTM F138	1.76	This study
	Arenysaurus ardevoli	MPZ2008/1	0.64	Cruzado-Caballero et al. (2015)
	Corythosaurus sp.	CMN 34825	1.84	Evans et al. (2009)
	Hypacrosaurus altispinus	ROM 702	1.71	Evans et al. (2009)
Ankylosauridae	*Euoplocephalus tutus*	AMNH 5405	1.86	Leahey et al. (2015)
Ceratopsidae	*Triceratops* sp.	FPDM-V-9677	1.61	Sakagami & Kawabe (2020)
Dromaeosauridae	*Saurornitholestes langstoni*	Not recorded	1.54	Zelenitsky et al. (2009)
	Bambiraptor feinbergi	Not recorded	1.45	Zelenitsky et al. (2009)
	Velociraptor mongoliensis	Not recorded	1.55	Zelenitsky et al. (2009)
Oviraptoridae	*Citipati osmolskae*	Not recorded	1.50	Zelenitsky et al. (2009)
Pachycephalosauridae	*Stegoceras validum*	UALVP2	1.60	Bourke et al. (2014)
Stegosauridae	*Stegosaurus stenops*	CM 106	1.80	Leahey et al. (2015)
Thecelosauridae	*Thescelosaurus neglectus*	NCSM 15728	1.84	Button & Zanno (2023)
Tyrannosauridae	*Albertosaurus sarcophagus*	Not recorded	1.85	Zelenitsky et al. (2009)
	Gorgosaurus libratus	Not recorded	1.84	Zelenitsky et al. (2009)
	Tarbosaurus bataar	Not recorded	1.81	Zelenitsky et al. (2009)
	Tyrannosaurus rex	Not recorded	1.82-1.85	Zelenitsky et al. (2009)

6.4.2. Hearing Acuity. The hearing ranges were calculated only from OTM F138 due to the lack of preservation of the endosseous labyrinth and deformation on the braincases of TMDC F139 and TMDC F140. The calculated hearing ranges of OTM F138 were obtained from both the right and left endosseous labyrinths and averaged to find the desired hearing calculations.

Utilizing the equations of Walsh et al (2009), the calculated mean best hearing (MBH) and best frequency of hearing (BFR) were 2050 Hz and 3380 Hz (Table 6.6), respectively, suggesting that *M. peeblesorum* could hear and vocalize best at a narrow, middle range frequency window. Conversely, using the equations of Gleich et al. (2005) of scaling the cochlear duct length, the best frequency of hearing (BF) and maximum frequency of hearing (MF) were calculated to be 270 Hz and 1700 Hz (Table 6.6), respectively, a much lower and narrower frequency range than calculated using the methods of Walsh et al. (2009). Calculating the ranges using a similar approach as Evans et al. (2009), with the equation of Gleich et al. (2005) and not scaling the cochlear duct length for the basilar papilla, gives a BF of 57 Hz and MF of 1311 Hz (Table 6.6). This poses numerous questions about the accuracy of the three methods for calculating the hearing frequencies of extinct taxa. Across Dinosauria, all calculation methodologies have been employed and similarly produce drastically different values for the hearing frequencies attainable by taxa (Evans et al., 2009; Lautenschlager and Hübner, 2013; Sakagami and Kawabe, 2020; King et al., 2021). Table 6.6 shows the hearing frequency calculations for various ornithischian taxa utilizing the equations of Walsh et al. (2009), Gleich et al. (2005), and modified Gleich et al. (2005) (Evans et al., 2009) for a direct comparison of the contrasting auditory sensory results.

Table 6.6 Hearing frequency calculations of ornithischian taxa using various methods.

Family	Taxon	Specimen ID	Gleich et al. (2005)		Walsh et al. (2009)		Altered Gleich et al. (2005), employed by Evans et al. (2009)		Reference
			BF	**MF**	**BFR**	**MBH**	**BF**	**MF**	
Hadrosauridae	*Maiasaura peeblesorum* (adult)	OTM F138	266	1696	3380	2050	57	1311	This study
	Arenysaurus ardevoli (subadult-adult)	MPZ2008/1	967*	2808*	-	-	396*	1755*	Cruzado-Caballero et al. (2015)
	Corythosaurus sp. (juvenile)	ROM 759	794	2507	-	-	295	1586	Evans et al. (2009)
	Corythosaurus sp. (subadult)	CMN 34825	743	2412	-	-	267	1534	Evans et al. (2009)
	Hypacrosaurus altispinus (adult)	ROM 702	357	1700	-	-	80	1190	Evans et al. (2009)
	Lambeosaurus sp. (juvenile)	ROM 758	1245	3339	-	-	579	2110	Evans et al. (2009)
	Parasaurolophus sp. (juvenile)	RAM 1400	1626	4024	-	-	863	2617	Farke et al. (2013)

Table 6.6 Hearing frequency calculations of ornithischian taxa using various methods. (cont)

Ceratopsidae	*Triceratops* sp.	FPDM-V-9775	290	1577	2814*	1743*	65	1326	Sakagami and Kawabe (2020)
Dryosauridae	*Dysalotosaurus lettowvorbecki* (juvenile)	BSPG AS I 834	2694*	5993*	3571	2154	1841*	4420*	Lauten-schlager and Hübner (2013)
	Dysalotosaurus lettowvorbecki (subadult)	MB.R.137X	1152*	3149*	3490	2110	514*	1974*	Sobral et al. (2012)
Thescelosauridae	*Thescelosaurus neglectus*	NCSM 15728	~1100-1200	3051	1854	~1100-1200	-	-	Button and Zanno (2023)

* Calculated from linear extrapolated measurements from figures or measured values in tables displayed in referred study.
- Represents values that could not be determined through either of these methods.

6.4.3. Reptile Encephalization Quotient (REQ). The REQ value was only calculated from OTM F138. Since TMDC F139 and TMDC F140 were found in a mass bone bed that contained many ontogenetic stages of *Maiasaura peeblesorum* individuals, calculation errors could have occurred if a femur and humerus were selected as belonging to the braincases. Using the quadrupedal and bipedal formulas, the body mass of OTM F138 was estimated to be 2134.9 kg and 1251.7 kg, respectively. The mass of the brain was found to be 247.6 g. The REQ values for OTM F138 using the quadrupedal data set were calculated to be 2.1, assuming a 50% endocranial cavity fill, and 2.2, assuming a 60% endocranial cavity fill. The REQ values for OTM F138 using the bipedal data set were calculated to be 2.2, assuming a 50% endocranial cavity fill, and 2.3, assuming a 60% endocranial fill. Therefore, the range of REQ for an adult *M. peeblesorum* would be in the range of 2.1-2.3. This value indicates that the brain to body mass ratio of *M. peeblesorum* was average-to-large compared to its hadrosaurid and ornithopod relatives with a similar mass (Table 6.7).

6.4.4. Cerebrum Relative Volume (CRV). The cerebrum/endocranial volumetric relationship was calculated for all three cranial endocast specimens of the *Maiasaura peeblesorum* braincases in this study. OTM F138 showed a CRV of 49.6%, which represents the cerebral region to be housing almost half of the total endocranial space in the braincase. This value is larger compared to all other ornithopods, except *Arenysaurus ardevoli* (CRV = 53%; Cruzado-Caballero et al., 2015)*,* and very large when compared to other ornithischians. The calculated CRV values for TMDC F139 was similarly high with the cerebral hemispheres comprising 42.6% of the endocranial cavity. However, due to the fragmentary nature and missing portions of the basisphenoid, parasphenoid, and

Table 6.7. REQ values for various ornithopod and, more broadly, ornithischian taxa.

Family	Taxon	Specimen ID	REQ		Source
			50% fill	60% fill	
Hadrosauridae	*Maiasaura peeblesorum*	OTM F138	2.1-2.2	2.2-2.3	This study
	Amurosaurus riabinini	AEHM 1/232	2.0	2.4	Lauters et al. (2013)
	Edmontosaurus sp.	CMN 2289	1.7-2.5	2.0-2.9	Evans et al. (2009)
	Hypacrosaurus altispinus	ROM 702	2.3-2.7	3.7	Evans et al. (2009)
	Hadrosauriformes indet.	Not reported	0.6-2.6	-	Hurlburt (1996)
Ankylosauridae	*Euoplocephalus tutus*	AMNH 5405	0.8	1.0	Hopson (1977), Hopson (1979), Hurlburt (1996)
Camptosauridae	*Camptosaurus dispar*	Not reported	1.2	1.5	Jerison (1969), Hurlburt (1996)
Ceratopsidae	*Triceratops sp.*	FPDM-V-9677	0.5-0.8	0.6-1.0	Jerison (1969), Hurlburt (1996)

Table 6.7 REQ values for various ornithopod and, more broadly, ornithischian taxa. (cont)

Iguanodontidae	*Iguanodon bernissartensis*	RBINS R51	1.9	2.2	Lauters et al. (2012a)
	Lurdusaurus arenatus	MNHN GDF 1700	1.2	1.5	Lauters et al. (2012a)
	Mantellisaurus atherfieldensis	RBINS R57	1.7	2.0	Lauters et al. (2013)
	Proa valdearinnoensis	MAP AR-1-2012	2.5	2.8	Knoll et al. (2021)
Protoceratopsidae	*Protoceratops andrewsi*	Not reported	1.9	2.3	Jerison (1969)
Psittacosauridae	*Psittacosaurus lujiatunensis*	IVPP V14341	1.8	2.1	Zhao et al. (2007)
Stegosauridae	*Kentrosaurus aethiopicus*	Not reported	0.4-0.5	0.5-0.6	Hopson (1977), Hopson (1979), Hurlburt (1996)
Thescelosauridae	*Thescelosaurus neglectus*	NCSM 15728	0.7-0.8	0.9-1.0	Button and Zanno (2023)

- Not calculated in study

presphenoid bones constraining the anteriormost extent of the braincase of TMDC F139, the area ventral to the cerebral hemispheres was interpreted based on knowledge of the endocrania shape. This could have affected the calculated TMDC F139 CRV value because significant portions of the endocranial body and cerebrum could not have been reconstructed. TMDC F140 also showed a significant CRV value of 39.7% relative to the braincase size and interpreted younger ontogenetic age.

Table 6.8. CRV ratios for various dinosaurian and avalian taxa.

Family	Taxon	Specimen ID	CRV	Source
Hadrosauridae	*Maiasaura peeblesorum*	OTM F138	49.6%	This study
	Maiasaura peeblesorum	TMDC F139	42.6%	This study
	Maiasaura peeblesorum	TMDC F140	39.7%	This study
	Amurosaurus riabinini	AEHM 1/232	30%	Lauters et al. (2023)
	Arenysaurus ardevoli	MPZ2008/1	53%	Cruzado-Caballero et al. (2015)
	Corythosaurus sp.	CMN 34825	38%	Evans et al. (2009)
	Corythosaurus sp.	ROM 759	45%	Evans et al. (2009)
	Edmontosaurus	CMN 2289	~45%	Evans et al. (2009)
	Gryposaurus	AMNH 5350	~45%	Evans et al. (2009)
	Hypacrosaurus altispinus	ROM 702	41-43%	Evans et al. (2009)
	Lambeosaurus sp.	ROM 758	38%	Evans et al. (2009)
Archaeopterygidae	*Archaeopteryx lithographica*	Unknown specimen	45%	Jerison (1968)
Iguanodontidae	*Iguanodon bernissartensis*	RBINS R51	19%	Lauters et al. (2023)
	Lurdusaurus arenatus	MNHN GDF 1700	19%	Lauters et al. (2023)
Oviraptoridae	*Citipati osmolsake*	IGM 100/973	43%	Balanoff et al. (2018)
	Conchoraptor gracilis	ZPAL MgD-I/95	43%	Kundrat (2007)
	Incisivosaurus gauthieri	IVPP V 13326	45%	Balanoff et al. (2009)
Tyrannosauridae	*Tyrannosaurus rex*	AMNH FR 5117	33%	Witmer & Ridgely (2009)

7. DISCUSSION

7.1. ENDOCAST RECONSTRUCTION

The following sections discuss the ontogenetic stage and morphological characteristics of the *M. peeblesorum* endocasts.

7.1.1. Ontogenetic Stage. The exact ontogenetic age of each of the three *Maiasaura peeblesorum* specimens used in this study is indeterminate. In the cases of TMDC F139 and TMDC F140, specific growth stages cannot be accurately determined due to their recovery from a mass bone bed with no postcranial elements directly associated with either of the braincases. Although OTM F138 preserved numerous postcranial elements that could be utilized to determine ontogeny, no histological testing has been completed on these features. However, as a result of the immense diversification and number of hadrosaur species from the Late Cretaceous (Varricchio and Horner, 1993; Brett-Surman, 1997), the ontogenetic stages of hadrosaurs, and specifically *M. peeblesorum*, have been well-studied (Horner et al., 2000; Woodward et al., 2015). By referencing these studies, an approximate ontogenetic stage for each of the three braincases can be deduced through various non-histological methods.

Horner et al. (2000) recognized six ontogenetic stages for *M. peeblesorum* based on the histological patterns observed in the femur and the relative size of the individuals. These were attained through destructive testing methods to determine the lines of arrested growth (LAGs) and the bone wall thickness (BWT) observed in the femur in association with femoral linear measurements. *M. peeblesorum* is an exemplar taxon that represented the growth and development of Late Cretaceous hadrosaurs in this study since nestling

juveniles to mature adults are well-represented in the fossil record, allowing for ontogenetic stages and their parameters to be described and compared across Hadrosauridae (Table 7.1).

Table 7.1. Ontogenetic stages and their parameters observed from histological testing by Horner et al. (2000). Table edited from Horner et al. (2000).

Ontogenetic Stage	Femur Length/BWT	LAGs	Approx. Body Length	Specimen Number
Early Nestling	7 cm / 2.5 mm	0	45 cm	YPM-PU 22432
Late Nestling	12 cm / 2-4 mm	0	90 cm	YPM-PU 22400
Early Juvenile	18 cm / 3-7 mm	0	120 cm	YPM-PU 22472
Late Juvenile	50 cm / 10-15 mm	0-1	3.5 m	MOR-005JV
Subadult	68 cm / 11-22 mm	1-5	4.7 m	MOR-005SA
Adult	100 cm/ 13-22 mm	2-6	7.0 m	MOR-005A

The femur associated with OTM F138 measures 103 cm in length, suggesting that the specimen belonged to a fully-grown adult based on the measurements and ontogenetic stages of Horner et al. (2000). Since no femora are associated with TMDC F139 and TMDC F140, other characteristics were used to interpret their ontogenetic stages. Although this is a flawed method, the only foreseeable solution for interpreting the ontogeny of TMDC F139 and TMDC F140 is comparative analysis with the cranial endocasts and/or skull lengths of saurolophine and closely related lambeosaurine hadrosaurs that have been

assigned growth stages. Optimally, cranial element measurements of each respective specimen in Horner et al. (2000) would have been described and correlated with the growth stages to enable for a more accurate comparison of the *M. peeblesorum* braincases used in this study. Inaccurate assumptions and interpretations about the ontogenetic stage of TMDC F139 and TMDC F140 could be influenced by numerous factors when comparing them to other related taxa, such as taphonomic deformation, inadequate preservation of the braincase, reconstruction errors, and physiological and morphological differences associated with relative body proportions, derivation, and the development of the nasal crest – or lack thereof in saurolophines. However, identifying an approximate ontogenetic stage for the braincases of TMDC F139 and TMDC F140 is crucial to understanding the development of the sensory systems and behavioral functions in *M. peeblesorum* with age.

As an example of how interspecific comparisons can vastly change biological, physiological, and ontogenetic interpretations, the cranial and endocranial measurements of a saurolophine hadrosaur can be compared to a lambeosaurine hadrosaur. Unfortunately, no other saurolophine endocranial cavities have been reconstructed, thus a comparison with a lambeosaurine is the most optimal method in this case. As noted earlier, the measured femur length of *M. peeblesorum* OTM F138 in comparison to histologically sampled specimens (Horner et al., 2000) suggests it was an adult. Utilizing the morphological, linear, volumetric observations associated with the cranial endocast and skull of this age-known specimen relative to the measurements of a lambeosaurine hadrosaur however provides differing results in the ontogenetic growth stage of OTM F138. Geologically coeval and closely related, the lambeosaurine hadrosaur *Hypacrosaurus altispinus* ROM 702 (Evans et al., 2009) can be used as a suitable example: *M. peeblesorum* has skull and

cranial endocast lengths of 769 mm and 149.0 mm, respectively, and an endocranial volume of 253.3 cm^3, whereas *H. altispinus* has skull and cranial endocast lengths of ~700 mm and 204.0 mm, respectively, and an endocranial volume of 289.9 cm^3 (Evans et al., 2009). While the skull length of *M. peeblesorum* is very similar to *H. altispinus*, the endocranial length is closer to that of a subadult lambeosaurine *Corythosaurus*, which measures 142.0 mm (Evans et al., 2009). However, the endocranial volumes of *M. peeblesorum* and *H. altispinus* are within a reasonable similarity to one another, especially due to the incompleteness of the anteriormost olfactory apparatus for OTM F138.

To account for and better understand the endocast length difference between the two adults, the REQ values can be compared; this endocranial mass to body mass ratio shows if the measured values are proportionate to each other given the body size difference between saurolophine *M. peeblesorum* and lambeosaurine *H. altispinus*. It is worth noting that comparing the REQ of individuals is a more accurate form of determining the ontogenetic stage, even though the REQ values of TMDC F139 and TMDC F140 cannot be calculated. *H. altispinus* ROM 702 did not have an associated femur, therefore the REQ from a different *H. altispinus* specimen (CMN 8501) was used to calculate the REQ for the taxon (Evans et al., 2009), altering the value calculated for *H. altispinus*. Regardless, the REQ of *M. peeblesorum* calculated in this study was approximately 2.1-2.3, while the REQ of *H. altispinus* was found to be 2.3-3.7 (Evans et al., 2009), assuming a 50-60% endocranial fill for both specimens. Given the body mass of the *H. altispinus* specimen was approximately larger by up to 1200 kg, these REQ values are inferred to be very similar. Therefore, a cranial endocast length of *M. peeblesorum*, or any other similarly sized and temporally concurrent saurolophine dinosaur, could be as small as approximately three-

quarters the length of a relatively similar growth stage lambeosaurine dinosaur. However, these preliminary results and comparison of the skull and endocranial cavity lengths for saurolophines and lambeosaurines need further investigation because these interpretations are based solely on the calculation methods employed here for one specimen. The length difference between the two tribes has been previously noted and is believed to be attributed to the caudodorsal elongation of the nasal cavities during the development of the crest in lambeosaurines (Evans et al., 2009). Through this convoluted method, one can see how preservation quality and lack of associated bone material can make both quantitative and qualitative analyses very difficult in paleoneurology.

The length and volume of the cranial endocast for TMDC F139 are 129.7 mm and 134.4 cm^3, respectively. TMDC F139 is, however, assumed to have undergone a combination of anteroposterior and dorsoventral deformation, thus slightly altering the measurable length. This deformation should not have an impact on the interpretations that are drawn from the usable endocranial reconstruction since the volumetric analysis and anatomy were not affected. Nonetheless, for the purpose of interpreting the ontogenetic stage, longitudinal shortening slightly affects the comparability and should be noted. The length and volume of the cranial endocast for TMDC F140 is 137.5 mm and 123.8 cm^3, respectively. The length measurements for both specimens fall between the measured values of two juvenile specimens, *Lambeosaurus* sp. (113.2 mm) and incomplete *Corythosaurus* sp. (110.1 mm), and subadult *Corythosaurus* sp. (142.0 mm) (Evans et al., 2009). Their respective endocast volumes, including the olfactory system, are 94.1 cm^3, 97.9 cm^3, and 145.4 cm^3, respectively. Therefore, given the knowledge that the endocranial lengths will be shorter but will have similar endocranial volumes, *M. peeblesorum* TMDC

F139 and TMDC F140 are assumed to be late juvenile to subadult ontogenetic stages. The conditions of these two braincases and inability to precisely calculate the ages of each specimen histologically make it difficult to determine which specimen was ontogenetically more mature.

7.1.2. Morphological Characteristics and Comparisons. The morphologies of the three reconstructed cranial endocast in this study are similar to those of related Late Cretaceous hadrosaurs *Hypacrosaurus altispinus*, *Corythosaurus* sp., and *Lambeosaurus* sp. (Evans et al., 2009). Differing morphological traits most easily observed in the endocrania of Late Cretaceous hadrosaurs (including the cranial endocast of this study and Evans et al., 2009) to more basal ornithopods (such as those of Lauters et al., 2012, 2013, 2022) are the enlargement of the entire endocrania body, enlargement of the cerebral hemispheres relative to the endocrania body and body mass, and the shortening and widening of the olfactory tract (Evans, 2005; Evans et al., 2009; Lauters et al., 2012, 2012, 2022; Lautenschlager and Hübner, 2013). This can directly be seen in the CRV, REQ, and higher olfaction acuity for the Late Cretaceous hadrosaurs (see Cerebrum Relative Volume, Reptile Encephalization Quotient, and Olfactory Ability discussions, respectively). Measurement and morphological endocrania comparisons of various Late Cretaceous hadrosaur taxa can be seen in Table 7.2 and Figure 7.1, respectively, for insight into the similarity of endocrania features. Given taphonomic deformation and damage is going to directly alter characteristics and measurements, differences resulting from these natural processes are noted, but not looked at as variations in the endocranial anatomy and morphology. This is especially important for TMDC F139 and TMDC F140 which have undergone severe postmortem alterations.

The morphology of the endosseous labyrinth varies little in the Ornithopoda taxa the endosseous labyrinths have been reconstructed for; the greatest variation observable is the lengthening of the cochlear duct in the Late Cretaceous ornithopods relative to the Early-Middle Cretaceous ornithopods. This corresponds to the lower frequencies of hearing attainable for the former taxa than the latter (see Hearing Acuity discussion). Regards about the attainable hearing in saurolophine and lambeosaurine hadrosaurs has been postulated before (Evans et al., 2005; 2009). This theory is supported by the small length and width difference seen in saurolophine *M. peeblesorum* OTM F138 and lambeosaurine *Hypacrosaurus altispinus* ROM 702 (Evans et al., 2009) that alters the interpreted attainable hearing frequencies the two taxa could hear. The three semicircular canals of OTM F138 are consistent in shape and size with that seen in *H. altispinus* ROM 702 (Evans et al., 2009).

The cephalic and pontine flexures of OTM F138 and TMDC F149 resemble the more obtuse angled flexures characteristics of ornithopods, and more broadly ornithischians (Evans et al., 2009; Lauters et al., 2012; 2013; 2022; Lautenschlager and Hübner, 2013; Button and Zanno, 2023). The cephalic and pontine flexure of TMDC F139 cannot be compared well to other specimens due to the extreme taphonomic deformation to the braincase.

Anatomically, the cranial endocasts of OTM F138, TMDC F139, and TMDC F140 are highly analogous to the cranial endocasts of other taxa in Ornithopoda. All the main components of the endocast are visible and are in their standard localities of the dinosaurian brain (see Appendix 2 for reference). The presence of a highly defined dural peak on the dorsal surface of the cerebellum is absent in the three endocasts of this study – though a
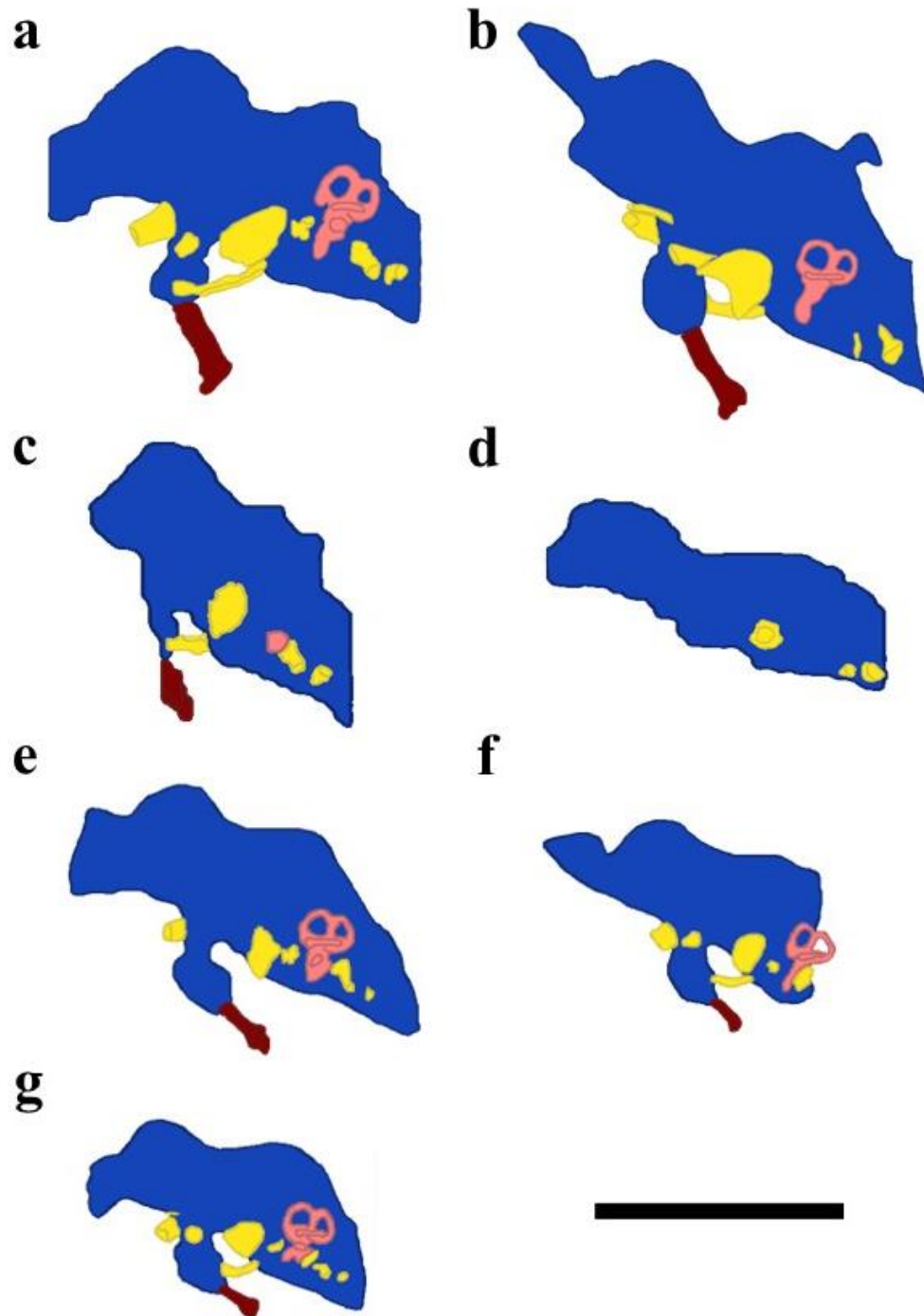
Figure 7.1 Line drawings of the cranial endocast from Late Cretaceous hadrosaur taxa (a) adult *M. peebleosurm* OTM F138, (b) adult *H. altipinus* ROM 702, (c) late juvenile-subadult *M. peeblesorum* TMDC F139, (d) late juvenile-subadult *M. peeblesorum* TMDC F140, (e) subadult *Corythosaurus* sp. CMN 34825, (f) juvenile *Corythosaurus* sp. ROM 759, and (g) juvenile *Lambeosaurus* sp. ROM 758. Endocast reconstruction of taxa other than *M. peeblesorum* provided by Evans et al. (2009). Scale bar = 100 mm.

Table 7.2 Volumetric and linear measurements for Late Cretaceous hadrosaur taxa.

Taxon	Specimen Number	Endocast Length (mm)	Total Endocast Volume (cm³)	Cerebrum max. width (mm)	Cerebrum volume (cm³)
Maiasaura peeblesorum	OTM F138 (adult)	149.0	253.3	59.3	118.5
Maiasaura peeblesorum	TMDC F139 (late juvenile–subadult)	129.7	134.4	48.5	57.2
Maiasaura peeblesorum	TMDC F140 (late juvenile–subadult)	137.5	123.7	53.7	48.7
*Hypacrosaurus altispinus**	ROM 702 (adult)	204.0	289.9	43.0	117.5
Corythosaurus sp.*	CMN 34825 (subadult)	142.0	145.4	46.5	51.1
Corythosaurus sp.*	ROM 759 (juvenile)	110.1 (incomplete)	97.9	44.7	41.6
Lambeosaurus sp.*	ROM 758 (juvenile)	113.2	94.1	63.2	35.1

*Data for taxa provided by Evans et al. (2009).

slight one is noted in OTM F138. However, it is not as prominent as the dorsal peak observed in *Hypacrosaurus altispinus* ROM 702 (see Figure 7a of Evans et al., 2009). Regardless, dorsal peaks are a common trait observed in ornithopod taxa (Evans et al., 2009; Lauters et al., 2012; 2013; 2022; Button and Zanno, 2023). The lack of a dural peak in OTM F138, TMDC F139, and TMDC F140 that is regarded as easily viewable in hadrosaurs (Evans, 2005; Evans et al., 2009) could be entirely phylogenetically based; limited cranial endocasts from saurolophine have been reconstructed, therefore

saurolophines may not exhibit a dural peak to the same degree – if at all – to their lambeosaurine relatives. Therefore, limitations in comparing the peak seen in *M. peeblesorum* to the peaks in the lambeosaurines described in Evans (2005) and Evans et al. (2009) are present. The low quality of CT scanner used in this study could also be affecting the anatomy visible.

7.2. NEUROSENSORY FUNCTION

The following sections discuss the sensory function and volumetric analyzes calculated on the *M. peeblesorum* endocasts.

7.2.1. Olfactory Ability. The development of olfaction throughout Dinosauria – and more broadly Tetrapoda – is a derived trait for both herbivorous (Zelenitsky et al., 2009; Evans et al., 2009; Sakagami and Kawabe, 2020) and carnivorous taxa (Zelenitsky et al., 2009, 2011). The highest olfactory ratios calculated across Dinosauria to date have been from Late Cretaceous taxa as follows: the theropods *Tyrannosaurus rex* (1.82-1.85: Zelenisky et al., 2009), *Gorgosaurus libratus* (1.84: Zelenitsky et al., 2009), and *Albertosaurus sarcophagus* (1.85: Zelenitsky et al., 2009); the ankylosaurid *Euplocephalus tutus* (1.86: Sakagami and Kawabe, 2020); the neornithischian *Thescelosaurus neglectus* (1.84: Button and Zanno, 2023); and the ornithopod *Corythosaurus* sp. (1.84: Evans et al., 2009). A distinct trend can be observed regarding when the aforementioned organisms lived: all were found in Upper Cretaceous formations. Direct quantitative evidence supports the higher olfaction acuity in these Upper Cretaceous dinosaurs, although noteworthy is the possible collection, research, and preservation bias for these taxa. The enhancement of the olfactory sense with time and across species is consistent with a

heightened sense of smell for prey identification and predator avoidance, promoting evolutionary success.

The olfactory ratio calculated for *M. peeblesorum* (OTM F138) shows an average value when compared to other ornithopods and, more broadly, ornithischians (see Table 6.5). The ratio for *M. peeblesorum* is low when compared to highly specialized Late Cretaceous carnivorous dinosaurs and aligns more with an herbivorous diet similar to that of its ornithischian relatives and their analogous olfaction ratios. However, as the olfactory ratios of numerous ornithischian species is greater than or equivalent to those of these Late Cretaceous predatory dinosaurs, the olfactory ratio value itself does not necessarily determine the trophic ecology of the organism without further context. Broader context with other morphological traits (e.g., teeth (Ballell et al., 2022) or morphology of the pelvic girdle (Weishampel and Norman, 1989; Makovicky and Zanno, 2011)) or ecological studies (i.e. coprolite analysis (Chin, 2007) on the taxa needs to be employed to assess these ecological traits with certainty.

The olfaction ratio calculated for *M. peeblesorum* could be a lower representation of the interpreted olfactory acuity, due to the non-preservation of the entire olfactory bulb in OTM F138. Comparing the morphology and size of the reconstructed olfactory apparatus of OTM F138 to other ornithopods (see Evans et al., 2009, Figure 5 and Table 2; Lauters et al., 2012, Figure 16.3) it appears that the widest portion of the olfactory bulbs is at or very near the anteriormost preserved region of the endocast. Furthermore, it has been noted that the volume of the olfactory apparatus in most ornithopods, specifically saurolophines and lambeosaurines, accounts for ~5% of the total endocranial volume (Evans et al., 2009; Lauters et al., 2012). The olfactory apparatus reconstructed for *M.*

peeblesorum OTM F138 accounts for 5.7% of the total endocranial volume, thereby inferring that almost the entire olfactory system is represented in the specimen. Since the size of the olfactory bulbs has been shown to correlate with the olfaction development (Rombaux et al., 2009), measuring the most accurate representation of the olfactory bulbs is important for sensory calculation and comparison.

Among ornithopods, very few olfactory ratios have been calculated for basal taxa. Knoll et al. (2021) described and reconstructed three cranial endocasts of the Early Cretaceous iguanodontian *Proa valdearinnoensis*, two of which preserved the olfactory lobes. However, neither of the olfactory bulbs was measured and scale bars were not included in the figures; therefore, olfactory ratios could not be calculated for their project. Knoll et al. (2021) note that the olfactory lobes are very large in *P. valdearinnoensis*, unlike the narrow olfactory bulbs exhibited by lambeosaurines (Knoll et al., 2021). Therefore, quantitative comparisons cannot be made.

With *M. peeblesorum* showing an average olfactory acuity across Ornithopoda and Dinosauria (Table 6.5), it does not appear that the sense of smell had a great influence on successful parental care. Although *M. peeblesorum* is evolutionarily separated from crocodylomorphs, *Alligator mississippiensis* can be used as a modern analog to illustrate how an olfactory acuity can influence complex behavior such as parental care. The olfactory ratio for *Alligator mississippiensis* has been calculated to be in the range of 1.70-1.74 (Zelenisky et al., 2009), a value slightly less than that of *M. peeblesorum*. Modern studies on the nesting areas of *Alligator mississippiensis* show a successful form of parental care in regard to warning off potential threats and noting when juveniles from other pods interacted with the organism's offspring (Hunt and Watanabe, 1982). Furthermore, studies

have shown that crocodilians were able to presumably identify food sources based on olfaction alone, whether in a terrestrial or fluvial environment (e.g., Reber, 2020). This leads to the conclusion that *M. peeblesorum* did not exhibit an enhanced olfactory ratio compared to its Late Cretaceous dinosaurian or modern archosaurian relatives. Therefore, the average olfactory acuity demonstrated by *Maiasaura* was not specialized in regard to the parental behaviors that the taxa is well-known for.

  7.2.2. Hearing Acuity. The hearing frequencies of *M. peeblesorum* OTM F138 were calculated using the three methods – Gleich et al. (2005): BF: 266 Hz and MF: 1696 Hz; Walsh et al. (2009): BFR: 3380 Hz and MBH: 2050 Hz; and the altered Gleich et al. (2005) that was employed by Evans et al. (2009): BF: 57 Hz and MF: 1311 Hz. Employing these three methods provides the broadest comparable study of the saurolophine hearing frequency against lambeosaurine, ornithopod, and ornithischian taxa. While the three unique methods give a wide auditory range from 57-3380 Hz, these calculated low values of hearing frequencies are similar to other ornithopods (Table 6.6). To date, no other saurolophine endosseous labyrinths have been reconstructed. The endosseous labyrinths belonging to lambeosaurine hadrosaurs have been reconstructed and quantitatively analyzed in great amount due to the curiosity behind the nasal crest functionality relative sound production and resonation, and therein hearing frequencies (Evans et al., 2009; Sobral et al., 2012; Farke et al., 2013; Lautenschlager and Hübner, 2013; Cruzado-Caballero et al., 2015). Since not all three methods for calculating the hearing frequencies were employed in these studies, comparisons across all the methods could not be made. Interestingly, the best hearing frequencies and maximum hearing frequencies of *M. peeblesorum* and the ceratopsian *Triceratops* sp. NCSM 15728 (Sakagami and Kawabe,

2020) were the most similar for both sets of Gleich et al. (2005) equations. They were used to infer that adult saurolophines and ceratopsians could possibly best hear, and thereby vocalize, in a similar narrow, low frequency range between 50-1700 Hz (Table 6.6). Unfortunately, an approximate ontogenetic stage was not assigned to the *Triceratops* sp. specimen NCSM 15728, and no age correlation could be inferred.

The hearing frequency of the adult lambeosaurine *Hypacrosaurus altispinus* ROM 702 is relatively similar to *M. peeblesorum* using the two methods of Gleich et al. (2005) – with a BF of 80-357 and MF of 1190-1700 (Evans et al., 2009) – but the hearing frequencies calculated for other lambeosaurine taxa greatly differs (Table 6.6). The difference between the attainable hearing frequencies of saurolophines and lambeosaurines is interpretably attributed to the development of nasal crests in lambeosaurines, which is believed to have altered their hearing to slightly higher frequencies than the saurolophines (Evans et al., 2009; Sobral et al., 2012; Lautenschlager and Hübner, 2013). Ontogenetic age could also alter the comparisons between the taxa shown in Table 6.6, given that the majority of calculations were based on from ontogenetically young specimens. Logically an adult organism should be able to hear a juvenile's vocalization, and vice versa, with the interpretation that an organism will most likely be able to vocalize in the range they can hear, therefore indicating that the auditory senses should be relatively similar throughout all stages of ontogeny. However, broad assumptions about the attainable hearing frequencies of extinct taxa cannot be made because biological and ecological characteristics possibly severely affect the ranges. For example, age segregation within a taxon group (Zhao et al., 2014) could limit the communication between different

ontogenetic stages, therefore hindering the need for the inner ears to develop the capabilities of enhanced hearing frequencies.

Studies of the modern American alligators (*Alligator mississippiensis*) show that limited communication is performed between ontogenetically young and old organisms. Upon hatching, nestlings make high pitched called, signaling to the female adult they have hatched (Joanen and McNease, 1989). After this process though, almost non-existent communication is demonstrated between the juveniles and adults (Joanen and McNease, 1989). Communication between alligators is present, and significantly peaks, during mating season (Joanen and McNease, 1989) with deep bellowing and low grunts demonstrated during this time between sexually mature subadult-adult stages (Garrick et al., 1978; Joanen and McNease, 1989). *M. peeblesorum* would be an exemplary taxon to test the retention or change of hearing capabilities through ontogeny, since the known parental care could allow for a direct examination into the hearing frequencies that would have to be attainable to hear the youth. Evident though is *M. peeblesorum* had a sufficient hearing range to hear both juveniles and adults, as implied by fossilized evidence of parental care and gregarious life patterns. However, the degree to which this sensory function was – or was not – specialized is indeterminable without a full ontogenetic sequence.

The acquisition of advanced auditory senses is crucial for the success of a single individual in their given environment for activities such as predation. Expanding this to a group situation involving numerous organisms increases the need for an acute sensory system for the evolutionary success of a taxon. To maintain their gregarious lifestyle, it would have been vital that *M. peeblesorum* had hearing capabilities that aided in the

protection of individuals in nesting colonies. Furthermore, with the knowledge that *M. peeblesorum* had similar auditory senses to that of other saurolophines and lambeosaurines, this supports the interpretation that related hadrosaurs were of a gregarious lifestyle as well. Across the limited database for ornithischian taxa, the calculated auditory frequencies appear to be similar in the relative range of *M. peeblesorum*, which attained a low frequency and narrow range.

      7.2.3. Reptile Encephalization Quotient (REQ). Intelligence in extinct taxa can be difficult to quantify within organisms, especially when behavioral and ecological characteristics cannot be directly studied. Encephalization quotients have been shown to correlate with an increase in complexity of behaviors (Jerison, 1969; Jerison, 1973; Hopson, 1977; Button and Zanno, 2023). Therefore, calculating the REQ for extinct dinosaurian taxa allows for the determination of the likelihood that they had the capabilities of behavioral complexity. By observing the volume of the brain relative to the body mass to determine if the brain had a specialized increase through ontogenetic or evolutionary processes, insights into the probability of different behavioral and ecological traits can be inferred.

      The REQ value calculated for *M. peeblesorum* is average when compared to related ornithopods and other ornithischian taxa (Table 6.7). Expanding across Dinosauria, *M. peeblesorum* still demonstrates an average REQ value; higher than those calculated for taxa in Sauropoda (Franzosa, 2004; Sereno et al., 2007) and Ceratopsia (Zhou et al., 2007), while lower than most REQs calculated in Theropoda (Franzosa, 2004). This is a similar trend that is observed across all of Ornithopoda (Lauters et al., 2023). The higher REQ in Theropoda, especially that of Eumaniraptorans, has been attributed to the development of

complex thinking for predation (Franzosa, 2004) and the acquisition of flight in later derived taxa (Balanoff et al., 2013), while the low REQ in Ceratopsia has been linked to a passive and defensive strategy along with their frills and horns, as a means of predator defense and deterrence (Bauchot et al., 1977). Since ornithopods did not have defensive mechanisms that were similar to ceratopsians nor predatory behaviors as carnivores, the high encephalization quotient observed in Ornithopoda, relative to other ornithischian taxa, could be linked to the need for higher complex abilities to avoid predation (Persons, 2011; Persons and Currie, 2014). This could have been achieved through gregarious social behaviors and maternal care of protecting young, both of which have been directly identified in the fossilization record for ornithopods (Varricchio and Horner, 1993).

With the immense quantity of mass bone beds in the Two Medicine Formation recording a gregarious lifestyle and nesting behaviors of *M. peeblesorum*, assumptions that the REQ value would be higher compared to those of other ornithopods and ornithischians are reasonable. The calculation performed on OTM F138 shows an average value (2.1-2.3), signifying that the brain volume of *M. peeblesorum* was not greater than that expected in dinosaurs with the same relative body mass. Furthermore, the REQ of *M. peeblesorum* is situated closer to that of the Middle Jurassic *Iguanodon bernissartensis* (1.9-2.2: Lauters et al., 2012a) and Early Cretaceous *Protoceratops andrewsi* (1.9-2.3: Jerison, 1969), rather than its relative Late Cretaceous hadrosaurs. With the knowledge that the Late Cretaceous hadrosaurs were greatly specialized in numerous morphological and behavioral aspects, the similarity between *M. peeblesorum* and more basal ornithopod and ornithischian taxa is surprising. This unexpected comparison stems from the fact that complex behaviors and high intelligence have never been associated with these earlier dinosaurian taxa, while

these traits are the main characteristics described with *M. peeblesorum*. Note that this REQ value for *M. peeblesorum* is based on the sole reconstruction of OTM F138 in this study. However, the lack of enlargement of the entire brain relative to the body mass observed in *M. peeblesorum* suggest that further inquiries about the ecological behavior associated with higher REQ values should be tested, especially regarding the possibilities of linking complex behaviors to sociality or predator avoidance in all Jurassic to Late Cretaceous ornithischians. This average REQ, coupled with the knowledge that gregarious and parental actions were demonstrated by *M. peeblesorum*, shows that organisms did not necessarily need a highly derived and volumetrically large brain to successfully demonstrate complex behaviors.

7.2.4. Cerebrum Relative Volume (CRV). Modern research trends show that the enlargement of the cerebral hemispheres relative to the endocranial cavity is associated with increased complexity of behaviors (Button and Zanno, 2023). Therefore, the cerebral/endocranial volumetric measurement is calculated to infer the likelihood of an organism exhibiting these behaviors. Since the cerebral hemispheres are the regions of the brain where informational processing and sensory data coalescing occurs, a CRV ratio calculation is the best way to interpret an extinct organism's capabilities of exhibiting complex behavior, second only to direct fossilization evidence of these traits. With complex and parental behaviors directly observed in the fossilized record for *M. peeblesorum*, questions regarding how the CRV of this dinosaur compares with its archosaurian relatives can be postulated.

The cerebrum volume to endocranial cavity volume of *M. peeblesorum* OTM F138 is much greater than almost all other CRV values calculated throughout Ornithopoda. This

value (49.6%) is only less than that of *Arenysaurus ardevoli* (CRV: 53%; Cruzado-Caballero et al., 2015) however minimally ~5% higher than those of other related saurlophine and lambeosaurine hadrosaurs (*Amurosaurus* (Lauters et al., 2013)*, Corythosaurus* (Evans et al., 2009)*, Edmontosaurus* (Evans et al., 2009), *Gryposaurus* (Evans et al., 2009), *Hypacrosaurus* (Evans et al., 2009), *Lambeosaurus* (Evans et al., 2009), and well over twice the CRV calculated for more basal ornithopods (*Iguanodon* (Lauters et al., 2012), *Lurdusaurus* (Lauters et al., 2012)). Similar to OTM F138, TMDC F139 and TMDC F140 demonstrate high CRV values, 42.6% and 39.4% respectively, compared to their assumed ontogenetic stages. A very distinct plesiomorphic feature of the brain of ornithopods is the enlargement and rounding of the cerebral hemisphere region, relative to the rest of the brain (Giffin, 1989; Lauters et al., 2023), which can be observed in this study. This enabled inferences to be made about how confidently we can attribute complex behaviors to the ecological lifestyles of *M. peeblesorum*, across Ornithopoda, and relative to modern Archosauria.

Throughout Dinosauria, ornithopods and maniraptorans display the greatest CRV; specifically, the highest CRV value calculated across Dinosauria to date is for the Late Cretaceous European lambeosaurine *Arenysaurus ardevoli* with a cerebral hemisphere to endocrania cavity volumetric ratio of 53% (Crusado-Caballero), with *M. peeblesorum* the next greatest. Other high CRV values are found in the Late Cretaceous *Gryposaurus, Edmontosaurus,* and *Corythosaurus* – all showing a cerebral volume that encompasses ~45% of the endocrania body (Evans et al., 2009) – and the Early to Late Cretaceous *Incisivosaurus gauthieri* (Balanoff et al., 2009) *Conchoraptor gracilis*, (Kundrat, 2007), and *Citipati osmolsake* (Balanoff et al., 2018) – all showing cerebral volumes that comprise

43-45% of the endocrania body. Demonstration of behaviorally complex actions have been well associated with these taxa, ranging from gregarious nesting groups (Horner and Makela, 1979; Varricchio and Horner, 1993) and potential pack hunting styles (Gishlick, 2001; King et al., 2020).

As evident from modern studies, birds are able to perform behaviorally complex abilities such as nesting behaviors and parental care that have been associated with *M. peeblesorum* (Sol et al. 2005a, 2005b). While these performances are naturally ingrained into the organisms for evolutionary success, the brain had to be developed to execute and replicate these behaviors. From volumetric comparisons, the social complexity of *Archaeopteryx* (CRV = 45%; Lauters et al., 2013), an avialan accepted to be bridging the gap between dinosaurs and avians, is likely to have been very similar with that of diamond doves (*Geopelia cuneata*: CRV = 45%) and modern domesticated chickens (*Gallus domesticus*: CRV = 44%) (Burish et al., 2004). Modern birds that demonstrate a CRV value similar to *M. peeblesorum* (range of 48-53%) include the blue-tailed emerald (*Chlorostilbon mellisugus*), common quail (*Coturnix coturnix*), red-throated loon (*Gavia stellata*), wild turkey (*Meleagris gallopavo*), killdeer (*Charadrius vociferus*), common sandpiper (*Tringa hypoleucos*), Eurasian sparrowhawk (*Accipiter nisus*), common tern (*Sterna hirundo*), black grouse (*Tetrao tetrix*), and gray partridge (*Perdix perdix*) (Burish et al., 2004). It is important to note that there is a large variability in the CRV value of modern birds. The highest CRV value calculated for a modern bird was 82.3% and observed in the blue-and-yellow macaw (Burish et al., 2004). Comparisons between these highly specialized and behaviorally complex birds and ornithopods are rather unreasonable, because birds have acquired further macroevolutionary traits over millions

of years since the extinction of the non-avian dinosaur lineage. However, it is reasonable to assume that if modern and ancient birds with a cerebral hemisphere to endocrania volumetric ratios similar to that of *M. peeblesorum* are able to demonstrate forms of complex behaviors, *M. peeblesorum* may have been able to perform them as well, as supported by the fossil record. Since the CRV for *M. peeblesorum* is much higher than those of other dinosaurs, it is logical to infer that these two traits – that is, the dinosaur demonstrating complex behaviors and characterized by a large cerebral hemisphere volume relative to the brain - are interconnected.

Other Late Cretaceous hadrosaurs had relatively similar CRV values to that of *M. peeblesorum* and birds. Therefore, a question regarding this trait can therefore be postulated: was this volumetric increase in the cerebral hemispheres needed for the non-avian dinosaurs to develop complex behaviors or did the acquisition of behavioral complexity evolve through time and a preservational bias hindered the evidence of the trait in related and/or time concurrent ornithopods? Direct evidence of gregarious behavior has been noted in numerous hadrosaur taxa through discoveries of track sites (Currie, 1983; Lockley and Matsukawa, 1999) and mass bonebeds (Varricchio and Horner, 1993). This supports the inference that the abilities for advanced processing skills were present, leading to the belief that parental care could have been an evolved and acquired trait for Late Cretaceous hadrosaurs with large CRV values. The taphonomic conditions needed to preserve dinosaur eggs and juvenile bones are highly specific and very rare, and the Two Medicine Formation provides the conditions needed to preserve the soft, unossified bone of young organisms and the calcitic carbonate shells of eggs (Varricchio and Horner, 1993; Scherzer and Varricchio, 2010). Thus, a degree of preservational bias could have affected

the social complexity in the form of nesting sites seen in Late Cretaceous hadrosaurs. However, quantitative comparisons of the cerebral hemisphere volume relative to the endocrania do favor *M. peeblesorum* as the dinosaur with the highest likelihood to display complex behaviors among the group. This is in contrast to the average REQ value observed. Since taphonomic processes are random, the questions regarding the social complexity and intelligence of related Late Cretaceous ornithopods currently lie solely on the comparison methods and paleoneurological inferences Future research focusing on the cerebral region of ornithopods, specifically *M. peeblesorum*, would allow for greater insight into these behaviors and the evolution of the cerebral hemisphere through the Late Cretaceous.

8. CONCLUSIONS

In the present study, digital reconstructions of a partial ontogenetic series consisting of three cranial endocasts of *Maiasaura peeblesorum* have allowed for the first glimpse into the neuroanatomy and sensory system of this "good mother" dinosaur to provide further inferences about the species' behavior. Evidence from the reconstructed cerebrum region of OTM F138, TMDC F139, and TMDC F140 match expectations and inferences that *M. peeblesorum* could have exhibited a form of behaviorally complex abilities, as supported by the fossil record. With the enlarged cerebral region, the likelihood of demonstrating these behaviors is greater than that of other members of Ornithopoda and, broadly, ornithischians. This conclusion is derived from the enlargement of the cerebrum relative to the endocranial volume observed in *M. peeblesorum*, as is typical for Late Cretaceous hadrosaurs. Demonstrated is a calculated cerebral to endocrania volume ratio (CRV) of 49.5% in ontogenetically mature *M. peeblesorum* adult specimens – a value at minimum 5% higher than related ornithopods – while ontogenetically younger specimens show CRV values closer to 39.7-42.6%. Given the evidence of complex behaviors in the form of parental care and gregarious behavior associated with the species, these CRV values are consistent for *M. peeblesorum* to demonstrate behaviorally complex actions. An olfactory ratio of 1.76 and a narrow, low frequency hearing range of 57-3380 Hz confirmed average results that are consistent with those of other related Late Cretaceous hadrosaur taxa, implying that neither smell nor hearing were incredibly enhanced traits for *M. peeblesorum*. With the poor preservation of TMDC F139 and TMDC F140, ontogenetic changes in the olfactory ability and hearing frequencies need further investigation to

observe how these sensory functions changed with age. An average reptile encephalization quotient (REQ) of 2.1-2.3 for *M. peeblesorum* was observed in comparison with other ornithopods, indicating that the total brain volume was not significantly increased relative to the taxon's body size. Without the analysis of partitioned endocrania volumes across Dinosauria, the degree of volumetric enlargement or reduction of other anatomical features, such as the cerebral hemispheres, within the REQ cannot be interpreted. However, the CRV of this study suggests that a possible specialization and volumetric increasement in the brain of *M. peeblesorum* was centralized to the cerebrum region.

Before the discovery of nestling *M. peeblesorum* specimens in a nest-like structure, limited evidence was available to demonstrate that non-avian dinosaurs exhibited complex behavior associated with parental care. The findings in this study offer preliminary evidence about the sensory system of a dinosaur exhibiting these traits. As demonstrated by modern archosaurian studies (e.g., American alligator), specialized sensory systems – such as olfaction and hearing – are not necessary for having gregarious or complex parental behaviors. Coupled with the fossilized evidence of gregarious social behaviors, the enlarged cerebrum in the reconstructed cranial endocast of *M. peeblesorum* is evidence that a behaviorally complex lifestyle could have been demonstrated by the "good mother" dinosaur through parental care.

APPENDIX A.

HISTORY OF NON-AVIAN DINOSAUR PALEONEUROLOGY

1. OTHNIEL MARSH

Othniel Marsh (1831-1899) was an American vertebrate paleontologist at the U.S. Geological Survey and the first professor of paleontology in the United States at Yale University. He excavated and described numerous genera of dinosaurs and other Mesozoic faunas from the western United States during the "Bone Wars" of the late 19th Century, including *Triceratops, Stegosaurus, Apatosaurus* (and therein *Brontosaurus*), *Diplodocus*, and *Allosaurus* – thus establishing himself as one of the first premier American dinosaurian paleontologists. During his career, Marsh also established the roots of modern vertebrate paleoneurology between 1874 and 1896 (Marsh, 1874, 1881, 1884a, 1884b, 1886, 1890, 1891, 1896), as he was the first person to question the neuroanatomy and evolution of the braincase in the vertebrate groups he studied. Perhaps most importantly, his work on the endocasts and braincases of extinct taxa (Marsh 1886) led to the formulation of a series of laws about brain evolution that consisted of eight rules he deemed to be constant. They are listed as follows (Marsh, 1886; p. 58-59):

1. All Paleogene and Neogene mammals had small brains.

2. There was a gradual increase in the size of the brain during this period.

3. This increase was confined mainly to the cerebral hemispheres, or higher portion of the brain.

4. In some groups, the convolutions of the brain have gradually become more complex.

5. In some, the cerebellum and the olfactory lobes have even diminished in size.

6. There is some evidence that the same general law of brain growth holds good for Birds and Reptiles from the Cretaceous to present time.

7. The brain of a mammal belonging to a vigorous race, fitted for a long survival, is larger than the average brain, or that period, in the same group.

8. The brain of a mammal of a declining race is smaller than the average of its contemporaries of the same group.

These laws were disproved by numerous studies in the years following Marsh's proposal, but they provided a baseline for future paleontologists to modify, expand, and quantify brain evolution. From this spark of interest in the inner working of the braincase of extinct organisms, the subfield of paleoneurology was born. Marsh's greatest, or at least most relevant, contribution to paleoneurology was his observation that brains were not a consistent size throughout the fossil record and changed both morphologically and volumetrically over time.

A major flaw in Marsh's research and proposed laws on the size and development of the brain was that they were based entirely on the stratigraphic positioning of an organism in the fossil record. In modern studies, paleoneurologists make note of organisms' sizes, phylogenetic relationships, paleoecological traits, and other cranial or postcranial paleobiological features as a means to compare brain sizes and behavioral capabilities of extinct taxa. Holistic methods of gaining endocranial or behavioral information have been shown to be prudent to the understanding of the neurological and sensory systems. Studies have shown that most animals have the tendency to increase in the complexity and relative size of the brain when compared to body mass (encephalization), rather than shift back to more basal brain characteristics (Jerison, 1955,

1961). Evolutionary trends and speeds among phylogenetically unrelated organisms are varied; therefore, assessment of morphological and developmental features of the brain cannot solely based on positioning within geological time.

Most of the laws Marsh proposed centered around mammalian vertebrates, with the sixth law being the outlier, focusing on the archosaurian branch of vertebrates. During his research, Marsh discovered and described two Late Cretaceous birds *Ichthyornis dispar* (Marsh, 1873) and *Hesperornis regalis* (Marsh, 1880). His conclusions, based on the analysis of the specimens, how the two birds' brains would have appeared in life, and how the bird brain had similar characteristics to dinosaur brains led to the derivation of the sixth law. In today's prospective of having found 70 genera of Mesozoic birds (Chiappe and Dyke, 2002), Marsh's work seems based on admittedly limited research, but these two birds represented the second and third birds to ever be found from the Mesozoic, behind *Archaeopteryx* (which now considered an avialan). Therefore, upon his extensive research for the time, he claimed:

> "More recent research renders it probable that the same general law of brain growth holds good for birds and reptiles from the Mesozoic to the present time. The Cretaceous birds, that have been investigated with reference to this point, had brains only about one-third as large in proportion as those nearest allied among living species. The Dinosaurs from our Western Jurassic follow the same law, and had brain cavities vastly smaller than any existing reptiles. (Schuchert, 1938; p. 56-57)"

In the above statement, Marsh relates the proportion of brain to the endocast volume of Cretaceous aged birds and non-avian dinosaurs. This is the first connection noted on the phylogenetic relationship, and by extension, paleoneurological traits, between birds and

non-avian dinosaurs. Because of this, the connection is considered the beginning of qualitative research into the non-avian dinosaur endocranium.

While Othniel Marsh's contributions to paleoneurological studies were based on conclusive information during his time and were then later falsified by other studies and research, his role played a part in the advancement of investigations into the brains of extinct organisms. His preliminary study on the endocranial evolution of mammals (Marsh, 1874) and Mesozoic birds (Marsh, 1880), paved the way for the first paleoneurological studies to be applied directly to dinosaurs.

2. TILLY EDINGER

Johanna Gabrielle Ottilie "Tilly" Edinger (1897-1967) was a German-born vertebrate paleontologist who is widely accepted as the founder of modern paleoneurology (Buchholtz and Seyfarth 1999, 2001). While Marsh's research and proposals about the brain of extinct and modern animals was completed before she was born, Tilly was the scientist that began integrating comparative anatomical interpretations of the brain with functionality, sensory, stratigraphic, and geologic aspects. Her extensive work and findings (Edinger 1921, 1926, 1929, 1933a, 1933b, 1939, 1941, 1942, 1948, 1955, 1961, 1962, 1964, 1975; Romer and Edinger, 1942), paved the way for this field of paleontology and inspire many today.

Born the daughter of Ludwig Edinger, a highly influential comparative neurologist and founder of Frankfurt's first neurological research institute (Kreft, 1997), Tilly was no stranger to academics and neurological sciences from a very young age. She was first educated by private tutors, then attended the only secondary school for girls of the time in Frankfurt, leading her to study at the Universities of Heidelberg, Frankfurt, and Munich where she first focused in zoology, but later turned to a specialization in paleontology and geology. Her first interaction with a "fossil brain," a natural cast of the endocranial cavity that had been formed by the cementation of sediments in in the braincase, was during her doctoral research on the Mesozoic marine reptile *Nothosaurus* (Buchholtz and Seyfarth, 2001). Her description of the specimen and endocast was the topic of her first publication (Edinger, 1921).

With her background in neurological studies under her father, Edinger began speculating on the nature of other fossilized brains and their significance for the understanding of modern and extinct organisms. During her unpaid volunteer work at the Geological-Paleontological Institute of the University of Frankfurt (1921-1927), she undertook the self-assigned task of gathering all previously described or noted endocasts, taxonomically organizing and classifying them, and providing conclusions that could be drawn from them. This rigorous task was completed and published as a book titled Die fossilen Gehirne (Fossil Brains) (Edinger, 1929) and is regarded as one of Edinger's most influential accomplishments, because it defined paleoneurology as the new subfield of paleontology. The topics, methodologies, interpretations, and hypothesis presented in the book would comprise the bulk of her research focus in her career.

Over the next decade, Edinger would continue to develop new endocranial interpretations in numerous taxonomic classes. This was progressively more challenging with time due to the Nazi invasion and overtaking of Germany. With Edinger's Jewish background, her life and career were thrown into disarray, beginning with the event infamously known as "Kristallnacht" on November 9-10, 1938, and the continued rise of antisemitism in fascist Germany. By the next day, Edinger was no longer allowed to continue her work at the Senckenberg Museum where she was "employed" as an unpaid curator. Luckily, her correspondence, collaborative nature, and existing professional relationships with other paleontologists allowed her to achieve permits to immigrate first to England and then the United States, though not without struggles and hardships (Buchholtz and Seyfarth, 2001). Once in the United States, Edinger continued her

paleoneurological work and documented and described many organisms' neuroanatomy, including pterosaurs (Edinger, 1941), horses (Edinger, 1948), and whales (1955).

Throughout her career, Edinger made observations that quickly disproved or contradicted Marsh's statements about the brain. Most notably, she observed that the size of the brain did not necessarily correlate with the body size or stratigraphic occurrence (Edinger 1948, 1962). Her studies on horses were the defense of this, as she noticed the equid body size increased and the brain size decreased over the Paleogene and Neogene periods. While originally a supporter of Marsh's work at the beginning of her career (Buchholtz and Seyfarth, 2001), Edinger later became one of his harshest critics (Edinger, 1962) and proved that his incorrect laws were derived from his background in earth sciences rather than comparative anatomy (Buchholtz and Seyfarth, 1999). Furthermore, her contributions in the field expanded the limited "descriptions" of size and primitive detailing of the brain, to complex analyses that allowed for the interpretations of sensory and functionality processes of the extinct organisms. This is attributed to her familiarity with neuroanatomy; she understood the central nervous system present in modern organisms that she could then apply to extinct ones. Her extensive documentation of the anatomical and morphological changes across time still forms the basis for current studies of the olfactory, optical, and auditory senses from the cranial endocast. While Tilly Edinger did not work directly with nor study non-avian dinosaur cranial endocasts, her contributions to the field paved the way for later scientists to apply her methods to dinosaur faunas.

3. HARRY JERISON

Whereas Othniel Marsh and Tilly Edinger laid the groundwork for qualitative paleoneurological research, Harry Jerison was the paleoneurologist who introduced quantitative analysis to the field. Jerison was a professor at the University of California, Los Angeles from 1969-1992 and became a Professor Emeritus until his passing in January 2023. During his early research career, he was a colleague and close friend of Tilly Edinger. His research focused on investigating the correlation between the volume of the brain and the body mass of modern organisms and dinosaurs. This was discussed in two of his most well-known publications "Brain evolution and dinosaur brains" (Jerison, 1969) and "Evolution of the brain and intelligence" (Jerison, 1973). His developments lead to his own eight "orderliness to brain evolution" laws (Jerison and Barlow, 1985; p. 24-25), similar to that of Othniel Marsh.

1. "A basal lower vertebrate grade of encephalization evolved in the earliest bony fish, amphibians and reptiles and has continued to the present as a steady-state or equilibrium maintained for at least 350 million years. Since about two-thirds of living vertebrate species are members of these three classes of vertebrates, this basal grade is the norm for vertebrates.

2. There are variations in encephalization within the lower vertebrate groups, the most interesting being between herbivorous and carnivorous dinosaurs. The carnivores were apparently significantly more encephalized.

3. The earliest fossil birds and mammals with known endocasts had evolved to a higher grade, representing at least three or four times as much brain as in lower

vertebrate species of comparable body size. This progressive or 'anagenetic' evolution occurred at least 150 million years ago, and in the case of the mammals may have begun with their reptilian ancestors at least 50 million years earlier.

4. Within the mammals there is a good fossil record of the brain, which is consistent with a picture of steady-states punctuated by rapid evolution to higher grades. However, many grades of encephalization are represented in living mammalian species, with some (opossum, hedgehog) at the same grade as the earliest of the mammals.

5. Two unusual conclusions are evident in the history of encephalization in primates. First primates have always been a brainy order, perhaps doing with their brains what many other species did by morphological specializations. Second, the evolution of encephalization in the primates followed rather than preceded or even accompanied other adaptations by primates to their niches. Washburn (1978) has pointed this out as a feature of hominid evolution, but it appears to have been true for prosimians and simians as well (Jerison 1979).

6. The highest grade of encephalization is shared by humans and bottlenosed dolphins (Tursiops truncatus). The sapient grade was attained about 200,000 years ago, but cetaceans may have reached their highest grade 18 million years ago.

7. Encephalization in the hominids is a phenomenon of the past three to five million years, and its rapidity appears to have been unique in vertebrate evolution.

8. These results suggest two complementary conclusions. First, the long steady-states that occurred in most groups indicate that, on the whole, encephalization was not a major element in vertebrate evolution. A particular grade of encephalization tended to be maintained once it was achieved. On the other hand, its appearance in many different and distantly related groups is evidence of some Darwinian 'fitness' for encephalization."

These laws were based on the work Jerison completed in previous studies, and further elaborated and modified the preliminary laws set by Marsh. They provide a much deeper, and more accurate, understanding of the quantitative and developmental aspect of paleoneurology. Specifically, Jerison and his laws disproved Marsh's theory of "bigger is better" by utilizing numerous specimens to show that there is variability of encephalization in successful forms. Encephalization is defined as the correlation or ratio of the brain volume relative to the body mass of the organism and/or evolutionary time (Jerison, 1969; Jerison and Barlow, 1985). Jerison was able change the assumed conception that dinosaurs had unusually small brains (Jerison, 1969), which was made through comparing the encephalization ratios of dinosaurs to mammals without regards to the difference in derived evolutionary traits in archosaurs and mammals. Therefore, Jerison compared the brain size of dinosaurs to that of modern reptiles to illustrate that the dinosaurian brain was within expected size bounds when compared to their reptilian and avian relatives (Jerison, 1969).

Harry Jerison was able to quantitively demonstrate this feature seen in the dinosaur endocrania with the development of the encephalization quotient (Jerison and Barlow, 1985). An encephalization quotient (EQ) is the correlation of the brain mass to the body mass of an organism to its perceived cognitive ability. Jerison was the first to apply these

mathematical approaches to the endocranium of both extinct and extant organisms to better infer how cognitive abilities and complex behaviors have evolved through time. By calculating the endocranial volume of organisms and relating this to the expected or seen body mass, trends and inferences in cognitive abilities were able to be traced among vertebrates based on phylogeny. Broadly, the encephalization quotient also allows for a direct correlation of how the brain and body of organisms are evolving alongside and relative to one another. Regardless of applicability to dinosaurs or other specimens, these laws provided a new complexity and revitalization to understanding and detailing the brain in relation to quantitative and evolutionary studies.

APPENDIX B.

DINOSAUR NEUROANATOMY: GENERAL FORM AND FUNCTION

1. OVERVIEW

The cranial endocast is the reconstructed internal area of the braincase, where soft anatomy related to the central nervous system was located during a vertebrate organism's life. When reconstructions are made, regardless of the method, the resulting endocast is composed of the brain, cranial nerves, endosseous labyrinths, dural tissues, vascularization, and a phylogenetically variable amount of soft anatomy and cartilage. Since the endocranial segmentation reconstructs the hollow area inside the braincase, it means that there is no true preservation of all these anatomical features. For example, the foramina where the cranial nerves nucleated and exited the braincase in life are preserved rather than the actual nerves. These areas are still important to segment, describe, and investigate as they allow for the reconstruction of the pathways these nerves would have traversed in life, providing insight into the specific functions of each nerve and respective brain region they are stemming from. Further, cranial endocasts cannot be used to find a true volumetric measurement of the brain, so paleoneurologist use the total volume of the endocast to make inferences on an organism's sensory system and behavior.

There are different ways to define and portray a cranial endocast (Evans et al., 2009; Buchholtz, 2012; Bever et al., 2013), but the method chosen to separate the endocranium for easier classification divides it into three regions: the forebrain, midbrain, and hindbrain. This is meant to aid in describing anatomical locations without sacrificing accuracy. The forebrain includes the olfactory apparatus (the combination of the olfactory bulbs and olfactory tract), including the olfactory nerve, both cerebral hemispheres (collectively called the "cerebrum"), pituitary body, and optic nerve. The midbrain includes the optic

lobes, oculomotor nerve, and the trochlear nerve. The hindbrain includes the cerebellum,

brainstem, endosseous labyrinths, and the trigeminal, abducens, facial, vestibulocochlear,

glossopharyngeal, vagus, accessory, and hypoglossal cranial nerves. The aforementioned

cranial nerves will be described all together in one section, rather than by separate regions

of the brain.

2. FOREBRAIN

2.1 OLFACTORY APPARATUS

The olfactory apparatus is located at the anteriormost area of an endocast and extends rostrally from the cerebrum. The olfactory tract's morphology varies dramatically between taxa and ontogenetic stages, but the olfactory bulb is relatively similar among groups as a split oval protrusion with a tranversely-oriented notch at the anteriormost extent of the anatomy (Jerison, 1969; Evans, 2005; Lautenschlager and Hübner, 2013; Muller, 2021). The main function of the olfactory apparatus is the acquisition and transmission of sensory data related to olfaction, or smell. During an organism's life, the olfactory epithelium, the specialized epithelial tissue that is responsible for gathering and transmitting scent via nerve axons, would be housed in the nasal cavity. Since scent data would be gathered across the nasals and epithelium, information would be transmitted through to the olfactory bulbs and forebrain for further data processing.

Olfaction is one of the most important senses for animals for food acquisition (Togunov et al., 2017; Molina-morales et al., 2020), reproduction (Balthazart and Taziaux 2009; Caro et al. 2015), and predator avoidance (Kats and Dill, 1998; Webb et al., 2010) are just a few situational experiences during which animals would need to develop a heightened sense of smell. Preservation of the olfactory tract without the olfactory bulb occurs more often than not, as the olfactory bulb is not covered by bony material (Lauters et. al, 2021). In some cases, though, the olfactory bulbs can be studied by impressions preserved on the ventral surface of the frontals (Martinez et al., 2012, Bronzati et al., 2019; Langer et al., 2019).

The size and development of the olfactory bulbs are directly correlated with the development and olfactory ability in vertebrates (Edinger, 1908; Rombaux et al., 2009). Across Dinosauria, numerous studies on the olfactory apparatus have been conducted to determine and better understand olfactory acuity and function (Zelenitsky et al., 2009; Evans et al., 2009; Hughes and Finarelli, 2019; Sakagami and Kawabe, 2020; Müller, 2021). Specifically, extinct non-avian theropod dinosaurs have been frequently studied due to their relationship to modern birds and the interest in how this sensory system functioned and/or evolved in the predatory realm of Dinosauria. The availability of a direct comparison with descendant modern analogs is crucial in paleontological studies as it allows for more detailed general and macroevolutionary interpretations to be made. Interestingly, a comparative study on the olfactory bulb size in extinct theropod taxa and *Archaeopteryx* showed that the previously presumed oldest known bird had the same olfactory abilities of the similarly sized theropods (Zelenitsky et al., 2009). Of the non-avian theropods, tyrannosaurids and dromaeosaurids have the largest olfactory bulb to cerebral hemisphere and olfactory bulb to body mass ratios, leading to the conclusion that these groups would have had the highest olfactory abilities (Zelenitsky et al., 2009, 2011). Olfactory studies in sauropodomorphs indicate varied acuity of olfaction, but overall trends show larger olfactory bulbs in sauropodomorphs than other dinosaurs with similar body mass sizes (Müller, 2021). In comparison with these other groups of dinosaurs, the olfactory bulb and tract size seen in ornithopods is smaller (Hopson, 1979; Witmer and Ridgely, 2008; Evans et al., 2009). Specifically, studies comparing the olfaction acuity in lambeosaurines and hadrosaurines have taken place because of the hypothesis made by Ostrom (1961, 1962) that the development and derivation of the nasal crests in

lambeosaurines could increase the olfactory region surface area for olfactory epithelium, and therefore, increase the olfactory sensitivity. This was disproven by Evans (2005) who demonstrated that the olfactory system did not dramatically change from the plesiomorphic conditions. Further studies have confirmed that the olfactory acuity in lambeosaurines was slightly greater than that of their non-crested hadrosaurine relatives (Lauters et al., 2013).

2.2 CEREBRUM

The cerebrum is the large, usually round to diamond shaped mass located in the posterior region of the forebrain (Lautenschlager and Hübner, 2013; Lauters et al., 2022) and represents the widest portion of the endocast (Franzosa, 2004). It is medially split into right and left hemispheres by a longitudinal fissure, **al**though this is rarely observable in non-maniraptoran or avialan endocasts due to the thickness of the dural covering in this region. The cerebrum lies posteriodorsally to the olfactory tract and is distinguished by its wider shape than the olfactory tract and cerebellum posterior to it, with the widest point typically seen at the most posterior extent of the forebrain region of non-avian dinosaurs. The cerebrum contacts with the ventral side of the frontals, which can then leave impressions of endocranial valleculae in cases of exceptional preservation and/or the presence of a large brain-to-braincase volume. When compared to other non-avian dinosaurian groups, the cerebrum of hadrosaurs, notably both saurlophines and lambeosaurines, had a larger volume than that of other non-hadrosaur ornithischian and large theropods (Lauters et al. 2012), and a similar volume when compared to some smaller theropods, such as the maniraptorans (Balanoff et al., 2009**;** Lauters et al., 2012). With time, the cerebrum in ornithopods notably had a monospecific volumetric enlargement with

more derived taxa having larger cerebral areas than basal ornithopod species (Lauters et al., 2012).

Functionally, the cerebrum is considered to be the center of informational processing and sensory data coalescing. One of the primary roles of the cerebrum is to process olfactory information, but it is also responsible for interpreting other sensory information gathered in the brain (Buchholtz, 2012). Intellectual ability and complexity of behavioral traits can be inferred from the size of the cerebral hemispheres through quantitative and comparison methods (Larsson et al., 2000). A larger cerebrum size is therefore associated to a higher likelihood of greater intellectual ability and complex behaviors. However, since intelligence and behavioral traits are not preserved in the fossil record, this information is only interpreted through direct fossilization evidence. Ornithopods have been of special interest to the study of the volumetric relationship between the cerebrum and intelligence from mass bone beds discovered suggesting gregarious behavior among the extinct taxa (Varricchio et al., 1993).

Unfortunately, the endocranial cavity does not give us an accurate representation of the actual volume of the cerebrum, as noted earlier for the entire brain. Other anatomical features, such as the dura mater and cranial sinuses are housed in the braincase alongside the brain itself and the volume at which this soft anatomy is consumed is unknown. Vascular valleculae are anatomical impressions left by blood vessels on the surface of the bones created if the brain completely filled the endocranial chamber and compressed the soft anatomy against the ventral side of bones surrounding the braincase. The vascularization impressions left on the interior walls of the braincase allow for inferences about the size, shape, and volume of the anatomical features in the endocast (Osmolska,

2004; Evans, 2005; Godefroit et al, 2012a; Lauters et al., 2013, 2022). Evans (2005) was the first person to report vascularized valleculae impressions in ornithopods, specifically in hadrosaurs and pachycephalosaurs. Following this study, impressions have been documented in numerous ornithopod specimens and have aided in better understanding and determining the shape, volumetric size, and space consumed in the cerebral hemispheres in the forebrain region (Godefroit et al., 2012a; Lauters et al., 2013; Lauters et al, 2022). Lauters et al. (2022) estimated that the cerebral hemispheres of ornithopods were in close contact with the interior surface of the braincase and filled more than half the space of the endocranial cavity from the high frequency of seeing these impressions in specimens.

2.3 PITUITARY

In archosaurs, the pituitary is located ventrally to posteroventrally from the cerebral area, connected to the endocast dorsally via the infundibulum encased in the basisphenoid bone of the braincase floor. Functionally, the pituitary gland is responsible for the production, regulation, and spread of hormones used for growth and development in the body (Lauters et al., 2022; Evans et al., 2009). The pituitary fossa houses the pituitary gland, therefore preservation of this in the endocast allows for a close proxy to the true size of the pituitary gland (Sampson and Witmer, 2007). Early studies on this region proposed that the size of the pituitary gland and the adult individual could be related and correlated (Edinger 1964), which was then proven in numerous studies of various groups of dinosaurs showing smaller bodied taxa having smaller pituitary glands and larger bodied taxa having larger pituitary glands (Sereno et al., 2007; Sander et al., 2011, Godefroit et al., 2012a; Godefroit et al., 2012b; Lauters et al., 2013). Interpretations could lead to the hypothesis

that the evolutionarily ancestral smaller form of a groups would have a smaller pituitary size when compared to the same more derived, larger taxa (Lauters et al., 2022), but more work on this comparison needs to be conducted. Further, a study conducted by Morhardt et al. (2017), showed that the pituitary could evolve independently of the rest of the brain, allowing for the postcranial growth and larger development of more derived species, while keeping a similar brain, braincase, and skull size to their basal relatives.

The internal carotid arteries are commonly preserved along with the pituitary, extending posteroventrally from the pituitary and appear as a wishbone shaped structure in Dinosauria in anterioposterior view (Witmer and Ridgely 2008, Figure 1; Evans et al., 2009, Figure 7). Two foramina at the posteroventral bases of the arteries can be present, depending on preservational conditions, representing the area in which the anatomy exited the osteological braincase and would continue traversing to the specific region of the body. The location of the artery itself and its foramina in the endocranial cavity can vary slightly between groups of dinosaurs but is all located in the basicranium (Rogers 1998; Carabajal, 2012; Paulina-Carabajal et al., 2016). The responsibility of the arteries is to supply the narial, facial, and braincase region of the skull with oxygenated blood (Porter and Witmer, 2020).

3. MIDBRAIN

3.1 OPTIC LOBES

The midbrain region is primarily associated with vision, as the only anatomical feature classified in this region is the optic lobes (Buchholtz, 2012). In non-avian dinosaurs and basal archosaurs, the optic lobes are located posterior to the cerebrum and anterior to the cerebellum in the dorsal endocast (Hu et al., 2021). This is important to note because there is a ventrolateral shift of the optic lobe location in birds (Franzosa and Rowe, 2005) resulting from the enlargement of the forebrain and hindbrain in derived avian species (Witmer and Ridgely, 2009; Hu et al., 2021). In dinosaurian species that are closely related to birds, such as tyrannosaurs and ornithomimids, a transitional state could be observed as their brains were becoming larger and more developed, with a more "bird-like" organization (Witmer and Ridgely, 2009). However, the optic lobes are very difficult or near impossible to observe in non-avian dinosaurian endocasts due the coverage of thick venous sinuses or dural matter that do not allow for definitive morphological structures to be observed (Franzosa and Rowe, 2005; Witmer and Ridgely, 2009; Buchholtz, 2012; Lautenschlager and Hübner, 2013; Hu et al., 2021). This limits the comparisons that can be made from the differing localities of the optic lobes and the taxa. The orientation of the optic lobes relative to the osteological braincase differ phylogenetically; the optic lobes of non-avian dinosaurs and archosaurs are located ventrally to the frontals, while the optic lobes of birds and closely related dinosaurs are located laterally to the laterosphenoids.

The optic lobes observable in endocasts represent the enlargement of the optic tecta of the brain (Buchholtz, 2012). Functionally, the optic tectum is the anatomical region

responsible for the processing and interpretation of visual information that is gathered through the eyes. The size of the optic lobes can be correlated with vision acuity, with larger optic lobes representing larger optic tecta and more reliance on high visual acuity. Due to the infrequency of observing them in ornithopod specimens it has been hypothesized that the relative size of the optic lobes to the overall brain was small (Evans et al., 2009; Lauters et al., 2022).

4. HINDBRAIN

4.1 CEREBELLUM

The cerebellum is located in the hindbrain region of the brain, posterior to the cerebrum and optic lobes in non-avian dinosaurs. Due to the lateral shift of the optic lobes in avian taxa, the location of the cerebellum differs between the groups, as it will sit directly posterior and come in contact with the cerebrum in avian taxa. The cerebellum is defined by a slightly smaller, relative to the cerebrum, round bulge that tapers anterior to the brainstem and foramen magnum. Osteologically, it is encased by the parietals and supraoccipitals dorsally, the exoccipital-opisthotic laterally, and the basisoccipital ventrally (McFeeters et al., 2021). On the dorsal surface between the parietals and the cerebellum, preservation of vascular elements is possible in cranial endocasts, similar to the cerebrum. Here specifically, a large caudally oriented longitudinal venous sinus runs over the cerebellum that terminates at the occipital region. The preservation appears as a ridge or peak on the dorsocaudal surface of the cerebellum in the cranial endocast (Carabajal, 2012) and can be observed in varying definitions in some dinosaurs, crocodilians, and birds (Wharton, 2000). Functionally, this sinus is presumed to have transmitted blood to the different regions of the brain via smaller laterally extending veins (Witmer et al., 2008; Wharton, 2000). Floccular lobes can also be seen projecting laterally from the posterior region of the cerebellum, encircled by the endosseous labyrinths (Rogers, 1998).

The cerebellum's main role is centered around movement and muscle control, so it coincides heavily with the vestibular (balance), auditory, visual, and somatic (muscular)

systems (Franzosa, 2004). The floccular lobes are also an important part of this system, as they are the main controllers of balance and posture in the body and stability and orientation of the head, linking it to the agility of a vertebrates (Ferreira Cardoso, 2015; Witmer and Ridgely, 2009). The size of the floccular lobes can be interpreted to measure and quantify these abilities when relating different dinosaurian taxa; the larger sizes seen in carnivores (King et al., 2020) pterosaurs, and birds (Chatterjee, 1991; Franzosa, 2004) could be correlated with the need for well-balanced and agile movements. However, depending on the thickness of the dural covering in the hindbrain region, the floccular lobes may not be observable in specimens (Ballell et al., 2021), but they are present in different sizes and forms since they are crucial to an organism's motor function and stability. Studies by Ferreira-Cardoso (2015) and Ferreira-Cardoso et al. (2017) postulate that there is no precise or direct correlation between floccular size and the ability of these motor functions in birds, and further testing is required. Changes in the floccular lobe sizes through ontogeny can be linked with the shift from bipedal locomotion in the younger organism to quadrupedal locomotion in adulthood. This is especially important to note in ornithopods, and comparisons done by Lauters et al. (2022) show that they are quite apparent in most species, especially in the basal ornithopods. This dramatic and specialized shift in balance would require refined neuromuscular coordination (Jerison, 1973); therefore, it is not outrageous to speculate about the increase in size of floccular lobes in ornithopods.

4.2 ENDOSSEOUS LABYRINTH

Similar to the cranial endocast itself noted by Witmer et al. (2009), the labyrinth of the inner ear used for reconstruction from CT data does not truly show the shape, structure,

and perfect outline of the osseous labyrinth. Therefore, it is referred to as the endosseous labyrinth, although it is more commonly known as the inner ear structure. The auditorial sensory anatomy is situated posterior to the trigeminal nerve, lateral to the cerebellum, and encircling the floccular lobes, in the hindbrain region of dinosaurs (Evans, 2005; Witmer and Ridgely, 2009; Evans et al., 2009; Buchholtz, 2012; Lauters et al., 2013). The structure comprises two main features: the vestibular system and the cochlear duct. The vestibular system contains three distinct semicircular canals that are visible in lateral view in well preserved vertebrate specimens. They are rightfully named based on their location relative to the braincase itself: the anterior semi-circular canal, the lateral semi-circular canal, and the posterior semicircular canal. The orientation and overall structure of these portions are widely variable in not only archosaurs but all vertebrate organisms as well (Wever, 1978; Georgi and Sipla, 2008; Witmer et al., 2009; Georgi et al., 2013; Evers et al., 2019). In general, the anterior semicircular canals of derived ornithopods (Evans et al., 2009), non-avian theropods (Sampson and Witmer, 2007; Smith et al., 2011) and ceratopsians (Witmer and Ridgely, 2008) are longer than the posterior and lateral semicircular canals. Unique cases are present where the three canals are very similar lengths (Sobral et al., 2012). The cochlear duct occurs as a stem, trending ventrally from the vestibule region and similarly varies in both length and thickness among vertebrate organisms (Witmer and Ridgely, 2008; Lautenschlager et al., 2012; Button and Zanno, 2023). In ornithopods, an elongated cochlear duct is present (Sobral et al., 2012) and, thus, linked to an increase in auditory capabilities related to low-frequency sounds (Wever, 1978; Walsh et al., 2009).

Functionally, the endosseous labyrinth is the organ responsible for the sensory functions of balance and hearing. The vestibular system of the inner ear, the combined

region of the three semicircular canals, detects and helps control the vertical and lateral positioning of the head, as well as the pitch, roll, and yaw of the skull. This is attained by a viscous liquid, called perilymph moving through the semicircular canals and innervating tiny hair cells along the base of each canal, called the canal ampulla (Purves et al., 2001). In response to the movement, the 3D spatial location of the skull is collected in the semicircular canals and transmitted to the brain via the vestibular branch of the vestibulocochlear cranial nerve (CN VIII). Horizontal and rise/fall movement of the skull are transmitted in this way as well but are collected by the utricle and saccule, two other fluid filled cavities housed in the same region that similarly contain canal ampulla.

The cochlear system of the inner ear, found in the cochlear duct, is responsible for the acquisition of auditory senses (Casale et al., 2018). The basilar papilla, which is housed in the cochlear duct, is the main region where auditory sound is processed. Sound vibrations are sensed and collected in the oval window and transmitted to the round window where vibrations in opposition of the collected vibrations are created, inducing movement of perilymph and reaction of epithelial cells in the basilar papilla. This information is then transmitted to the brain via CN VIII.

The endosseous labyrinth in ornithopods has been sparsely studied, given the importance of hearing abilities in herbivorian group that enabled them to escape predation (Kats and Dill, 1998; Webb et al., 2010). Specifically, studies on the endosseous labyrinths of lambeosaurine hadrosaurids have been shown to provide crucial information for making inferences on the vocal resonation of the crest relative to the hearing sensitivity (Evans et al., 2009). Ontogenetic processes have also been recorded in the preservation of the semicircular canals, with juveniles having thinner, more delicate, and circular shaped

canals in comparison to the thicker, elliptical-triangular shaped subadult and adult specimens (Lautenschlager and Hübner, 2013). In previous studies, orientation of the lateral semicircular, which can be an indicator for the alert and raised posture of the head (Witmer and Ridgely, 2009), did not appear to change during ontogeny (Sobral et al., 2012; Lautenschlager and Hübner, 2013). However, it has been attributed that the orientation of the three semicircular canals relative to the endocast can be indicative of locomotory styles (Button and Zanno, 2023) This can be especially vital information to understanding the shift from bipedalism to quadrapedalism in ornithopods.

4.3 BRAINSTEM

The brainstem is the caudalmost extent of the cranial endocast since it is located immediately posterior to the cerebellum and differentiable by the posterior dorsoventral decrease in height. The anatomy terminates at the foramen magnum, located at the posteriormost end of the osteological braincase. In hadrosaurines and lambeosaurines, comparative anatomy has shown the width of the brainstem is almost consistent with the widths measured in the midbrain and hindbrain regions (Evans et al., 2009; Lauters et al., 2022), with the largest width being measured across the cerebral hemispheres. Functionally, this region is the main root and transmitting system for neural passageways that run from the forebrain to the central nervous system (Buchholtz, 2012).

5. CRANIAL NERVES

Twelve cranial nerves (CN) are recognized in the dinosaurian brain (Evans et al., 2009). Ten of these are viewable as paired nerves that extend laterally or rostrally from of the fore-, mid- and hindbrain regions of the endocast. The other two (CN I and CN II) are also paired nerves, although they are often not preserved with the fine septa (Evans et al., 2009; Button and Zanno, 2023) that extend ventrally from the forebrain region of the endocast. Due to the lack of preservation of nerves, like the brain, a foramen in the osteological braincase is considered the evidence for the existence of cranial nerves (Hopson, 1979). The preservation quality of the foramen will vary among specimens due to taphonomic processes causing cracks, and therefore, mechanical preparational reconstruction, deformation, and lost pieces of the braincase will lead to misidentification or no foramen being present. A review of numerous studies shows that the foramen shape, location, and size will vary slightly based on the dinosaurian taxon (Sanders et al., 2005; King et al., 2020; Lauters et al., 2022), but general regional trends remain stable. It is important to note that the cranial nerve foramina only show the location where the nerve exited the osteological braincase, but not the exact nucleation site to the brain. This information could only be determined from the fossilization of cephalic and somatic musculature fibers, which is very rare (Hopson, 1979). Each cranial nerve, labelled in Table A.1, has a respective sensory function that controls and innervates a specific region. The function of each nerve is inferred based on comparative anatomy of modern archosaurian studies.

Table A.1: List of all cranial nerves found in non-avian dinosaurs and their specialized functions (Buchholtz, 2012).

Label	Cranial Nerve Name	General Function
I	Olfactory Nerve	Olfaction (smell)
II	Optic Nerve	Sight
III	Oculomotor Nerve	Innervates 4 out of 6 fine muscles for the eye and eyelid
IV	Trochlear Nerve	Innervates muscle for downward and diagonal eye rotation
V_1	Trigeminal Nerve: Ophthalmic Branch	Sensory innervation of face region
V_2	Trigeminal Nerve: Maxillary Branch	Sensory and motor control of maxillary region
V_3	Trigeminal Nerve: Mandibular Branch	Sensory and motor control for mandibular region
VI	Abducens Nerve	Innervates muscle for outward eye rotation and maintaining proper alignment during horizontal gaze
VII_{hy}	Facial Nerve: Hyomandibular Branch	Innervates facial muses of the lower jaw and face
VII_{pal}	Facial Nerve: Palatine Branch	Innervates facial muscles used for expression and taste
VIII	Vestibulocochlear Nerve	Innervates balance, hearing, and head orientation
IX	Glossopharyngeal Nerve	Sensory innervation from tongue, pharynx, and motor innervation for swallowing and noise production
X	Vagus Nerve	Longest nerve in the body, responsible for regulating involuntary necessary body functions
XI	Accessory Nerve	Motor and muscle innervation for head rotation and stabilization of shoulders
XII	Hypoglossal Nerve	Sensory and motor innervation of tongue

6. FLEXURE

The brains of most archosaurian taxa are described by the measurement of the cephalic flexure and the pontine flexure (Hopson, 1979; Lautenschlager et al., 2013; Lauters et al., 2022). The cephalic flexure angle is measured between the rostrocaudal axis that extends through the cerebral hemispheres, beginning at the most posterior end of the olfactory tract to the most posterior end of the cerebral hemispheres, and the oblique axis of the midbrain, running from the most posterior end of the cerebral hemispheres to the most anterior end of the middle cerebellum. The pontine flexure angle is measured between the oblique axis of the midbrain and the rostrocaudal axis that passes through the cerebellum and brainstem. Flexure angle values will vary dramatically depending on different biological factors, such as ontogeny/growing rate (Lauters et al., 2022) and phylogeny (Watanabe et al., 2021). Flattening of flexure angles – which becomes closer to 180 degrees – can occur when there is a dramatic increase in body size due to a possible faster growth rate of the braincase relative to the brain, leaving plenty of space for the brain to elongate anterioposteriorly (Lautenschlager and Hübner, 2013). Conversely, flexures will be more defined when the brain is developing faster than the braincase is growing, or has the ability to grow, and there is limited room for the expansion and further enlargement of the brain (Lautenschlager and Hübner, 2013). Flexure angles in ornithopods are shown to be less than those of their other dinosaurian relatives (Giffin, 1989, Buchholtz, 2012), and is likely due to the endocranial cavity in derived ornithopods becoming straighter (Lauters et al., 2022).

7. DURAL ENVELOPE

The dural envelope, or sometimes referred to as the dural covering, is the protective and supportive external covering of the brain in the braincase. It surrounds the entire brain, and therefore contacts all the bones of the braincase. Anatomically, it is made up of dense connective tissues and can be distinguished by up to three major layers depending on the organism: the outermost dura mater, the middle arachnoid mater, and the innermost pia mater. These layers, however, can only be described and separated in modern specimens, because the separate layers are not preserved during the fossilization process. Therefore, for dinosaurian taxa, these regions are all classified as the dural envelope. The dural envelope houses vascular blood veins, cranial sinuses, and cerebrospinal fluid, allowing for these features to perform their functions in association with the brain.

The dura mater is the externalmost and thickest layer that comprises the envelope and is situated against the braincase. Functionally, it is responsible for protecting and supporting the brain and cranial sinuses. Due to this protective and thick nature in dinosaurs, there is a risk that it could block anatomical and surficial features from being viewed on the endocast (Buchholtz, 2012). Unfortunately, CT scanning cannot differentiate the boundary between the brain and the dural mater; therefore, if the dural material was thicker in the living organism, the endocranial cavity shape would not be reflective of the true brain shape (Lautenschlager and Hübner, 2013). On the contrary, it has been shown to be successful in the identification of valleculae, specifically in ornithischian dinosaurs (Evans, 2005). In regions where this dura mater was thin, there is a chance of attaining impressions on the osteological braincase of valleculate veins that are

situated right against the true brain of an organism. This allows for a better, if not close to true, representation of the size and morphology of the brain within the braincase (Evans, 2005). A "dural peak" can also sometimes be visible on the dorsal region of the cerebellum, representing the area where the longitudinal sinus was located, but this is only present in certain taxa and well-preserved specimens (Button and Zanno, 2023).

The arachnoid mater is the second layer in the dural envelope complex. This layer is named so for its spiderweb appearance of fibrous veinlets and contains and uses the cerebrospinal fluid as a protective and cushion layer between the outer dura mater and inner pia mater. The pia mater is the innermost layer of the envelope and situated closest to the brain. It is responsible for the production of cerebrospinal fluid in life. Neither the arachnoid or pia mater has been observed on a steinkern or CT reconstruction, and are, therefore, unknown for non-avian dinosaurs. However, it is assumed that these two layers were probably present in non-avian dinosaurs since they are observed in modern birds (Monchaux, 2019) and reptiles (Kondrashova et al., 2020).

BIBLIOGRAPHY

Adeeb, N., Deep, A., Griessenauer, C.J., Mortazavi, M.M., Watanabe, K., Loukas, M., Tubbs, R.S., and Cohen-Gadol, A.A. (2013). The intracranial arachnoid mater: A comprehensive review of its history, anatomy, imaging, and pathology. *Child's Nervous System* 29(1), 17–33. https://doi.org/10.1007/s00381-012-1910-x

Anderson, J.F., Hall-Martin, A., and Russell, D.A. (1985). Long-bone circumference and weight in mammals, birds and dinosaurs. *Journal of Zoology* 207(1), 53–61. https://doi.org/10.1111/j.1469-7998.1985.tb04915.x

Balanoff, A.M., Bever, G.S., Rowe, T.B., and Norell, M.A. (2013). Evolutionary origins of the avian brain. *Nature* 501(7465), 93–96. https://doi.org/10.1038/nature12424

Balanoff, A.M., Norell, M.A., Hogan, A.V.C., and Bever, G.S. (2018). The endocranial cavity of oviraptorosaur dinosaurs and the increasingly complex, deep history of the avian brain. *Brain, Behavior and Evolution* 91(3), 125–135. https://doi.org/10.1159/000488890

Balanoff, A.M., Xu, X., Kobayashi, Y., Matsufune, Y., and Norell, M.A. (2010). Cranial osteology of the theropod dinosaur *Incisivosaurus gauthieri* (Theropoda: Oviraptorosauria). *American Museum Novitates* 3651, 1–34. https://doi.org/10.1206/644.1

Balanoff, A.M., and Bever, G.S. (2017). The role of endocasts in the study of brain evolution. *In*: J. H. Kaas (ed.), *Evolution of Nervous Systems*, 2nd ed. vol. 1. pp. 223–241. Elsevier, Oxford.

Ballell, A., Benton, M.J., & Rayfield, E.J. (2022). Dental form and function in the early feeding diversification of dinosaurs. *Science Advances* 8(50). https://www.science.org/doi/10.1126/sciadv.abq5201

Ballell, A., King, J.L., Neenan, J.M., Rayfield, E.J., and Benton, M.J. (2021). The braincase, brain and palaeobiology of the basal sauropodomorph dinosaur *Thecodontosaurus antiquus*. *Zoological Journal of the Linnean Society* 193, 541–562. https://doi.org/10.5523/bris.1hm

Balshine, S. (2012). Patterns of parental care in vertebrates. *In*: Royle, N.J., Smithset, P.T., and Koliker, M. (eds.), *The Evolution of Parental Care*, pp. 62–80. Oxford University Press. https://api.semanticscholar.org/CorpusID:146269928

Balthazart J., and Taziaux, M. (2009). The underestimated role of olfaction in avian reproduction? *Behavioral Brain Research* 200(2), 248–259. doi:10.1016/j. bbr.2008.08.036

Barrett, P.M., and Maidment, S.C.R. (2017). The evolution of ornithischian quadrupedality. *Journal of Iberian Geology* 43(3), 363–377). https://doi.org/10.1007/s41513-017-0036-0

Bell, P.R. (2014). A review of hadrosaur skin impressions. In: Ebert, D., and Evans, D. (eds.), *The Hadrosaurs*, pp. 572–590. Indiana University Press. https://www.researchgate.net/publication/257446562

Benson-Amram, S., Dantzer, B., Stricker, G., Swanson, E.M., and Holekamp, K.E. (2016). Brain size predicts problem-solving ability in mammalian carnivores. *Proceedings of the National Academy of Sciences* 113(9), 2532–2537. https://doi.org/10.1073/pnas.1505913113

Bever, G.S., Brusatte, S.L., Carr, T.D., Xu, X., Balanoff, A.M., and Norell, M.A. (2013). The braincase anatomy of the late cretaceous dinosaur *Alioramus* (Theropoda: Tyrannosauroidea). *Bulletin of the American Museum of Natural History* 376, 1–72. https://doi.org/10.1206/810.1

Bourke, J.M., Porter, W.R., Ridgely, R.C., Lyson, T.R., Schachner, E.R., Bell, P.R., and Witmer, L.M. (2014). Breathing life into dinosaurs: Tackling challenges of soft-tissue restoration and nasal airflow in extinct species. *Anatomical Record* 297(11), 2148–2186. https://doi.org/10.1002/ar.23046

Brasier, M.D., Norman, D.B., Liu, A.G., Cotton, L.J., Hiscocks, J.E.H, Garwood, R., Antcliffe, J.B., and Wacey, D. (2017). Remarkable preservation of brain tissues in an Early Cretaceous iguanodontian dinosaur. *The Geological Society of London Special Publications 448*, 383–398. https://doi.org/10.6084/m9.figshare.c.3519984

Brett-Surman, M.K. (1979). Phylogeny and palaeobiogeography of hadrosaurian dinosaurs. *Nature* 277, 560–562.

Brett-Surman, M.K. (1997). Ornithopods. *In*: Farlow, J.O., and Brett-Surman, M.K. (eds.), *The Complete Dinosaur*, pp. 330–346. Indiana University Press.

Briggs, D.E G., Kear, A.J., Martill, D.M., and Wilby, P.R. (1993). Phosphatisation of soft tissue in experiments and fossils. *Journal of the Geological Society, London* 150, 1035–1038. https://doi.org/10.1144/gsjgs.150.6.1035

Bronzati, M., Müller, R.T., and Langer, M.C. (2019). Skull remains of the dinosaur *Saturnalia tupiniquim* (Late Triassic, Brazil): With comments on the early evolution of sauropodomorph feeding behaviour. *PLoS ONE*, 14(9). https://doi.org/10.1371/journal.pone.0221387

Brown, B. (1916). *Corythosaurus casuarius*: skeleton, musculature and epidermis. *Bulletin of the American Museum of Natural History* 35(38), 709–716.

Buchholtz, E. (2012). Dinosaur Paleoneurology. *In* Brett-Surman, M.K., Holtz, T.R., and Farlow, J.O. (eds.), *The Complete Dinosaur,* 2nd ed., pp. 191–208. Indiana University Press.

Buchholtz, E., and Seyfarth, E.A. (1999). The gospel of the fossil brain: Tilly Edinger and the science of paleoneurology. *Brain Research Bulletin* 48, 4, 351–361. https://doi.org/10.1016/S0361-9230(98)00174-9

Buchholtz, E., and Seyfarth, E.A. (2001). The Study of "Fossil Brains." *Bioscience* 51(8), 674–682.

Burish, M.J., Kueh, H.Y., and Wang, S.S.H. (2004). Brain Architecture and Social Complexity in Modern and Ancient Birds. *Brain, Behavior and Evolution* 63(2). 107–124. https://doi.org/10.1159/000075674

Burnham, D.A., Derstler, K.L., Currie, P.J., Bakker, R.T., Zhonghe, Z., and Ostrom, J.H. (2000). Remarkable new birdlike dinosaur (Theropoda: Maniraptora) from the Upper Cretaceous of Montana. *The University of Kansas Paleontological Contributions* 13, 1–14.

Button, D.J., and Zanno, L.E. (2023). Neuroanatomy of the Late Cretaceous *Thescelosaurus neglectus* (Neornithischia: Thescelosauridae) reveals novel ecological specialisations within Dinosauria. *Scientific Reports* 13(1). https://doi.org/10.1038/s41598-023-45658-3

Carabajal, A.P. (2012). Neuroanatomy of titanosaurid dinosaurs from the Upper Cretaceous of Patagonia, with comments on endocranial variability within Sauropoda. *Anatomical Record* 295(12), 2141–2156. https://doi.org/10.1002/ar.22572

Caro, S.P., Balthazart, J., and Bonadonna, F. (2015). The perfume of reproduction in birds: chemosignaling in avian social life. *Horm Behav*. 68, 25–42.

Carr, T.D., Varricchio, D.J., Sedlmayr, J.C., Roberts, E.M., and Moore, J.R. (2017). A new tyrannosaur with evidence for anagenesis and crocodile-like facial sensory system. *Scientific Reports* 7. https://doi.org/10.1038/srep44942

Casale, J., Kandle, P.F., Murray, I.V., and Murr, N. (2018). Physiology, cochlear function. *In*: StatPearls. StatPearls Publishing, Treasure Island (FL); PMID: 30285378.

Cerroni, M.A., and Paulina-Carabajal, A. (2019). Novel information on the endocranial morphology of the abelisaurid theropod *Carnotaurus sastrei*. *Comptes Rendus - Palevol*, 18(8), 985–995. https://doi.org/10.1016/j.crpv.2019.09.005

Chadwick, R.A. (1981). Chronology and structural setting of volcanism in southwestern and central Montana. *Montana Geological Society Field Conference and Symposium Guidebook to Southwest Montana*, 301–310.

Chatterjee, S. (1991). Cranial anatomy and relationships of a new Triassic bird from Texas. *Philosophical Transactions: Biological Sciences* 332(1265).

Chiappe, L.M., and Dyke, G.J. (2002). The Mesozoic radiation of birds. *Annual Review of Ecology and Systematics* 33, 91–124. https://doi.org/10.1146/annurev.ecolsys.33.010802.150517

Chin, K. (2007). The paleobiological implications of herbivorous dinosaur coprolites from the Upper Cretaceous Two Medicine Formation of Montana: Why eat wood? *Palaios* 22(5), 554-566.

Cruzado-Caballero, P., Fortuny, J., Llacer, S., and Canudo, J.I. (2015). Paleoneuroanatomy of the European lambeosaurine dinosaur *Arenysaurus ardevoli*. *PeerJ*, 2015(2). https://doi.org/10.7717/peerj.802

Cubo, J., Woodward, H., Wolff, E., and Horner, J. R. (2015). First reported cases of biomechanically adaptive bone modeling in non-avian dinosaurs. *PLoS ONE*, 10(7). https://doi.org/10.1371/journal.pone.0131131

Cunningham, J.A., Rahman, I.A., Lautenschlager, S., Rayfield, E.J., and Donoghue, P.C.J. (2014). A virtual world of paleontology. *Trends in Ecology and Evolution* 29(6), 347–357). https://doi.org/10.1016/j.tree.2014.04.004

Currie, P.J. (1983). Hadrosaur trackways from the Lower Cretaceous of Canada. *Second Symposium on Mesozoic Terrestrial Ecosystems* 28(1), 63-73.

Dendy, A. (1911). On the structure, development and morphological interpretation of pineal organs and adjacent parts of the brain in the Tuatara (*Sphenodon punctatus*). *Philosophical Transactions of the Royal Society B: Biological Sciences* 201, 227–331.

Dilkes, D. (2000). Appendicular myology of the hadrosaurian dinosaur *Maiasaura peeblesorum* from the Late Cretaceous (Campanian) of Montana. *Transactions of the Royal Society of Edinburgh: Earth Sciences* 90, 87–125. https://www.researchgate.net/publication/287832765

Dufeau, D.L., Morhardt, A.C., and Witmer, L.M. (2012). Ontogenetic change in the cranial endocast and endosseous labyrinth of American alligator (*Alligator mississippiensis*): Implications for the interpretation of extinct archosaurs. *Journal of Vertebrate Paleontology* 32, 89.

Eberth, D.A., and Hamblin, A.P. (1993). Tectonic, stratigraphic, and sedimentologic significance of a regional discontinuity in the upper Judith River Group (Belly River wedge) of southern Alberta, Saskatchewan, and northern Montana. *Canadian Journal of Earth Sciences*, 30(1), 174–200. https://doi.org/10.1139/e93-016

Edinger, T. (1929). Die fossilen Gehirne. Ergebnisse Der Anatomie Und Entwicklungsgeschichte 28,1–249.

Edinger, T. (1942). The pituitary body in giant animals fossil and living: a survey and a suggestion. *The Quarterly Review of Biology* 17, 31–45.

Edinger, T. (1948). *Evolution of the Horse Brain*. Geological Society of America, 192 pp.

Edinger, T. (1951). The brains of the Odontognathae. *Evolution* 5, 6–24.

Edinger, T. (1955). Hearing and smell in cetacean history. *Monatsschrift Für Psychiatrie Und Neurologie* 129, 37–58.

Edinger, T. (1962). Anthropocentric misconceptions in paleoneurology. *Medical Society in the City of New York* 19, 56–107.

Edinger, T. (1975). *Paleoneurology 1804-1966: An Annotated Bibliography*. Springer Science & Business Media, 258 pp.

Evans, D.C. (2010). Cranial anatomy and systematics of *Hypacrosaurus altispinus*, and a comparative analysis of skull growth in lambeosaurine hadrosaurids (Dinosauria: Ornithischia). *Zoological Journal of the Linnean Society*, 159(2), 398–434. https://doi.org/10.1111/j.1096-3642.2009.00611.x

Evans, D.C.E. (2005). New evidence on brain−endocranial cavity relationships in ornithischian dinosaurs. *Acta Palaeontologica Polonica*, 50(3), 617–622. http://app.pan.pl/acta50/app50

Evans, D.C., Ridgely, R., and Witmer, L.M. (2009). Endocranial anatomy of lambeosaurine hadrosaurids (Dinosauria: Ornithischia): A sensorineural perspective on cranial crest function. *Anatomical Record*, 292(9), 1315–1337. https://doi.org/10.1002/ar.20984

Evers, S.W., Neenan, J.M., Ferreira, G.S., Werneburg, I., Barrett, P.M., and Benson, R.B.J. (2019). Neurovascular anatomy of the protostegid turtle *Rhinochelys pulchriceps* and comparisons of membranous and endosseous labyrinth shape in an extant turtle. *Zoological Journal of the Linnean Society* 187. https://academic.oup.com/zoolinnean/article/187/3/800/5552592

Falcon-Lang, H.J. (2003). Growth interruptions in silicified conifer woods from the Upper Cretaceous Two Medicine Formation, Montana, USA: Implications for palaeoclimate and dinosaur palaeoecology. *Palaeogeography, Palaeoclimatology, Palaeoecology* 199(3–4), 299–314. https://doi.org/10.1016/S0031-0182(03)00539-X

Farke, A.A., Chok, D.J., Herrero, A., Scolieri, B., and Werning, S. (2013). Ontogeny in the tube-crested dinosaur *Parasaurolophus* (Hadrosauridae) and heterochrony in hadrosaurids. *PeerJ* 2013(1). https://doi.org/10.7717/peerj.182

Ferreira Cardoso, S.F. (2015). On the function of the floccular complex of the vertebrate cerebellum: implications in paleoneuroanatomy. Master's thesis at the Universidade de Evora de Lisbon.

Ferreira-Cardoso, S., Araújo, R., Martins, N.E., Martins, G.G., Walsh, S., Martins, R.M.S., Kardjilov, N., Manke, I., Hilger, A., and Castanhinha, R. (2017). Floccular fossa size is not a reliable proxy of ecology and behaviour in vertebrates. *Scientific Reports* 7(1). https://doi.org/10.1038/s41598-017-01981-0

Foreman, B.Z., Rogers, R.R., Deino, A.L., Wirth, K.R., and Thole, J.T. (2008). Geochemical characterization of bentonite beds in the Two Medicine Formation (Campanian, Montana), including a new 40Ar/39Ar age. *Cretaceous Research* 29(3), 373–385. https://doi.org/10.1016/j.cretres.2007.07.001

Franzosa, J., and Rowe, T. (2005). Cranial endocast of the Cretaceous theropod dinosaur *Acrocanthosaurus atokensis*. *Journal of Vertebrate Paleontology* 25(4), 859-864.

Franzosa, J.W. (2004). Evolution of the Brain in Theropoda (Dinosauria).Ph.D dissertation at The University of Texas at Austin.

Freedman-Fowler, E.A., and Horner, J.R. (2015). A new brachylophosaurin hadrosaur (Dinosauria: Ornithischia) with an intermediate nasal crest from the Campanian Judith River Formation of northcentral Montana. *PLoS ONE* 10(11). https://doi.org/10.1371/journal.pone.0141304

Garamszegi, L.Z., and Eens, M. (2004). The evolution of hippocampus volume and brain size in relation to food hoarding in birds. *Ecology Letters* 7(12), 1216–1224. https://doi.org/10.1111/j.1461-0248.2004.00685.x

Garrick, L.D., Lang, J.W., and Herzog, H.A. (1978). Social signals of adult American alligator. *Bulletin of the American Museum of Natural History* 160(3), 155-192.

Gates, T.A., Horner, J.R., Hanna, R.R., and Nelson, C.R. (2011). New unadorned hadrosaurine hadrosaurid (Dinosauria, Ornithopoda) from the Campanian of North America. *Journal of Vertebrate Paleontology* 31(4), 798–811. https://doi.org/10.1080/02724634.2011.577854

Gavin, W.M.B. (1986). A paleoenvironmental reconstruction of the Cretaceous Willow Creek anticline dinosaur nesting locality: North Central Montana. Master's thesis at Montana State University.

Georgi, J.A., Sipla, J.S., and Forster, C.A. (2013). Turning semicircular canal function on its head: Dinosaurs and a novel vestibular analysis. *PLoS ONE* 8(3). https://doi.org/10.1371/journal.pone.0058517

Georgi, J., and Sipla, J. (2008). Comparative and functional anatomy of balance in aquatic reptiles and birds. *In*: Thewissen, J.G.M. and Nummela, S. (eds.), *Sensory Evolution on the Threshold: Adaptations in Secondarily Aquatic Vertebrates*, pp. 183–210. University of California Press.

Giffin, E.B. (1989). Pachycephalosaur paleoneurology (Archosauria: Ornithischia). *Journal of Vertebrate Paleontology* 9(1), 67-77.

Gilmore, C.W. (1917). *Brachyceratops*, a ceratopsian dinosaur from the Two Medicine Formation of Montana, with notes on associated fossil reptiles. *United States Geological Society Professional Paper*. 54 pp.

Gishlick, A.D. (2001). Predatory behaviour in maniraptoran theropods. *In*: Briggs, D.E.G and Crowther, P.R (ed.) *Palaeobiology II*, pp. 414–417. Wiley. https://doi.org/10.1002/9780470999295.ch99

Gleich, O., Dooling, R.J., and Manley, G.A. (2005). Audiogram, body mass, and basilar papilla length: Correlations in birds and predictions for extinct archosaurs. *Naturwissenschaften* 92(12), 595–598. https://doi.org/10.1007/s00114-005-0050-5

Godefroit, P., Bolotsky, Y.L., and Lauters, P. (2012a). A new saurolophine dinosaur from the latest Cretaceous of far eastern Russia. *PLoS ONE 7*(5). https://doi.org/10.1371/journal.pone.0036849

Godefroit, P., Escuillie, F., Bolotsky, Y.L., and Lauters, P. (2012b). A new basal hadrosauroid dinosaur from the upper cretaceous of Kazakhstan. *In*: Godefroit, P. (ed.), *Bernissart Dinosaurs and Early Cretaceous Terrestrial Ecosystems*, pp. 335–358. Indiana University Press, Bloomington.

Grellet-Tinner, G., Chiappe, L., Norell, M., and Bottjer, D. (2006). Dinosaur eggs and nesting behaviors: A paleobiological investigation. *Palaeogeography, Palaeoclimatology, Palaeoecology* 232(2–4), 294–321. https://doi.org/10.1016/j.palaeo.2005.10.029

Hirsch, K.F., and Quinn, B. (1990). Eggs and eggshell fragments from the Upper Cretaceous Two Medicine Formation of Montana. *Journal of Vertebrate Paleontology* 10(4), 491-511.

Holloway, R.L. (2018). On the making of endocasts: The new and the old in paleoneurology. *In*: Bruner, E. et al. (eds.) *Digital Endocasts*, pp. 1–8. Springer Japan. https://doi.org/10.1007/978-4-431-56582-6_1

Hopson, J.A. (1977). Relative brain size and behavior in archosaurian reptiles. *Annual Review of Ecology and Systematics* 8, 429-448. https://www.jstor.org/stable/2096736?seq=1&cid=pdf-

Hopson, J.A. (1979). Paleoneurology. *In*: Gans, C., Northcutt, R.C., and Ulinski, P. (eds.), *Biology of the Reptilia* (Neurology A), vol. 9, pp. 39–146. Academic Press Inc., New York, New York.

Horner, J.R. (1982). Evidence of colonial nesting and "site fidelity" among ornithischian dinosaurs. *Nature* 297(5868), 675–676. https://doi.org/10.1038/297675a0

Horner, J.R. (1983). Cranial osteology and morphology of the type specimen of *Maiasaura peeblesorum* (Ornithischia: Hadrosauridae), with a discussion of its phylogenetic position. *Journal of Vertebrate Paleontology* 3(1), 29–38. https://doi.org/10.1080/02724634.1983.10011954

Horner, J.R. (1988). A new hadrosaur (Reptilia, Ornithischia) from the Upper Cretaceous Judith River Formation of Montana. *Journal of Vertebrate Paleontology* 8(3), 314-321.

Horner, J.R. (1992). Cranial morphology of *Prosaurolophus* (Ornithischia: Hadrosauridae) with descriptions of two new hadrosaurid species and an evaluation of hadrosaurid phylogenetic relationships. *Museum of the Rockies, Occasional Paper 2*, 1–119.

Horner, J.R., and Currie, P.J. (1994). Embryonic and neonatal morphology and ontogeny of a new species of *Hypacrosaurus* (Ornithischia: Lambeosaurinae) from Montana and Alberta. *In*: Carpenter, K., Hirsch, K.F., and Horner, J.R. (eds.), *Dinosaur Eggs and Babies*, pp. 312–336. Cambridge University Press.

Horner, J.R., and Makela, R. (1979). Nest of juveniles provides evidence of family structure among dinosaurs. *Nature* 282(5736), 296–298. https://doi.org/10.1038/282296a0

Horner, J.R., and Weishampel, D.B. (1988). A comparative embryological study of two ornithischian dinosaurs. *Nature* 332(17), 256–257.

Horner, J.R., de Ricqlès, A., and Padian, K. (2000). Long bone histology of the hadrosaurid dinosaur *Maiasaura peeblesorum*: Growth dynamics and physiology based on an ontogenetic series of skeletal elements. *Journal of Vertebrate Paleontology* 20(1), 115-129.

Horner, J.R., Jackson, F.D., Schmitt, J.G., and Hanna, R. (2001). Bones and rocks of the Upper Cretaceous Two Medicine–Judith River clastic wedge complex, *Guidebook for the Society of Vertebrate Paleontology 61st Annual Meeting.* https://www.researchgate.net/publication/341030291

Horner, J.R., Weishampel, D.B., and Forster, C.A. (2004). Hadrosauridae. *In*: Weishampel, D.B., Dodson, P., Osmolska, H. (eds.) *The Dinosauria*, pp. 438–463. University of California Press. https://doi.org/10.1525/california/9780520242098.003.0023

Hu, K., King, J.L., Romick, C.A., Dufeau, D.L., Witmer, L.M., Stubbs, T.L., Rayfield, E.J., and Benton, M.J. (2021). Ontogenetic endocranial shape change in alligators and ostriches and implications for the development of the non-avian dinosaur endocranium. *Anatomical Record* 304(8), 1759–1775. https://doi.org/10.1002/ar.24579

Huene, F. (1914). III.—Saurischia and Ornithischia. *Geological Magazine* 1(10), 444-445. doi:10.1017/S0016756800153166

Hughes, G.M., and Finarelli, J.A. (2019). Olfactory receptor repertoire size in dinosaurs. *Proceedings of the. Royal Society B: Biological Sciences* 286(1904).

Hunt, R.H., and Watanabe, M.E. (1982). Observations on maternal behavior of the American alligator, *Alligator mississippiensis*. *Journal of Herpetology* 16(3); 235-239.

Hurlburt, G.R. (1996). Relative brain size in recent and fossil amniotes: Determination and Interpretation. Ph.D thesis at the University of Toronto. https://doi.org/10.13140/RG.2.2.26802.07362

Hurlbert, G.R., Ridgely, R.C., and Witmer, L.M. (2013). Relative size of brain and cerebrum in *Tyrannosaurus rex*: an analysis using brain-endocast quantitative relationships in extant alligators. *In*: Parrish, J.M., Henderson, M., Currie, P.J., Koppelhus, E. (eds.) *Origin, Systematics, and Paleobiology of the Tyrannosauridae,* pp. 134-154. Indiana University Press.

Jackson, F.D., Schaff, R.J., Varricchio, D.J., and Schmitt, J.G. (2015). A theropod nesting trace with eggs from the Upper Cretaceous (Campanian) Two Medicine Formation of Montana. *PALAIOS* 30(5), 362–372. https://doi.org/10.2110/palo

Jarvik, E. (1954). On the visceral skeleton in *Eusthenopteron*, with a discussion of the parasphenoid and palatoquadrate in fishes. *Kungl. Svenska Vetenskapsakademiens Handlingar* 4, 1–104.

Jerison, H.J. (1955). Brain to body ratios and the evolution of intelligence. *Science* 121(3144), 447–449.

Jerison, H.J. (1961). Quantitative analysis of evolution of the brain in mammals. *Science* 133, 1012–1014.

Jerison, H.J. (1969). Brain evolution and dinosaur brains. *The American Naturalist* 103(934), 575–588.

Jerison, H.J. (1973). *Evolution of the Brain and Intelligence*. Academic Press, New York, 482 pp.

Jerison, H.J. (2004). Dinosaur brain. *In*: Adelman, G., and Smith, B.H. (eds.) *Encyclopedia of Neuroscience 3rd Edition*, pp. 1-6 Amsterdam, Elsevier.

Jerison, H.J., and Barlow, H.B. (1985). Animal intelligence as encephalization [and discussion]. *Animal Intelligence* 308(1135), 21–35.

Jirak, D., and Janacek, J. (2017). Volume of the crocodilian brain and endocast during ontogeny. *PLoS ONE* 12(6). https://doi.org/10.1371/journal.pone.0178491

Joanen, T., and Mcnease, L.L. (1989). Ecology and physiology of nesting and early development of the American alligator. *American Zoology* 29, 987–998. https://academic.oup.com/icb/article/29/3/987/294223

Kats, L.B., and Dill, L.M. (1998). The scent of death: Chemosensory assessment of predation risk by prey animals. *Écoscience* 5(3), 361-394.

King, J.L., Sipla, J.S., Georgi, J.A., Balanoff, A.M., and Neenan, J.M. (2020). The endocranium and trophic ecology of *Velociraptor mongoliensis*. *Journal of Anatomy* 237(5), 861–869. https://doi.org/10.1111/joa.13253

King, J.T. (1994). Facies analysis of the volcaniclastic Two Medicine Formation, Wolf Creek Montana. Master's thesis at the University of Montana. https://scholarworks.umt.edu/etd/7569

Knoll, F., Lautenschlager, S., Kawabe, S., Martínez, G., Espílez, E., Mampel, L., and Alcalá, L. (2021). Palaeoneurology of the Early Cretaceous iguanodont *Proa valdearinnoensis* and its bearing on the parallel developments of cognitive abilities in theropod and ornithopod dinosaurs. *Journal of Comparative Neurology* 529(18), 3922–3945. https://doi.org/10.1002/cne.25224

Kondrashova, T., Blanchard, J., Knoche, L., Potter, J., and Young, B.A. (2020). Intracranial pressure in the American alligator (*Alligator mississippiensis*): reptilian meninges and orthostatic gradients. *Journal of Comparative Physiology A* 206(1), 45–54. https://doi.org/10.1007/s00359-019-01386-6

Kotrschal, A., Corral-Lopez, A., Amcoff, M., and Kolm, N. (2015). A larger brain confers a benefit in a spatial mate search learning task in male guppies. *Behavioral Ecology* 26(2), 527–532. https://doi.org/10.1093/beheco/aru227

Kotrschal, A., Rogell, B., Bundsen, A., Svensson, B., Zajitschek, S., Brännström, I., Immler, S., Maklakov, A.A., and Kolm, N. (2013). Artificial selection on relative brain size in the guppy reveals costs and benefits of evolving a larger brain. *Current Biology* 23(2), 168–171. https://doi.org/10.1016/j.cub.2012.11.058

Kreft, G. (1997). The work of Ludwig Edinger and his Neurology Institute. *In*: Korf, H.W., and Usadel, K.H. (eds), *Neuroendocrinology,* pp. 407-423. Springer, Berlin, Heidelberg. https://doi.org/10.1007/978-3-642-60915-2_31

Kundrát, M. (2007). Avian-like attributes of a virtual brain model of the oviraptorid theropod *Conchoraptor gracilis*. *Naturwissenschaften* 94(6), 499–504. https://doi.org/10.1007/s00114-007-0219-1

Langer, M.C., McPhee, B.W., de Almeida Marsola, J.C., Roberto-da-Silva, L., and Cabreira, S.F. (2019). Anatomy of the dinosaur *Pampadromaeus barberenai* (Saurischia—Sauropodomorpha) from the Late Triassic Santa Maria Formation of southern Brazil. *PLoS ONE* 14(2). https://doi.org/10.1371/journal.pone.0212543

Larsson, H.C.E., Sereno, P.C., and Wilson, J.A. (2000). Forebrain enlargement among nonavian theropod dinosaurs. *Journal of Vertebrate Paleontology* 20(3), 615–618. https://doi.org/10.1671/0272-4634(2000)020[0615:FEANTD]2.0.CO;2

Lautenschlager, S., and Hübner, T. (2013). Ontogenetic trajectories in the ornithischian endocranium. *Journal of Evolutionary Biology* 26(9), 2044–2050. https://doi.org/10.1111/jeb.12181

Lautenschlager, S., Rayfield, E.J., Altangerel, P., Zanno, L.E., and Witmer, L.M. (2012). The endocranial anatomy of *Therizinosauria* and its implications for sensory and cognitive function. *PLoS ONE* 7(12). https://doi.org/10.1371/journal.pone.0052289

Lauters, P., Coudyzer, W., Vercauteren, M., and Godefroit, P. (2012). The brain of *Iguanodon* and *Mantellisaurus*: Perspectives on ornithopod evolution. *In*: Godefroit, P. (ed.), *Bernissart Dinosaurs and Early Cretaceous Terrestrial Ecosystems*, pp. 213–224. Indiana University Press.

Lauters, P., Vercauteren, M., Bolotsky, Y.L., and Godefroit, P. (2013). Cranial endocast of the lambeosaurine hadrosaurid *Amurosaurus riabinini* from the Amur Region, Russia. *PLoS ONE* 8(11). https://doi.org/10.1371/journal.pone.0078899

Lauters, P., Vercauteren, M., and Godefroit, P. (2023). Endocasts of ornithopod dinosaurs: Comparative anatomy. *Progress in Brain Research* 275, 1–23. https://doi.org/10.1016/bs.pbr.2022.10.002

Leahey, L.G., Molnar, R.E., Carpenter, K., Witmer, L.M., and Salisbury, S.W. (2015). Cranial osteology of the ankylosaurian dinosaur formerly known as *Minmi* sp. (Ornithischia: Thyreophora) from the Lower Cretaceous Allaru Mudstone of Richmond, Queensland, Australia. *PeerJ* 2015(12). https://doi.org/10.7717/peerj.1475

Liang, X., Wen, S., Yang, D., Zhou, S., and Wu, S. (2009). Dinosaur eggs and dinosaur egg-bearing deposits (Upper Cretaceous) of Henan Province, China: Occurrences, palaeoenvironments, taphonomy and preservation. *Progress in Natural Science* 19(11), 1587–1601. https://doi.org/10.1016/j.pnsc.2009.06.012

Lockley, M.G., and Matsukawa, M. (1999). Some observations on trackway evidence for gregarious behavior among small bipedal dinosaurs. *Palaeogeography, Palaeoclimatology, Palaeoecology* 150, 25-31.

Lorenz, J.C. (1981). Sedimentary and tectonic history of the Two Medicine Formation, Late Cretaceous (Campanian), northwestern Montana. Master's thesis at the University of Montana.

Lorenz, J.C., and Gavin, W. (1984). Geology of the Two Medicine Formation and the sedimentology of a dinosaur nesting ground. *Montana Geological Society, 1984 Field Conference, Symposium Guidebook*, 175–186.

Mak, G.K., and Weiss, S. (2010). Paternal recognition of adult offspring mediated by newly generated CNS neurons. *Nature Neuroscience* 13(6), 753–758. https://doi.org/10.1038/nn.2550

Makovicky, P.J., and Zanno, L.E. (2011). Theropod diversity and the refinement of avian characteristics. *In*: Dyke, G., and Kaiser, G. (eds.), *Living Dinosaurs*, pp. 9–29. Wiley. https://doi.org/10.1002/9781119990475.ch1

Manning, P.L., Morris, P.M., McMahon, A., Jones, E., Gize, A., Macquaker, J.H.S., Wolff, G., Thompson, A., Marshall, J., Taylor, K.G., Lyson, T., Gaskell, S., Reamtong, O., Sellers, W.I., van Dongen, B.E., Buckley, M., and Wogelius, R.A. (2009). Mineralized soft-tissue structure and chemistry in a mummified hadrosaur from the Hell Creek Formation, North Dakota (USA). *Proceedings of the Royal Society B: Biological Sciences* 276(1672), 3429–3437. https://doi.org/10.1098/rspb.2009.0812

Mantell, G.A. (1825). Notice on the Iguanodon, a newly discovered fossil reptile, from the sandstone of Tilgate forest, in Sussex. *Philosophical Transactions of the Royal Society of London* 115, 179–186.

Marsh, O.C. (1873). Notice of a new and remarkable fossil bird. *Annals and Magazine of Natural History* 11(61), 80.

Marsh, O.C. (1874). Small size of the brain in tertiary mammals. *Annals and Magazine of Natural History* 14, 167.

Marsh, O.C. (1880). *Odontornithes: A Monograph on the Extinct Toothed Birds of North America.* U.S. Government Printing Office, 201 pp.

Marsh, O.C. (1881). Principal characters of American Jurassic dinosaurs, Part V. *American Journal of Science* 21, 417–423.

Marsh, O.C. (1884a). Principal characters of American Jurassic dinosaurs; Part VII, on the Diplodocidae, a new family of the Sauropoda. *American Journal of Science* 27, 161–167.

Marsh, O.C. (1884b). Principal characters of American Jurassic dinosaurs; Part VIII, the order Theropoda. *American Journal of Science* 27, 329–340.

Marsh, O.C. (1886). *Dinocerata: A Monograph of an Extinct Order of Gigantic Mammals*. U.S. Government Printing Office, 522 pp.

Marsh, O.C. (1889). Notice of gigantic horned Dinosauria from the Cretaceous. *American Journal of Science* 38, 173–176.

Marsh, O.C. (1890). Additional characters of the *Ceratopsidae, with notice of new Cretaceous dinosaurs. American* Journal of Science 39, 418–426.

Marsh, O.C. (1891). The gigantic Ceratopsidæ, or horned dinosaurs, of North America. *Geological Magazine* 8, 193–199.

Marsh, O.C. (1896). *The Dinosaurs of North America*. United States Geological Survey, Washington D. C., 244 pp.

Martínez, R.N., Haro, J.A., and Apaldetti, C. (2012). Braincase of *Panphagia protos* (Dinosauria, Sauropodomorpha). *Journal of Vertebrate Paleontology* 32(sup1), 70–82. doi:10.1080/02724634.2013.819009

McDonald, A.T., Wolfe, D.G., Freedman Fowler, E.A., and Gates, T.A. (2021). A new brachylophosaurin (Dinosauria: Hadrosauridae) from the Upper Cretaceous Menefee Formation of New Mexico. *PeerJ* 9. https://doi.org/10.7717/peerj.11084

McFeeters, B., Evans, D.C., and Maddin, H.C. (2021). Ontogeny and variation in the skull roof and braincase of the hadrosaurid dinosaur *Maiasaura peeblesorum* from the Upper Cretaceous of Montana, USA. *Acta Palaeontologica Polonica* 66(3), 485-507. https://doi.org/10.4202/APP.00698.2019

Meganck, J.A., and Liu, B. (2017). Dosimetry in micro-computed tomography: a review of the measurement methods, impacts, and characterization of the Quantum GX Imaging System. *Molecular Imaging and Biology* 19(4), 499–511. https://doi.org/10.1007/s11307-016-1026-x

Molina-Morales, M., Castro, J., Albaladejo, G., and Parejo, D. (2020). Precise cache detection by olfaction in a scatter-hoarder bird. *Animal Behaviour* 167, 185–191. doi:10.1016/j.anbehav.2020.07.002.

Monchaux, M. (2019). Neurology in exotic animals. [Paper presentation]. *VIII FAUNA International Conference, Lisbon*.

Morhardt, A.C., Ridgely, R., and Witmer, L.M. (2017). Gross Anatomical Brain Region Approximation (GABRA): a new landmark-based approach for estimating brain regions in dinosaurs and other archosaurs. *Federation of American Societies for Experimental Biology* 31, 251.2-251.2.

Müller, R.T. (2022). Olfactory acuity in early sauropodomorph dinosaurs. *Historical Biology* 34(2), 346–351. https://doi.org/10.1080/08912963.2021.1914600

Murphy, N., Trexler, D., and Thompson, M. (2007). "Leonardo," a mummified *Brachylophosaurus* (Ornithischia: Hadrosauridae) from the Judith River Formation of Montana. *In*: Carpenter. K. (ed.), *Horns and Beaks: Ceratopsian and Ornithopod Dinosaurs*, pp. 117–133. Indiana University Press.

Newton, E.T. (1888). On the skull, brain, and auditory organ of a new species of pterosaurian *Scaphognathus purdoni*, from the upper Lias near Whitby, Yorkshire. *Philosophical Transactions of the Royal Society, London B: Biological Sciences* 179, 503–537.

Osmolska, H. (2004). Evidence on relation of brain to endocranial cavity in oviraptorid dinosaurs. *Acta Palaeontologica Polonica* 49(2), 321–324. http://app.pan.pl/acta49/app49

Osborn, H.E. (1905). *Tyrannosaurus* and other Cretaceous carnivorous dinosaurs: *Bulletin of the American Museum of Natural History* 21, 259–265.

Ostrom, J.H. (1961). Cranial morphology of the hadrosaurian dinosaurs of North America. *Bulletin of the American Museum of Natural History* 122, 33–186.

Ostrom, J.H. (1962). The cranial crests of hadrosaurian dinosaurs. *Postilla* 62, 1–29.

Ostrom, J.H. (1976). *Archaeopteryx* and the origin of birds. *Biological Journal of the Linnean Society* 8, 91–182.

Overington, S.E., Morand-Ferron, J., Boogert, N.J., and Lefebvre, L. (2009). Technical innovations drive the relationship between innovativeness and residual brain size in birds. *Animal Behaviour* 78(4), 1001–1010. https://doi.org/10.1016/j.anbehav.2009.06.033

Padian, K., Lamm, E.T., and Werning, S. (2013). Selection of specimens. *In*: *Bone Histology of Fossil Tetrapods: Advancing Methods, Analysis, and Interpretation,* pp. 35–54. University of California Press. https://doi.org/10.1525/california/9780520273528.003.0003

Paulina-Carabajal, A., Lee, Y.N., and Jacobs, L.L. (2016). Endocranial morphology of the primitive nodosaurid dinosaur *Pawpawsaurus campbelli* from the Early Cretaceous of North America. *PLoS ONE* 11(3). https://doi.org/10.1371/journal.pone.0150845

Pérez-Barbería, F.J., and Gordon, I.J. (2005). Gregariousness increases brain size in ungulates. *Oecologia* 145(1), 41–52. https://doi.org/10.1007/s00442-005-0067-7

Persons, W.S., and Currie, P.J. (2015). Duckbills on the run: The cursorial abilities of hadrosaurs and implications for tyrannosaur-avoidance strategies. *In*: Eberth, D.A., and Evans, D.C. (eds.), *Hadrosaurs*, pp. 449–458. Indiana University Press.

Porter, W.R., and& Witmer, L.M. (2020). Vascular patterns in the heads of dinosaurs: Evidence for blood vessels, sites of thermal exchange, and their role in physiological thermoregulatory strategies. *Anatomical Record* 303(4), 1075–1103. https://doi.org/10.1002/ar.24234

Prieto-Marquez, A. (2005). New information on the cranium of *Brachylophosaurus canadensis* (Dinosauria, Hadrosauridae), with a revision of its phylogenetic position. *Journal of Vertebrate Paleontology* 25(1), 144–156. https://doi.org/10.1671/0272-4634(2005)025[0144:NIOTCO]2.0.CO;2

Prieto-Marquez, A. (2007). Postcranial osteology of the hadrosaurid dinosaur *Brachylophosaurus canadensis* from the Late Cretaceous of Montana. *In*: Carpenter, K. (ed.), *Horns and Beaks: Ceratopsian and Ornithopod Dinosaurs*, pp. 91–116. Indiana University Press.

Prieto-Márquez, A. (2010a). Global historical biogeography of hadrosaurid dinosaurs. *Zoological Journal of the Linnean Society* 159(2), 503–525. https://doi.org/10.1111/j.1096-3642.2010.00642.x

Prieto-Márquez, A. (2010b). Global phylogeny of hadrosauridae (Dinosauria: Ornithopoda) using parsimony and Bayesian methods. *Zoological Journal of the Linnean Society* 159(2), 435–502. https://doi.org/10.1111/j.1096-3642.2009.00617.x

Prieto-Marquez, A. (2010). The braincase and skull roof of *Gryposaurus notabilis* (Dinosauria, Hadrosauridae), with a taxonomic revision of the genus. *Journal of Vertebrate Paleontology* 30(3), 838–854. https://doi.org/10.1080/02724631003762971

Prieto-Marquez, A., and Guenther, M.F. (2018). Perinatal specimens of *Maiasaura* from the Upper Cretaceous of Montana (USA): Insights into the early ontogeny of saurolophine hadrosaurid dinosaurs. *PeerJ* 2018(5). https://doi.org/10.7717/peerj.4734

Prieto-Márquez, A., and Wagner, J.R. (2013). A new species of saurolophine hadrosaurid dinosaur from the Late Cretaceous of the Pacific coast of North America. *Acta Palaeontologica Polonica* 58(2), 255–268. https://doi.org/10.4202/app.2011.0049

Racicot, R. (2016). Fossil secrets revealed: X-Ray CT scanning and application in paleontology. *The Paleontological Society Papers* 22, 21–38. https://doi.org/10.1017/scs.2017.6

Radinsky, L.B. (1968). A new approach to mammalian cranial analysis, illustrated by examples of prosimian primates. *Journal of Morphology* 124, 167–179.

Reader, S.M., and Laland, K.N. (2002). Social intelligence, innovation, and enhanced brain size in primates. *Proceedings of the National Academy of Sciences* 99(7), 4436–4441. https://www.pnas.org

Reber, S.A. (2020). Crocodilians are promising intermediate model organisms for comparative perception research. *Comparative Cognition & Behavior Reviews* 15, 111–129. https://doi.org/10.3819/ccbr.2020.150004

Rogers, R.R. (1990). Taphonomy of three dinosaur bone beds in the Upper Cretaceous Two Medicine. *Palaios* 5, 394–413.

Rogers, R.R. (1998). Sequence analysis of the Upper Cretaceous Two Medicine and Judith River Formations, Montana: Nonmarine response to the Claggett and Bearpaw marine cycles. *Journal of Sedimentary Research* 68(4); 615-631. http://pubs.geoscienceworld.org/sepm/jsedres/article-pdf/68/4/615/2812375/615.pdf?casa_token=QCOEKvgGZF8AAAAA:vbXaMCYGKjMlbQVkze-I3t5dEQBXI3agEOokY_UcRuGhilYHUD0VwHOMhnlRkwBfc0F0

Rogers, R.R., Swisher III, C.C., and Horner, J.R. (1993). ^{40}A/^{39}Ar age and correlation of the nonmarine Two Medicine Formation (Upper Cretaceous), northwestern Montana, USA. *Canadian Journal of Earth Sciences* 30, 1066–1075.

Rogers, S.W. (1998). Exploring dinosaur neuropaleobiology: Computed tomography scanning and analysis of an *Allosaurus fragilis* endocast. *Neuron* 21, 673–679.

Rogers, S.W. (1999). Allosaurus, crocodiles, and birds: Evolutionary clues from spiral computed tomography of an endocast. *Anatomical Record* 257(5), 162–173). https://doi.org/10.1002/(SICI)1097-0185(19991015)257:5<162::AID-AR5>3.0.CO;2-W

Rombaux, P., Duprez, T., and Hummel, T. (2009). Olfactory bulb volume in the clinical assessment of olfactory dysfunction. *Rhinology* 47, 3–9.

Romer, A., and Edinger, T. (1942). Endocranial casts and brains of living and fossil amphibia. *Journal of Comparative Neurology* 77(2), 355–389

Sakagami, R., and Kawabe, S. (2020). Endocranial anatomy of the ceratopsid dinosaur *Triceratops* and interpretations of sensory and motor function. *PeerJ* 8. https://doi.org/10.7717/peerj.9888

Sampson, S.D. (1995). Two new horned dinosaurs from the Upper Cretaceous Two Medicine Formation of Montana; With a phylogenetic analysis of the Centrosaurinae (Ornithischia: Ceratopsidae). *Journal of Vertebrate Paleontology* 15(4), 743-760.

Sampson, S., and Witmer, L.M. (2007). Craniofacial anatomy of *Majungasaurus crenatissimus* (Theropoda: Abelisauridae) from the Late Cretaceous of Madagascar. *Journal of Vertebrate Paleontology* 27(2), 32-104.

Sanders, R.K., Sanders, D.K.S., and Smith, R.K. (2005). The endocranium of the theropod dinosaur *Ceratosaurus* studied with computed tomography. *Acta Palaeontologica Polonica* 50(3), 601–616. http://app.pan.pl/acta50/app50

Sandy, M.R. (1989). Preparation of serial sections. *The Paleontological Society Special Publications* 4, 146-156. doi: 10.1017/S2475262200005086

Saveliev, S.V., Alifanov, V.R., and Bolotsky, Y.L. (2012). Brain anatomy of *Amurosaurus riabinini* and some neurobiological peculiarities of duck-billed dinosaurs. *Paleontological Journal* 46(1), 79–91. https://doi.org/10.1134/S003103011201011X

Scherzer, B.A., and Varricchio, D.J. (2010). Taphonomy of a juvenile lambeosaurine bonebed from the Two Medicine formation (Campanian) of Montana, United States. *Palaios* 25(12), 780–795. https://doi.org/10.2110/palo.2009.p09-143r

Scott-Persons, W. (2011). Duckbills on the run: comparing the cursorial abilities of hadrosaurs and tyrannosaurs. *In*: Braman, D.R., Eberth, D.A., Evans, D.C., and Taylor, W. (eds.), *International Hadrosaur Symposium Abstract Volume*, pp. 117–121. Royal Tyrell Museum of Paleontology, Drumheller.

Schuchert, C. (1938). Biographical memoir of Othniel Charles Marsh 1831–1899. National Academy of Sciences 20, 1–78.

Sereno, P.C. (2007). Logical basis for morphological characters in phylogenetics. *Cladistics* 23(6), 565–587. https://doi.org/10.1111/j.1096-0031.2007.00161.x

Shultz, S., and Dunbar, R. (2010). Encephalization is not a universal macroevolutionary phenomenon in mammals but is associated with sociality. *Proceedings of the National Academy of Sciences* 107(50), 21582–21586. https://doi.org/10.1073/pnas.1005246107

Sobral, G., Hipsley, C.A., and Müller, J. (2012). Braincase redescription of *Dysalotosaurus lettowvorbecki* (Dinosauria, Ornithopoda) based on computed tomography. *Journal of Vertebrate Paleontology* 32(5), 1090–1102. https://doi.org/10.1080/02724634.2012.693554

Sol, D., Duncan, R.P., Blackburn, T.M., Cassey, P., and Lefebvre, L. (2005). Big brains, enhanced cognition, and response of birds to novel environments. *Proceedings of the National Academy of Sciences* 102(15), 5460–5465. www.pnas.orgcgidoi10.1073pnas.0408145102

Sol, D., Lefebvre, L., and Rodríguez-Teijeiro, J.D. (2005). Brain size, innovative propensity and migratory behaviour in temperate Palaearctic birds. *Proceedings of the Royal Society B: Biological Sciences* 272(1571), 1433–1441. https://doi.org/10.1098/rspb.2005.3099

Sollas, W.J. (1904). A method for the investigation of fossils by serial sections. *Philosophical Transactions of the Royal Society of London. B: Biological Sciences* 196, 259–265.

Sollas, W.J. (1915). On the restoration of certain fossils by serial sections. Rep. Brit. Assoc. 1915. 426-427.

Sollas, W.J. (1917). The skull of *Ichthyosaurus* studied in serial sections. *Philosophical Transactions of the Royal Society of London B: Biological Sciences* 208, 63-126

Sollas, W. J. (1920). On the structure of *Lysorophus* as exposed by serial sections. *Philosophical Transactions of the Royal Society of London B: Biological Sciences* 209, 481-527

Sollas, W.J. (1921). On *Saccamina carteri*, Brady, and the minute structure of the foraminiferal shell. *Quarterly Journal of the Geological Society* 77, 193-212.

Sollas, W.J. (1926). On a sagittal section of the skull of *Australopithecus africanus*. *Quarterly Journal of the Geological Society* 82, 1-11

Sollas, W.J., and Sollas, I.B.J. (1904). An account of the Devonian fish, *Pauospondylus gunni*, Traquair. *Philosophical Transactions of the Royal Society of London B: Biological Sciences* 196, 267-294

Sollas, W.J., and Sollas, I.B.J. (1913). A study of the skull of a *Dicynodon* by means of serial sections. *Philosophical Transactions of the Royal Society of London B: Biological Sciences,* 204, 201-225

Starck, D. (1979). Cranio–cerebral relations in recent reptiles. *In*: Gans, C., Northcutt, R.G., and Ulinski, P. (eds.), Biology of the Reptilia (Neurology A), Vol. 9, pp. 1–38. Academic Press, New York.

Sternberg, C.M. (1953). A new hadrosaur from the Oldman Formation of Alberta: discussion of nomenclature. *Canada Department of Mines Geological Survey Bulletin* 128, 275–286.

Stidham, T.A., and Hutchison, J.H. (2001). The North American avisaurids (Aves: Enantiornithes): new data on biostratigraphy and biogeography. *Asociacion Paleontologica Argentina* 30(6), 30–36.

Togunov, R.R., Derocher, A.E., and Lunn, N.J. (2017). Windscapes and olfactory foraging in a large carnivore. *Scientific Reports* 7. https://doi.org/10.1038/srep46332

Trexler, D. (1995). A detailed description of newly-discovered remains of *Maiasaura peeblesorum (*Reptilia: Ornithischian*)* and a revised diagnosis of the genus. Master's thesis at The University of Calgary.

Varricchio, D.J., and Horner, J.H. (1993). Hadrosaurid and lambeosaurid bone beds from the Upper Cretaceous Two Medicine Formation of Montana: taphonomic and biologic implications. *Canadian Journal of Earth Sciences* 30, 997–1006.

Varricchio, D.J., Jackson, F., Borkowski, J.J., and Horner, J.R. (1997). Nest and egg clutches of the dinosaur *Troodon formosus* and the evolution of avian reproductive traits. *Nature* 385(6613), 247–250. https://doi.org/10.1038/385247a0

Varricchio, D.J., Jackson, F.J., and Trueman, C.N. (1999). A nesting trace with eggs for the Cretaceous theropod dinosaur *Troodon formosus*. *Journal of Vertebrate Paleontology* 19(1), 91–100.

Viele, G.W., & Harris III, F.G. (1965). Montana Group stratigraphy, Lewis and Clark County, Montana. *Bulletin of the American Association of Petroleum Geologists* 49(4), 379–417.

Walsh, S.A., Barrett, P.M., Milner, A.C., Manley, G., and Witmer, L.M. (2009). Inner ear anatomy is a proxy for deducing auditory capability and behaviour in reptiles and birds. *Proceedings of the Royal Society of London B: Biological Sciences* 276, 1355–1360.

Watanabe, A., Balanoff, A.M., Gignac, P.M., Gold, M.E.L., and Norell, M.A. (2021). Novel neuroanatomical integration and scaling define avian brain shape evolution and development. *ELife 10*. https://doi.org/10.7554/eLife.68809

Webb, J.K., Pike, D.A. and Shine, R. (2010). Olfactory recognition of predators by nocturnal lizards: safety outweighs thermal benefits. *Behav Ecol.* 21(1), 72–77. doi:10.1093/beheco/arp152

Weishampel, D.B., and Norman, D.B. (1989). Vertebrate herbivory in the Mesozoic; Jaws, plants, and evolutionary metrics. *In*: Farlow, J.O. (ed.), *Paleobiology of the Dinosaur*, Vol. 238, pp. 87–101. Geological Society of America. https://doi.org/10.1130/SPE238-p87

Werneburg, I., Evers, S.W., and Ferreira, G.S. (2021). On the "cartilaginous rider" in the endocasts of turtle brain cavities. *Vertebrate Zoology* 71, 403–418. https://doi.org/10.3897/VZ.71.E66756

Werneburg, I., Kyriakouli, C., and Szczygielski, T. (2022). A surface scan of the "Tübingen Steinkern", Holotype of *Proganochelys quenstedtii* (Testudinata), with some historical remarks. *MorphoMuseuM* 8(3), e168. https://doi.org/10.18563/journal.m3.168

Wever, E.G. (1978). Family Scincidae: The skinks. In: Wever, E.G. (ed.), *The Reptile Ear: Its Structure and Function*, pp. 623–657. Princeton University Press.

Wharton, D.S. (2000). An enlarged endocranial venous system in *Steneosaurus pictaviensis* (Crocodylia: Thalattosuchia) from the Upper Jurassic of Les Lourdines, France. *Earth and Planetary Sciences* 331, 221-226.

Witmer, L.M., and Ridgely, R.C. (2008). Structure of the brain cavity and inner ear of the centrosaurine ceratopsid dinosaur *Pachyrhinosaurus* based on CT scanning and 3D visualization. I: *A New Horned Dinosaur from an Upper Cretaceous Bone Bed in Alberta*, pp. 117–144. NRC Research Press.

Witmer, L.M., and Ridgely, R.C. (2009). New insights into the brain, braincase, and ear region of tyrannosaurs (Dinosauria, Theropoda), with implications for sensory organization and behavior. *Anatomical Record* 292(9), 1266–1296. https://doi.org/10.1002/ar.20983

Witmer, L.M., Ridgely, R.C., Dufeau, D.L., and Semones, M.C. (2008). Using CT to peer into the past: 3D visualization of the brain and ear regions of birds, crocodiles, and nonavian dinosaurs. *In*: Endo, H., and Frey, R. (eds), *Anatomical Imaging*, pp. 67-87. Springer, Tokyo. https://doi.org/10.1007/978-4-431-76933-0_6

Woodward, H.N., Fowler, E.A.F., Farlow, J.O., and Horner, J.R. (2015). *Maiasaura*, a model organism for extinct vertebrate population biology: a large sample statistical assessment of growth dynamics and survivorship. *Paleobiology* 41(4), 503–527. https://doi.org/10.5061/dryad.7vf45

Wosik, M., Chiba, K., Therrien, F., and Evans, D.C. (2020). Testing size-frequency distributions as a method of ontogenetic aging: a life-history assessment of hadrosaurid dinosaurs from the Dinosaur Park Formation of Alberta, Canada, with implications for hadrosaurid paleoecology. *Paleobiology* 46(3), 379–404. https://doi.org/10.5061/dryad.1jwstqjqr

Zelenitsky, D.K., Therrien, F., and Kobayashi, Y. (2009). Olfactory acuity in theropods: Palaeobiological and evolutionary implications. *Proceedings of the Royal Society B: Biological Sciences* 276(1657), 667–673. https://doi.org/10.1098/rspb.2008.1075

Zelenitsky, D. K., Therrien, F., Ridgely, R.C., McGee, A.R., and Witmer, L.M. (2011). Evolution of olfaction in non-avian theropod dinosaurs and birds. *Proceedings of the Royal Society B: Biological Sciences* 278(1725), 3625–3634. https://doi.org/10.1098/rspb.2011.0238

Zhao, Q., Barrett, P.M., and Eberth, D.A. (2007). Social behaviour and mass mortality in the basal ceratopsian dinosaur Psittacosaurus (Early cretaceous). *Palaeontology* 50(5), 1023–1029. https://doi.org/10.1111/j.1475-4983.2007.00709.x

Zhao, Q., Benton, M.J., Xu, X., and Sander, P.M. (2014). Juvenile-only clusters and behaviour of the early Cretaceous Dinosaur *Psittacosaurus*. *Acta Palaeontologica Polonica* 59(4), 827–833. https://doi.org/10.4202/app.2012.0128

VITA

Emma Rose Puetz received her Bachelor of Science degree in Geology and Geophysics and minor in French in December 2023 from the Missouri University of Science and Technology. She graduated with 4.0. Emma completed her Master of Science degree in Geology and Geophysics in May 2024 from the Missouri University of Science and Technology. Her love of paleontology was sparked when she was young, and she continues to enjoy research and field work associated with the discipline. Emma was also a student-athletes on the Missouri University of Science and Technology Women's Cross Country and Track teams where she beat the school record in the 5k (xc), 5k (outdoor track), and 6k (xc), placed 11th at the Cross Country Midwest Regional Meet, placed 2nd in Cross County GLVC Conference, earned the GLVC Scholar Athlete of the Year in 2023, received GLVC Athlete of the Week numerous times, and was named the Missouri S&T 2024 Student-Athlete of the Year. She will continue paleoneurological research in the Functional Anatomy and Evolution Ph.D. degree program at Johns Hopkins University.